POLYPUBLIE

Mixing of viscoelastic fluids by helical ribbon impellers with and without aeration

Jianya Cheng

Document en libre accès dans PolyPublie
Open Access document in PolyPublie

Date	1993
Type	Mémoire ou thèse / Dissertation or Thesis Thèse de doctorat/Ph.D. thesis
URL de PolyPublie PolyPublie URL	https://publications.polymtl.ca/57976/
Conditions d'utilisation Terms of use	© Tous droits réservés / All rights reserved
Référence Citation	Cheng, J. (1993). Mixing of viscoelastic fluids by helical ribbon impellers with and without aeration [Thèse de doctorat, Polytechnique Montréal]. PolyPublie. https://publications.polymtl.ca/57976/

Détails de la thèse
Thesis details

Directeurs de recherche Advisors	
Programme Program	Non spécifié

Ce fichier a été téléchargé à partir de PolyPublie, le dépôt institutionnel de Polytechnique Montréal
This file has been downloaded from PolyPublie, the institutional repository of Polytechnique Montréal
https://publications.polymtl.ca

UNIVERSITÉ DE MONTRÉAL

MIXING OF VISCOELASTIC FLUIDS BY HELICAL RIBBON IMPELLERS WITH AND WITHOUT AERATION

par

Jianya CHENG

DÉPARTEMENT DE GÉNIE CHIMIQUE

ÉCOLE POLYTECHNIQUE

THÈSE PRÉSENTÉE EN VUE DE L'OBTENTION

DU GRADE DE PHILOSOPHIAE DOCTOR (Ph.D.)

(GÉNIE CHIMIQUE)

Novembre 1993

© droits réservés de Jianya CHENG 1993.

National Library
of Canada

Acquisitions and
Bibliographic Services Branch

395 Wellington Street
Ottawa, Ontario
K1A 0N4

Bibliothèque nationale
du Canada

Direction des acquisitions et
des services bibliographiques

395, rue Wellington
Ottawa (Ontario)
K1A 0N4

Your file *Votre référence*

Our file *Notre référence*

The author has granted an irrevocable non-exclusive licence allowing the National Library of Canada to reproduce, loan, distribute or sell copies of his/her thesis by any means and in any form or format, making this thesis available to interested persons.

L'auteur a accordé une licence irrévocable et non exclusive permettant à la Bibliothèque nationale du Canada de reproduire, prêter, distribuer ou vendre des copies de sa thèse de quelque manière et sous quelque forme que ce soit pour mettre des exemplaires de cette thèse à la disposition des personnes intéressées.

The author retains ownership of the copyright in his/her thesis. Neither the thesis nor substantial extracts from it may be printed or otherwise reproduced without his/her permission.

L'auteur conserve la propriété du droit d'auteur qui protège sa thèse. Ni la thèse ni des extraits substantiels de celle-ci ne doivent être imprimés ou autrement reproduits sans son autorisation.

ISBN 0-315-90014-8

Canada

e JIANYA CHENG

ertation Abstracts International is arranged by broad, general subject categories. Please select the one subject which most y describes the content of your dissertation. Enter the corresponding four-digit code in the spaces provided.

Chemical Engineering | 0542 | U·M·I

SUBJECT TERM SUBJECT CODE

ect Categories

E HUMANITIES AND SOCIAL SCIENCES

AUNICATIONS AND THE ARTS
ecture 0729
story 0377
ıa 0900
..... 0378
rts 0357
ıation Science 0723
alism 0391
y Science 0399
Communications 0708
..... 0413
h Communication 0459
er 0465

ATION
ral 0515
nistration 0514
and Continuing 0516
ultural 0517
..... 0273
ual and Multicultural 0282
ess 0688
nunity College 0275
culum and Instruction 0727
Childhood 0518
ntary 0524
ce 0277
ance and Counseling 0519
n 0680
ar 0745
y of 0520
Economics 0278
trial 0521
uage and Literature 0279
ematics 0280
..... 0522
sophy of 0998
cal 0523

Psychology 0525
Reading 0535
Religious 0527
Sciences 0714
Secondary 0533
Social Sciences 0534
Sociology of 0340
Special 0529
Teacher Training 0530
Technology 0710
Tests and Measurements 0288
Vocational 0747

LANGUAGE, LITERATURE AND LINGUISTICS
Language
- General 0679
- Ancient 0289
- Linguistics 0290
- Modern 0291

Literature
- General 0401
- Classical 0294
- Comparative 0295
- Medieval 0297
- Modern 0298
- African 0316
- American 0591
- Asian 0305
- Canadian (English) 0352
- Canadian (French) 0355
- English 0593
- Germanic 0311
- Latin American 0312
- Middle Eastern 0315
- Romance 0313
- Slavic and East European 0314

PHILOSOPHY, RELIGION AND THEOLOGY
Philosophy 0422
Religion
- General 0318
- Biblical Studies 0321
- Clergy 0319
- History of 0320
- Philosophy of 0322

Theology 0469

SOCIAL SCIENCES
American Studies 0323
Anthropology
- Archaeology 0324
- Cultural 0326
- Physical 0327

Business Administration
- General 0310
- Accounting 0272
- Banking 0770
- Management 0454
- Marketing 0338

Canadian Studies 0385
Economics
- General 0501
- Agricultural 0503
- Commerce-Business 0505
- Finance 0508
- History 0509
- Labor 0510
- Theory 0511

Folklore 0358
Geography 0366
Gerontology 0351
History
- General 0578
- Ancient 0579
- Medieval 0581
- Modern 0582
- Black 0328
- African 0331
- Asia, Australia and Oceania 0332
- Canadian 0334
- European 0335
- Latin American 0336
- Middle Eastern 0333
- United States 0337

History of Science 0585
Law 0398
Political Science
- General 0615
- International Law and Relations 0616
- Public Administration 0617

Recreation 0814
Social Work 0452
Sociology
- General 0626
- Criminology and Penology ... 0627
- Demography 0938
- Ethnic and Racial Studies 0631
- Individual and Family Studies 0628
- Industrial and Labor Relations 0629
- Public and Social Welfare 0630
- Social Structure and Development 0700
- Theory and Methods 0344

Transportation 0709
Urban and Regional Planning 0999
Women's Studies 0453

IE SCIENCES AND ENGINEERING

OGICAL SCIENCES
ulture
eneral 0473
gronomy 0285
nimal Culture and Nutrition 0475
nimal Pathology 0476
ood Science and Technology 0359
orestry and Wildlife 0478
lant Culture 0479
lant Pathology 0480
lant Physiology 0817
ange Management 0777
Wood Technology 0746
gy
eneral 0306
natomy 0287
iostatistics 0308
otany 0309
ell 0379
cology 0329
ntomology 0353
enetics 0369
imnology 0793
Microbiology 0410
Molecular 0307
Neuroscience 0317
Oceanography 0416
hysiology 0433
adiation 0821
eterinary Science 0778
oology 0472
hysics
eneral 0786
Medical 0760

TH SCIENCES
eochemistry 0425
hemistry 0996

Geodesy 0370
Geology 0372
Geophysics 0373
Hydrology 0388
Mineralogy 0411
Paleobotany 0345
Paleoecology 0426
Paleontology 0418
Paleozoology 0985
Palynology 0427
Physical Geography 0368
Physical Oceanography 0415

HEALTH AND ENVIRONMENTAL SCIENCES
Environmental Sciences 0768
Health Sciences
- General 0566
- Audiology 0300
- Chemotherapy 0992
- Dentistry 0567
- Education 0350
- Hospital Management 0769
- Human Development 0758
- Immunology 0982
- Medicine and Surgery 0564
- Mental Health 0347
- Nursing 0569
- Nutrition 0570
- Obstetrics and Gynecology .. 0380
- Occupational Health and Therapy 0354
- Ophthalmology 0381
- Pathology 0571
- Pharmacology 0419
- Pharmacy 0572
- Physical Therapy 0382
- Public Health 0573
- Radiology 0574
- Recreation 0575
- Speech Pathology 0460
- Toxicology 0383

Home Economics 0386

PHYSICAL SCIENCES
Pure Sciences
Chemistry
- General 0485
- Agricultural 0749
- Analytical 0486
- Biochemistry 0487
- Inorganic 0488
- Nuclear 0738
- Organic 0490
- Pharmaceutical 0491
- Physical 0494
- Polymer 0495
- Radiation 0754

Mathematics 0405
Physics
- General 0605
- Acoustics 0986
- Astronomy and Astrophysics 0606
- Atmospheric Science 0608
- Atomic 0748
- Electronics and Electricity 0607
- Elementary Particles and High Energy 0798
- Fluid and Plasma 0759
- Molecular 0609
- Nuclear 0610
- Optics 0752
- Radiation 0756
- Solid State 0611

Statistics 0463

Applied Sciences
Applied Mechanics 0346
Computer Science 0984

Engineering
- General 0537
- Aerospace 0538
- Agricultural 0539
- Automotive 0540
- Biomedical 0541
- Chemical 0542
- Civil 0543
- Electronics and Electrical 0544
- Heat and Thermodynamics ... 0348
- Hydraulic 0545
- Industrial 0546
- Marine 0547
- Materials Science 0794
- Mechanical 0548
- Metallurgy 0743
- Mining 0551
- Nuclear 0552
- Packaging 0549
- Petroleum 0765
- Sanitary and Municipal 0554
- System Science 0790

Geotechnology 0428
Operations Research 0796
Plastics Technology 0795
Textile Technology 0994

PSYCHOLOGY
General 0621
Behavioral 0384
Clinical 0622
Developmental 0620
Experimental 0623
Industrial 0624
Personality 0625
Physiological 0989
Psychobiology 0349
Psychometrics 0632
Social 0451

UNIVERSITÉ DE MONTRÉAL

ÉCOLE POLYTECHNIQUE

Cette thèse intitulée

MIXING OF VISCOELASTIC FLUIDS BY HELICAL RIBBON IMPELLERS WITH AND WIHTOUT AERATION

présenté par: Jianya CHENG

en vue de l'obtention du grade de: PHILOSOPHIAE DOCTOR (Ph.D.)

a été dûment acceptée par jury d'examen constitué de:

M. Christophe GUY, Ph.D., président

M. Pierre CARREAU, Ph.D., membre et directeur de recherche

M. Lionel CHOPLIN, Ph.D., membre

M. Philippe TANGUY, Ph.D., membre

To little Victoria

Résumé

Le mélange des fluides non-newtoniens mécaniquement agités est utilisé dans plusieurs procédés industriels tels que la polymérisation, la bio-fermentation, etc. La complexité du comportement rhéologique des liquides non-newtoniens rend le contrôle de ces procédés de plus en plus difficile, particulièrement pour les mélanges en grande échelle, en régime transitoire ou avec aération. L'agitateur à ruban hélicoïdal est très efficace pour des liquides très visqueux, en particulier pour les fluides viscoélastiques, dû à la capacité de pompage axial. Bien que l'influence du comportement rhéologique sur le mélange des fluides a été étudiée depuis des dizaines d'années, plusieurs problèmes restent à résoudre. Par exemple, l'effet de la viscoélasticité sur la puissance requise, l'influence du comportement non-newtonien sur la vitesse de déformation effective, et le mélange avec agitateur à ruban hélicoïdal sous aération, etc. La puissance consommée est un paramètre important pour la conception du procédé; elle est aussi un indicateur de changement de mode d'écoulement dans le réservoir. La vitesse de déformation effective est un autre paramètre important. Le temps de mélange et le temps de circulation sont utilisés pour décrire la qualité du mélange. Le temps de mélange est défini comme le temps nécessaire pour atteindre un certain niveau d'homogénéité tandis que le temps de circulation est le temps nécessaire pour compléter une boucle fermée pour un élément du fluide.

L'objectif de ce travail est d'étudier l'influence du comportement non-newtonien

sur les paramètres qui caratérisent la qualité du mélange, tels la puissance consommée, le temps de mélange, le temps de circulation, la dispersion du gaz et les modes d'écoulement, etc. Nous étudierons les paramètres pour des mélanges en régimes laminaire et transitoire avec des agitateurs à ruban hélicoïdal avec ou sans aération.

Quatre liquides newtoniens et douze fluides non-newtoniens ont été choisis soigneusement comme fluides modèles pour couvrir une grand gamme de propriétés rhéologiques. Deux réservoirs de dimensions différentes et six combinaisons d'agitateurs à ruban hélicoïdal de géométrie différente ont été utilisés pour évaluer l'effet de la géométrie sur le processus de mélange. Du glycérol et du sirop de maïs ainsi que leurs solutions aqueuses diluées ont été utilisés comme liquides newtoniens. Les douze fluides non-newtoniens comprennent des solutions aqueuses rhéofluidifiantes de xanthane et de méthylcellulose carboxyle (CMC) et de gellane dans du sirop de maïs de concentrations différentes. Les solutions de xanthane et de CMC dissous dans un mélange de glycérol et d'eau ont été choisies comme des fluides élastiques rhéofluidifiants. Deux solutions élastiques avec viscosité indépendante de la vitesse de déformation, appelées fluides de Boger, ont été aussi utilisées dans ce travail: la première solution est un polyisobuthylène dissous dans un mélange de polybutène et de kérosène, l'autre est un polyacrylamide dans un sirop de maïs.

Pour les fluides inélastiques de rhéofluidifiance moyenne, la puissance consommée

ne dévie pas de la courbe correspondante obtenue pour les fluides newtoniens en régime laminaire, comme en régime transitoire. Pour les fluides inélastiques de forte rhéofluidifiance, le nombre de puissance montre une prolongation du régime laminaire; en d'autres termes, le début du régime transitoire est en quelque sorte retardé. L'élasticité d'un fluide augmente appréciablement la puissance requise (3.5 fois par rapport à la puissance d'un fluide newtonien dans le cas de la solution contenant 800 ppm de PAA). La déviation de la courbe de puissance non-newtonienne en régime laminaire est observée à des nombres de Reynolds plus faibles pour les fluides élastiques.

Deux modèles, basés sur l'analogie de l'écoulement Couette et sur la connaissance du couple ou de nombre de puissance pour les fluide newtoniens, ont été proposés pour décrire la vitesse de déformation effective en régime laminaire. L'influence de l'indice de comportement (paramètre de la loi de puissance) sur la vitesse de déformation effective a été étudiée attentivement pour une grande gamme d'indice de comportement avec agitateurs de différente géométrie. Les données expérimentales montrent que la vitesse de déformation effective augmente lorsque la rhéofluidifiance diminue (augmentation de l'indice du comportement). Les résultats expérimentaux obtenus suggèrent également que le dégagement entre la lame d'agitateur et le fond du réservoir n'affecte pas, de façon appréciable, la puissance consommée.

Sous aération et pour la premier fois, nous avons montré que la puissance

consommée pour les fluides de Boger est plus grande que celle sans aération et la puissance consommée augmente avec le débit du gaz. La puissance pour la solution contenant 800 ppm PAA (fluide de Boger) et un débit de gaz de 2.017 L/s est 3 fois plus grande que la puissance sous aération. La puissance d'aération diminue lors que le nombre de Reynolds augmente, et finalement approche le niveau de puissance requise pour des systèmes non aérés. L'augmentation de la puissance sous aération est due en parties à une augmentation de la viscosité apparente. La viscosité apparente pour le 800 ppm PAA avec une rétention de gaz de 6.6 % est 2 fois plus élevée que la viscosité sans gaz. Une diminution de la puissance consommée est observée pour des fluides inélastiques rhéofluidifiants et la puissance diminue lorsque le débit du gaz augmente. Le rapport de la puissance pour les systèmes aérés sur la puissance consommée en absence d'aération augmente lorsque le nombre de Reynolds diminue et finalement approche l'unité. La puissance en milieu aéré dépend aussi du caractère élastique et de la rhéofluidifiance.

Un concept de la vitesse de déformation effective en présence d'aération est suggéré pour corriger la vitesse de déformation effective. La vitesse de déformation sous aération est une combinaison des vitesses de déformation causées par la rotation de l'agitateur et par la présence des bulles et l'extension du fluide dues aux bulles. Deux corrélations basées sur l'analyse dimensionnelle sont proposées pour prédire la consommation de la puissance avec aération en fonction des nombres de Reynolds et de Weissenberg, et du nombre d'aération, en régimes laminaire et transitoire.

Les résultats expérimentaux de ce travail confirment les résultats publiés dans la littérature: la vitesse de déformation effective n'est plus proportionnelle à la vitesse de rotation de l'agitateur en régime transitoire, mais augmente avec la vitesse à un exposant de deux ou supérieur à deux. Pour un agitateur à ruban hélicoïdal, la vitesse de déformation effective augmente brutalement en régime transitoire pour les liquides inélastiques de forte rhéofluidifiance; par contre, une extension de la relation de Metzner-Otto est observée à des nombres de Reynolds plus élevés pour les fluides inélastiques de faible rhéofluidifiance. A partie des résultats de la littérature, une augmentation importante de la vitesse de déformation effective est observée dans tous les cas même pour des fluides inélastiques de faible rhéofluidifiance, agités par les agitateurs de type ancre, turbine à lames et disque plat.

Deux modèles analytiques et un modèle numérique basés sur des analyses uni ou bi-dimensionnelles de l'écoulement équivalent de Couette sont proposés pour décrire la vitesse de déformation effective en régime transitoire. Les prédictions de ces trois modèles sont comparés avec les résultats expérimentaux obtenus pour des agitateurs à ruban hélicoïdal dans travail, et avec les résultats de la littérature pour des agitateurs à ancre, turbine à lames et disque plat. L'accord entre les prédictions et les valeurs expérimentales est très satisfaisant. L'élasticité et les propriétés rhéofluidifiantes n'ont pas d'effet significatif sur le mélange sans dimension et le temps de circulation en régime transitoire alors qu'ils ont tendance à augmenter de façon marquée les temps de mélange et de circulation pour les faibles valeurs du nombre de Reynolds. Pour les fluides élastiques, la temps de mélange en régime

laminaire est de 4 fois plus long que pour les fluides newtoniens. On note finalement que le temps de mélange augmente quelque peu avec le pas du ruban hélicoïdal et diminue alors qu'on utilise un ruban plus large.

Abstract

This work has been carried out to investigate the influence of the non-Newtonian behaviour on the mixing performance parameters such as power requirement, mixing and circulation times, gas dispersion and flow patterns, etc, for the laminar and the transition flow regimes, of helical ribbon agitators, with and without aeration. Four Newtonian and twelve non-Newtonian fluids were carefully chosen as the test fluids to cover a wide range of the rheological complex properties. Two different scale mixers along with six different geometric combinations of the helical ribbon impellers were used to assess the geometry effects on the mixing.

Glycerol, corn syrup as well as their water dilute solutions were employed as Newtonian liquids. Twelve non-Newtonian fluids include shear-thinning xanthan and carboxyl methylcellulose (CMC) aqueous solutions and gellan in corn syrup of different concentrations. Solutions of xanthan and CMC dissolved in a mixture of glycerol and water were chosen as the shear-thinning and elastic fluids. Two elastic shear independent viscosity solutions, so called Boger fluids, were also used in this work. One of them is a polyisobutylene dissolved in the mixture of polybutene and kerosene while another is polyacrylamide in corn syrup.

For moderately shear-thinning inelastic fluids, the power consumption does not deviate from the corresponding Newtonian curve in the laminar flow regime as well as in the transition flow regime. For highly shear-thinning inelastic fluids, the power number shows an extended laminar flow regime, in other words, the onset of the transition regime is somewhat delayed. Fluid's elasticity increases appreciably the power requirement, and early departure from the Newtonian power curve in the laminar regime was observed at lower Reynolds numbers for viscoelastic fluids. Two models based on an analysis of the equivalent Couette flow, from the knowledge of torque or power number were proposed to predict the effective shear rate in the laminar flow regime. The influence of the flow index on the effective shear rate has

been intensively studied over the wide range of the flow index with different impeller geometries. Experimental data shows that the effective deformation rate increases with decreasing shear-thinning (e.g. increasing flow index). The present experimental results also suggest that the clearance between the agitator and the bottom does not influence the power consumption to an appreciable extent.

Under gassed conditions, for first time, the gassed power consumption in the Boger fluids (elastic, with shear independent viscosity) was found to be much higher than ungassed ones, while a decrease of gassed power was observed for the shear-thinning inelastic fluids. The gassed power is also dependent on the gas flow rate, Reynolds number and elastic level. A concept of aerated effective deformation rate is suggested to correct the effective deformation rate under gassed circumstances. Two correlations based on the dimensional analysis were proposed to predict the gassed power as functions of the aerated Reynolds number, the aeration and Weissenberg numbers, in both the laminar and the transition flow regimes. Gas hold-up, bubble sizes and gas dispersion performance were also studied.

The experimental results of this work confirm the previous finding in the literature, that is the effective shear rate is no longer proportional to the impeller rotational speed in the transition flow regime. With closer examination, for helical ribbon agitator, the effective deformation rate increases sharply in the transition flow regime for highly shear-thinning inelastic fluids; however, an extended linearity of Metzner-Otto's method was observed for moderately shear-thinning inelastic fluids. With reviewing other types of impellers in the literature, a sharp enhancement was found, even for the moderately shear-thinning liquids agitated by anchor, blade turbine and disc impellers. Two analytical and one numerical models based on one or two dimensional analysis of the equivalent Couette flow are proposed to predict the effective deformation rate in the transition flow regime. The predictions of three models are compared with experimental data obtained from helical ribbon agitators,

and with literature for anchor, blade turbine and flat disc agitators. The agreement between the predictions and the experimental values is quite good. The elasticity along with shear-thinning properties appear to have no significant effect on the dimensionless mixing and circulation times in the transition regime while they considerably increase the mixing and circulation times at lower Reynolds number.

Acknowledgement

First, I would gratefully express my sincere thanks to my supervisor Professor Dr. Pierre J. Carreau for giving me an opportunity and financial support to pursue Ph.D. degree under his guidance. His such high achievement, such bright and broad scientific knowledge, serious aptitude towards sciences and hard working habit have given me a very deep expression. Whenever I was wondering in the scientific crossroad, he could always point out the right direction. Although he's such a busy professor who is in charge of so many academic affairs, he is ready to advise me and willing to go into even detailed corners whenever I need his guidance. I would like to say that, his influence, in many ways, will remain on me in my life time.

It was such wonderful to have a chance to involve in a cooperating program with Professor L. Choplin and Dr. E. Brito. I wish to thank them for their quite helpful discussions and suggestions.

I also like to acknowledge Professor C. Chavarie, Professor M. Grmela and Professor P. Lafleur along with Professor P.J. Carreau, who have given me lectures during my studies. Through those courses, I have experienced some western educational training.

So many people have helped me via various ways during the course of this work. One of them is Mr. S. Brunet who helped me for the design of mixing systems and measurement methods, installation of experimental equipments, etc. Mr. R. Delisle installed the Labmaster data acquisition system and other electronic equipments, he also solved many problems encountered in PC and software. Mr. A. Lachapelle is first one to show me how to operate the Weissenberg rheogniometer. Ms. S. Pastuch, Mr. J. Larente and Miss D. Héroux have also helped me. Meanwhile, some students from Department of Mechanical Engineering have helped me to solve numerical problems. They are Mr. K. Zha, Mr. X. Wang and Mr. Z. Zhang.

It is always important to have some nice colleagues and graduate student fellows to deal with similar problems encountered and discuss interesting problems. Among them are Dr. A. Kamen, Mr. M. Jolicoeur, Mr. Z. Mao, Dr. M. Shi, Dr. B. Glugogorski, Dr. T. Ghosh, Dr. M. Karamanev and Miss C. Hyndmen.

Finally, I would express my thanks to my wife, Bin, for her encouragement and supports to let me to complete this thesis, and also thank my litter sweat heart, Vicky, for the happiness she brings to me.

TABLE OF CONTENTS

PAGE

RESUME v

ABSTRACT xi

ACKNOWLEDGEMENT xiv

TABLE OF CONTENTS xv

LIST OF FIGURES xviii

NOMENCLATURE xxiii

LIST OF APPENDICES xxvii

Chapter 1 - GENERAL INTRODUCTION 1

1.1 Introduction 2

1.2 Objectives 5

1.3 References 7

Chapter 2 - LITERATURE REVIEW 9

2.1 Rheological Properties 10

2.2 Effective deformation Rate 14

2.2.1 Influence of geometry on k_s 18

2.2.2 Influence of flow index on k_s 19

2.2.3 Influence of flow regime on k_s 20

2.2.4 Influence of aeration on k_s 21

2.3 Power Consumption 22

2.3.1 Dimensional analysis 23

2.3.2 Power correlations 25

2.3.3. Influence of non-Newtonian properties and flow regime on power input 28

2.4 Mixing and Circulation Times 29

2.5 References 33

Chapter 3 - POWER REQUIREMENT: Effect of Rheological Properties on Power Consumption with Helical Ribbon Agitators 40
3.1 Summary 41
3.2 Introduction 41
3.2.1 Previous work 43
3.3 Concept 44
3.3.1 Prediction of effective shear rate 45
3.4 Experimental 48
3.4.1 Test fluids 49
3.5 Results and Discussion 51
3.5.1 Newtonian liquids 51
3.5.2 Non-Newtonian fluids 52
3.5.3 Predicted and experimental effective shear rate 54
3.6 Conclusions 56
3.7 Acknowledgement 57
3.8 References 58
Chapter 4 - AERATED MIXING: Aerated Mixing of Viscoelastic Fluids with Helical Ribbon Impellers 78
4.1 Abstract 79
4.2 Introduction 79
4.3 Experimental 80
4.4 Results and Discussion 81
4.4.1 Mixing with aeration 82
4.4.2 Newtonian and inelastic fluids 84
4.4.3 Elastic fluids 85
4.4.4 Gassed power correlations 87
4.5 Conclusions 89

4.7 Acknowledgement 89
4.8 References 89
Chapter 5 - MIXING IN THE TRANSITION FLOW REGIME: Mixing in the Transition Flow Regime with Helical Ribbon Agitators 101
5.1 Abstract 102
5.2 Resume 102
5.3 Introduction 103
5.4 Concepts 105
5.4.1 Effective deformation rate 105
5.4.1.1 Approach 1 106
5.4.1.2 Approach 2 107
5.4.1.3 Approach 3 109
5.5 Experimental 112
5.5.1. Test fluids 113
5.6 Results and Discussion 113
5.6.1 Effective deformation rate 113
5.6.1.1 Helical ribbon agitators 114
5.6.1.2 Anchor, blade turbine and flat disc agitators 115
5.6.2 Mixing and circulation times 119
Chapter 6 - CONCLUSIONS 149
6.1 Conclusions 150
6.2 Recommendations for Future Work 152
APPENDICES 155

LIST OF FIGURES

PAGE

Chapter 2

Figure 1 Helical ribbon agitator system 15

Figure 2 Illustration of the procedure to calculate the effective deformation rate from power data using Metzner-Otto's method 17

Figure 3 Experimental data of the effective viscosity in the transition flow regime for an aqueous CMC solution (*from Forschner et al., 1991*) 21

Figure 4 Mixing time data in terms of $t_m^2\rho/\mu D^3$ *(from Hoogendooen and den Hartog)* 31

Chapter 3

Figure 1 Sketch of helical ribbon agitator system 63

Figure 2 Shear viscosity data for eight polymer solutions 64

Figure 3 Primary normal stress difference data for five polymer solution . . 65

Figure 4 Variation of elastic time constant with shear rate for five polymer solutions 66

Figure 5 Variation of $NpRe_g$ with Reynolds number for Newtonian fluids . 67

Figure 6 Power data for the shear thinning inelastic fluids 68

Figure 7 Power data for the viscoelastic fluids 69

Figure 8 Variation of $NpRe_g$ with Weissenberg number 70

Figure 9 Bottom effect on the power consumption 71

Figure 10 Variation of k_s with generalized Reynolds number for the shear thinning inelastic 72

Figure 11 Variation of k_s with generalized Reynolds number for the viscoelastic fluids 73

Figure 12 Dependence of k_s or k_s' on the flow index n 74

Figure 13 Dependence of D/d_e on the flow index n 75

Figure 14 Power predictions using d_e from Newtonian data (value reported in Table 1). Open symbols: experimental; solid symbols: predictions 76

Chapter 4

Figure 1 Sketch of experimental equipment 92

Figure 2 Variation of apparent viscosity of dispersion with time for the elastic 800 ppm PAA solution 93

Figure 3 Variation of apparent viscosity of dispersion with time for the shear-thinning 2.5% xanthan and 1% CMC aqueous solutions ($\dot{\gamma}$=42 s^{-1}) 94

Figure 4 Gassed power data for Newtonian and shear-thinning fluids . . . 95

Figure 5 Gassed power data for shear-thinning fluids (▵ □ ◯: 2.5% xanthan, ▲ ▼: 0.5% xanthan) 96

Figure 6 Gassed power data for elastic fluids (□ ◇ ◯: 800 ppm PAA, ■: 0.35% PIB, ●: 0.5% xanthan(gly/H_2O)) 97

Figure 7 Variation of gas hold-up with impeller rotational speed 98

Figure 8 Power correlations (▵: Newtonian and inelastic shear-thinning fluids, ▼: elastic fluids) 99

Chapter 5

Figure 1 Sketch of the two dimensional equivalent Couette flow 131

Figure 2 Helical ribbon system 132

Figure 3 Measurement of mixing and circulation times for 800 ppm PAA in impeller HR1 system, at 59 rev/min 133

Figure 4 Power curves for Newtonian and non-Newtonian test fluids . . . 134

Figure 5. Predictions of $\dot{\gamma}_e$ compared with the experimental data for the highly shear-thinning 2.5% xanthan solution with impeller HR3 135

Figure 6. Predictions of $\dot{\gamma}_e$ compared with the experimental data for the highly shear-thinning 2.5% xanthan solution with impeller HR1 136

Figure 7 Predictions of $\dot{\gamma}_e$ compared with the experimental data for the moderately shear thinning 1% CMC solution with impeller HR3 137

Figure 8 Predictions of $\dot{\gamma}_e$ compared with the data of Bourne et al.(1981) with anchor impeller 138

Figure 9 Prediction of $\dot{\gamma}_e$ compared with the data of Pollard and Kantyka (1969) with anchor impeller 139

Figure 10 Prediction of $\dot{\gamma}_e$ compared with the data of Metzner et al. (1961) with 6-bladed fan turbine impeller 140

Figure 11 Prediction of $\dot{\gamma}_e$ compared with the data of Nagata et al.(1971) with 6-blade turbine impeller 141

Figure 12 Prediction of $\dot{\gamma}_e$ compared with the data of Höcker et al. (1981) with flat disc impeller 142

Figure 13 Predictions of $\dot{\gamma}_e$ compared with the data of Forschner et al.(1991) with Inter-Mig turbine impeller 143

Figure 14 Comparison of power data evaluated via the effective shear rate obtained from Metzner-Otto's expression (Eq.1) and via Eqs. 7, 12 and 26 144

Figure 15 Dimensionless mixing time, Nt_m, versus generalized Reynolds number Re_g. □: glycerol (μ = 0.47 Pa.s), ◇: 1% CMC (H_2O), ○ ▵ ▽: 0.5 % xanthan in glycerol/H_2O, ▲ ■: 800 ppm PAA in

corn syrup; ◇ ◯ ▲: HR1 impeller, ▵: HR2 impeller, □ ▽ ■: HR3 impeller 145

Figure 16 Circulation number, *Ci*, versus generalized Reynolds number (symbols same as in Fig.15) 146

Figure 17 Distribution of circulation time for 0.5% Xanthan in glycerol/ H_2O 147

Figure 18 Dependence of t_m/t_c with generalized Reynolds number (symbols same as in Fig.15) 148

Appendices

Figure A1 Effect of the equivalent bottom clearance on k_s for impeller HR3 161

Figure A2 Effect of the equivalent bottom clearance on k_s for impeller HR4 162

Figure A3 Effect of the equivalent bottom clearance on the power consumption for impeller HR3 164

Figure A4 Frame of computer program for solving Model 3 in Chapter 5 166

Figure A5 Influence of the wall clearance on power number for corn syrup agitated by impeller HR3 171

Figure A6 Influence of the wall clearance on k_s for 3% CMC with impeller HR2 and HR3 173

Figure A7 Comparison of gassed power data with Michel and Miller's correlation 175

Figure A8 Dependence of *C* in Michel and Miller's correlation on flow index, *n* and elastic constant, λ 176

Figure A9 Illustration of reproducing the effective deformation rate

from the power data reported in the literature 177
Figure A10 Power data of Metzner et al. (1961) 179
Figure A11 Power data of Nagata et al. (1971) 179
Figure A12 Power data of Hocker et al. (1981) 180

NOMENCLATURE

A	parameter, Eq.11
a	power index, Eq.2 in Chapter 5
a_1 ~ a_7	exponent constant
B	proportionality constant of Rieger and Novak's correlation
C	proportionality constant, Eq.24 in Chapter 5
C	Constant, Eq. 6 in Chapter 4, or wall clearance, m
Ci	circulation number, Eq.28 in Chapter 5
C_1, C_4,	Constant Eq. 7 in Chapter 4
C_2, C_3, C_5,	Power index constants, Eq.7 in Chapter 4
c_1	integration constant, Eq.15 in Chapter 5
D	vessel diameter, m
d	impeller width, m
d_e	equivalent diameter of impeller, m
El	elastic number, Wi/Re_g
H	height of liquid in the vessel, m
h_c	bottom clearance, m
K_p	proportionality constant of the power number in laminar regime
K_p'	proportionality constant of power number in transition regime
$K_p(n)$	proportionality constant, Eq. 21 in Chapter 2
k_c	dimensionless circulation time constant
k_m	dimensionless mixing time constant
k_s	Metzner-Otto coefficient
k_s'	wall shear rate constant, Eq. 16 in Chapter 5
$k_{1,lam}$	proportionality parameter, Eq.27 in Chapter 5, mk_s^{n-1}
$k_{1,trans}$	proportionality parameter, Eq.27 in Chapter 5

l	length of impeller blade, m
m	power law parameter, Eq. 6, $Pa \cdot s^n$
m'	parameter, Eq. 18, $Pa \cdot s^{n'}$
N	impeller rotational speed, s^{-1}
Na	aeration number, Q/Nd^3
N_1	primary normal stress differences, Pa
n	power law index
n'	parameter, Eq. 18 in Chapter 4
n_b	number of impeller blade
P	power, W
P_g	Gassed power, W
P_o	Ungassed power, W
p	impeller pitch, m
Q	Gas flow rate in Chapter 4, or axial circulation flow rate, Eq.28 in Chapter 5, m^3/s
q	parameter in Eq. 7 in Chapter 5, $n(1-a)+a$
R	vessel radius, m
Re	Reynolds number, $d^2N\rho/\eta$
Re_g	generalized Reynolds number, $d^2N\rho/\eta_e$
Re_a	Aerated Reynolds number, calculated from aerated deformation rate $\dot{\gamma}_a$.
r	radial coordinate, m
s	parameter in Eq.26 in Chapter 5, $a(1-n)$
t_c	circulation time, s
t_m	mixing time, s
t_1	Cross model parameter, Eq. 16 in Chapter 3, s
V	volume of fluid in vessel, Eq. 28 in Chapter 5, m^3

v_g	Gas superficial velocity, Eq.5 in Chapter 4, m/s
v_r	radial velocity, $m \cdot s^{-1}$
v_z	axial velocity, $m \cdot s^{-1}$
v_z'	gradient of axial velocity, Eq. 19 in Chapter 5, $m \cdot s^{-2}$
v_ϑ	angular velocity, $m \cdot s^{-1}$
v_ϑ'	gradient of angular velocity, $m \cdot s^{-2}$
Wi	Weissenberg number, $\Psi_1 N/\eta_e$
w	impeller width, m

Greek letters

Γ	torque exerted on the vessel wall, N·m
$\dot{\gamma}$	shear rate s^{-1}
$\underline{\dot{\gamma}}$	rate of deformation tensor
$\dot{\gamma}_a$	aerated deformation rate, Eq.4 in Chapter 4, s^{-1}.
$\dot{\gamma}_b$	additional deformation rate due to bubble passing, Eq.5 in Chapter 4, s^{-1}.
$\dot{\gamma}_e$	effective deformation rate, s^{-1}
$\dot{\gamma}_{r\theta,wall}$	shear rate at the vessel wall, s^{-1}
η	non-Newtonian viscosity, Pa·s
η_a	aerated effective viscosity, Pa·s.
η_s	solvent viscosity, Pa·s
η_0	zero-shear viscosity, Pa·s
ε_g	gas hold-up, %.
ε_0	initial gas hold-up, %.
μ	Newtonian viscosity, Pa·s.
λ	characteristic elastic time, Eq. 19 in Chapter 3, s
ρ	liquid's density, kg/m^3

τ_{rz}	rz-component of shear stress, Pa
$\tau_{\theta z}$	θz-component of shear stress, Pa
$\tau_{r\theta}$	rθ-component of shear stress, Pa
τ_{11}	normal stress component, Pa
τ_{22}	normal stress component, Pa
Ψ_1	primary normal stress coefficient, $Pa \cdot s^2$
Ω	angular velocity of cylinder or impeller, s^{-1}
$II_{\dot{\gamma}}$	second invariant of rate of strain tensor, Eq. 20.

LIST OF APPENDICES

PAGE

Appendix I. Effective deformation rate in the laminar flow regime included bottom clearance effect 156

Appendix II. Computer program for solving Model 3 in Chapter 3 165

Appendix III. Influence of wall clearance on K_p and k_s 170

Appendix IV. Comparison of gassed power with the correlation of Michel and Miller 174

Appendix V. Reproduction of the effective deformation rate from the power data reported in the literature 177

Chapter 1

GENERAL INTRODUCTION

1-1. Introduction

Mechanical agitated mixing of non-Newtonian fluids, with and without aeration has been widely used in many industrial processes, which range from polymerization, biochemical fermentation, manufacture of detergents, fertilizers, and petrochemical refinery etc. Mixing degrees or levels will directly affect the commercial values of the final products which involve some sort of mixing processes. It is estimated that the expenditures involved in mixers in U.S. chemical process industries are around 150 M$/per year (exclusive of tanks and reactors, Smith, 1990). Due to the complex nature of mixing which is frequently accomplished with other unit operations, a poorly understanding of the mixing principles can lead to be very large error and considerable costs to the industry (Smith, 1990).

As pointed out by Carreau et al.(1976), the primary objects of the design of a mixing system are to attain a specific degree of homogeneity and to increase the rate of heat and/or mass transfer. Great attention should be drawn to select and design the mixing equipments to optimize the processes. Reviewing the literature over the past century (after Unwin, 1880), the fundamental theories about mixing are still in the developing stage, partially, due to the complicated flow geometry and hydrodynamics (Skelland, 1983). Empirical methods have been traditional ways to design and scale-up the industrial mixing reservoirs. Extrapolation of results obtained from a specific case into others can be totally misleading (Tatterson, 1991). However, no intensive effort has been devoted by the industry where mixing is routinely involved, to analyze these processes and to develop satisfying methods for further developments (Ulbrecht and Carreau, 1985).

Oldshue (1983) classified the fluid's mixing into five basic categories: liquid-solid, liquid-gas, immiscible liquids, miscible liquids and fluids motion. However, mixing can not be treated as simply as unit operations (Tatterson, 1991). Mixing is a complicated

process which is always accomplished with mass and heat transfer, chemical reactions and frequently occurs in other unit operations. Apparently, there no separated course, or even a separated chapter, in which mixing is being taught in undergraduate education in North American universities (Tatterson, 1991). Questions arise how those engineers to be, who have no knowledge of the mixing principles, can handle industrial mixing processes being encountered.

Non-Newtonian fluids, being involved in the industrial operations, make the processes much difficult, especially, coping with large difference in scale (Ulbrecht and Carreau, 1985, Smith, 1990). The non-Newtonian behaviour varies greatly with the applications. For instances, in polysacchrides fermentation, the batch varies initially from Newtonian, to shear-thinning and eventually viscoelastic fluid. Early works of Gray (1963) and Johnson (1967) compared the mixing performances of different agitator types and concluded that the close clearance agitators such as helical ribbon, helical screw or their combination, had better performances. These close clearance impellers rely on the axial pumping capacity rather than high radical gradient of momentum created by blade turbine style agitators (Ulbrecht and Carreau, 1985). The helical impellers can eliminate the stagnant zone within a reservoir, which is a constant problem in the mixing of the viscoelastic fluids.

Power requirement in a mixer is first an economic consideration. Over the years, the power consumption has also been an indicator of the changes of overall flow patterns (Ulbrecht and Carreau, 1985). Although, the power consumption has long been the topic of high interest, some conflicted results about the influence of non-Newtonian behaviour, especially elastic properties, can be found in the literature (Ulbrecht and Carreau, 1985). The partial reason is that the model fluids used in the literature frequently exhibit combined shear-thinning and elastic properties, and experiments cover different experimental regimes. Careful choice of the test fluids should be emphasized.

The difficulty, as one calculates the Reynolds number for non-Newtonian fluids in mixing systems, is to have the correct deformation rate. Metzner and Otto (1957) suggested a significant method to evaluate the effective deformation rate by comparing the non-Newtonian power data to the Newtonian one. Over the years, the effective deformation rate has being a sole topic of high interest, since the effective deformation rate has been recognized as one of the basic design parameters. Intensive study is still needed to ascertain the influence of rheological properties of non-Newtonian fluids and flow regime on the effective deformation rate.

Furthermore, mixing and circulation times have been investigated to assess the mixing performance since the power input not being enough information. Mixing time is taken as the time to achieve a certain degree of homogeneity while the circulation time is defined as the time for a fluid's element to complete a closed loop inside a mixer.

The flow regime in a mixing system has been classified into laminar, transition and turbulent flow regimes. Most processes involving viscoelastic fluids mixed by helical agitators fall in the categories of the laminar and transition regimes, because of the relative lower rotational speeds and high viscosity. Less attention has been drawn to the mixing in the transition flow regime. Intensive investigations have been carried out mainly at the laminar regime due to the difficulties and uncertainties faced at the transition regime. One of the practical topic is the effective shear rate in the transition regime. The effective shear rate is more complicated in the transition regime than in the laminar regime, as the previous experimental data have shown (from the early work of Metzner et al., 1961, to the more recent work of Forschner et al., 1991). However, very few efforts have been devoted to assess the key aspects and to develop appropriate models to correctively predict the effective shear rate. Except for the laminar regime, the influence of shear-thinning and elasticity on mixing time, and circulation time and flow patterns in the transition regime is far from being

clarified.

Hereby, another practical aspect of mixing is gas dispersion, particularly in rheologically complex fluids. Obviously, the mixing behaviour in a two-phase system is more complicated than that in a unique phase. Excellent reviews have been presented on the subject by Oldshue (1983), Nienow and Ulbrecht (1985), and Tatterson (1991). Gassed mixing in helical ribbon agitators has been barely studied by previous researchers, although sparged processes have been widely used. One is the fermentation of shear-sensitive cell cultures. Although some well studied results for other type agitators such as blade turbine, etc, are available, the extrapolation of these results to helical systems, without detailed investigation and verification, is quite doubtful. It is expected that the non-Newtonian behaviour of test fluids, gas sparger type, sparging rate and agitator geometry will mainly affect the gas dispersion and mass transfer performance.

The design and scale-up assisted by computer has been gradually accepted by the industry (Dickey and Hill, 1993). Smith (1990) has pointed out, from an industrial point of view, that the computational modelling , rather than empirical methods, may be likely much successful to describe the transition flow regime. This is of high interest.

Since the main body of this thesis consists of three articles which have been published or submitted, reported in Chapter 3 to Chapter 5, there is a detailed introduction for each article, to deal with the specific topics.

1-2. Objectives

The objectives of this work is to show the effect of non-Newtonian properties such as shear-thinning, elasticity and their combinations on power consumption, effective deformation rate, mixing and circulation times, flow behaviour with helical ribbon agitators of different geometries. The studies will be carried out in both laminar and

transition flow regimes, with and without aeration. The influence of non-Newtonian behaviour along with gas flow rate on the gassed power requirement, gas hold-up, gas dispersion performance, mixing and circulation times will be investigated.

Meanwhile, theoretical or semi-theoretical models will be developed to correctly predict the effective deformation rate at the laminar and transition flow regime, with and without aeration.

The test fluids will consist of Newtonian glycerol and corn syrup, and non-Newtonian shear-thinning inelastic xanthan and CMC aqueous solutions, gellan in corn syrup, viscoelastic xanthan and CMC solutions in the mixtures of glycerol and water, and elastic (with shear-independent viscosity) polyisobutylene in the mixture of polybutene and kerosene, polyacrylamide in corn syrup.

This thesis consists of a general literature review (Chapter 2), power consumption (Chapter 3), aerated mixing (Chapter 4) and mixing in the transition flow regime (Chapter 5).

In Chapter 2, the literature review includes the general rheological concepts of non-Newtonian fluids, effective shear rate, power correlation, mixing and circulation times. Although there is a specific introduction and literature review in each article, those reviews are relative brief due to the space limitations of the articles. It is desirable to give the detailed aspects of each domain concerning this thesis. For instances, some power data in the literature used to calculate the effective deformation rate, or some power correlations being employed for the calculation, are given in this chapter, but are not included in the articles.

In Chapter 3, the influence of shear-thinning, elasticity and their combination on power consumption with helical ribbon agitators is being investigated. Two semi-theoretical models, based on the knowledge of torque or based on an analysis of the equivalent Couette flow, are proposed to predict the effective shear rate in the laminar flow regime. The development of the models including bottom effects is given

in Appendix (A1), and the experimental data of the influence of wall clearance on power consumption is also shown in Appendix (A2).

The aerated mixing of viscoelastic fluids with helical ribbon impellers is reported in Chapter 4. The effects of non-Newtonian properties and gas sparging conditions on gassed power and gas-hold-up is investigated. Two empirical correlations from the dimensional analysis are suggested to predict the gassed power in both the laminar and transition flow regimes. A concept of aerated effective shear rate is proposed to correct the effective shear deformation under aerated conditions. The comparison of the gassed power data with the correlation of Michel and Miller (1962) is shown in Appendix (A4).

In Chapter 5, three models based on one or two dimensional analysis of the equivalent Couette flow, are proposed to predict the effective shear rate in the transition flow regime. The predictions are compared with the experimental data obtained using helical ribbon agitators, and with literature data for anchor, blade turbine and flat disc agitators. The study of the influence of non-Newtonian behaviour on mixing and circulation times in both the laminar and transition flow regimes is carried out. A computer program to solve a proposed numerical model is given in Appendix (A3).

1-3. References

Carreau, P.J., W.I. Patterson and C.Y. Yap., "Mixing of Viscoelastic Fluids with Helical Ribbon Agitators, I - Mixing Time and Flow Patterns", *Can. J. Chem. Eng.*, **54**,135-142 (1976).

Dickey, D.S. and R.S. Hill, "Use the Right Specialty-Polymer Pilot Plant", *Chem. Eng. Proc.*, **89**, 22-29(1993)

Forschner, P., R. Krebs and T. Schneider, "Scale-up Procedures for Power Consumption of Mixing in Non-Newtonian Fluids", *7th European Cong. on Mixing,*

Brugge, Belgium, 161-165(1991).

Gray, J.B., "Batch Mixing of Viscous Liquids", *Chem. Eng. Prog.,* **59**, 55-59(1963).

Johnson, R.T., "Batch Mixing of Viscous Liquids', *Ind. Eng. Chem. Proc. Des. Dev.*, **6**, 340-345(1967).

Metzner, A.B. and R.E. Otto, "Agitation of Non-Newtonian Fluids", *AIChE* J., **3**, 3-10(1957).

Metzner, A.B. and R.H. Feehs, H. Lopes Ramos and J.D. Tuthill, "Agitation of Viscous Newtonian and Non-Newtonian Fluids", *AIChE J.*, **7**, 3-9(1961).

Michel, B.J. and S.A. Miller, " Power Requirement of Gas-Liquid Agitated Systems", *AIChE J.*, **8**, 262-266(1962).

Nienow, A.W. and J.J. Ulbrecht, Gas-Liquid Mixing and Mass Transfer in High Viscosity Liquids, in *Mixing of Liquids by Mechanical Agitation* (Eds: Ulbrecht J.J. and G.K. Patterson), Goldon and Breach, New York (1985).

Oldshue, J.Y., Fluids Mixing Technology, McGraw-Hill, New York(1983).

Skelland, A.H.P, Mixing and Agitation of Non-Newtonian Fluids, in *Handbook of Fluids in Motion*, (Eds: N.P. Cheremisinoff and R. Gupta), Ann Arbor Science Publishers, Ann Arbor, MI(1983).

Smith J.M., "Industrial Needs for Mixing Research", *Trans, IChemE.*, **68**, 3-6(1990).

Tatterson, G.B., Fluids Mixing and Gas Dispersion in Agitated Tanks, McGraw-Hill, New York(1991).

Ulbrecht J.J. and P.J. Carreau, Mixing of Viscous Non-Newtonian Liquids, in *Mixing of Liquids by Mechanical Agitation* (Eds: Ulbrecht J.J. and G.K. Patterson), Goldon and Breach, New York (1985).

Unwin, W.C., *Proc. Roy. Soc.*, London, **A31**, 54(1880).

Chapter 2

CONCEPTS AND LITERATURE REVIEW

2-1. Rheological Properties

The media encountered in mixing processes are frequently non-Newtonian fluids ranging from inelastic shear thinning, viscoelastic and elastic fluids with the shear independent viscosity, even shear-thickening and Bingham type liquids with yield stress etc. In industrial processes such as the polysaccharides fermentation, the rheological properties vary as fermentation processes, from initially Newtonian behaviour to fairly and highly shear-thinning, and eventually viscoelastic behaviour. So model fluids are usually chosen for the mixing investigations to assess the influence of each aspect of rheological complexity of non-Newtonian fluids.

As seen in literature, the non-Newtonian viscosity and primary normal stress difference in simple shear flow have been chosen to describe the fluid's rheological characteristics in a mixing system and used in the expressions correlating the mixing variables. Questions arise about this traditional choice since the flow behaviour in a mixing system is far from being simple shear flow. Extensional flow could have a important role in a mixing process, especially, when mixing proceeds in the transition flow regime. Rheological information, other than in the simple shear deformation, could be quite useful to describe the mixing behaviour and correlate the mixing variables. However, difficulties arise for applying these rheological properties to the mixing systems at present stage, due to lack of the complete flow pictures inside reservoirs. For convenience, only viscosity and primary normal stress difference data measured under simple shear flow are being used in this work.

As indicated by Ulbrecht and Carreau (1985), the non-Newtonian viscosity is a local material property and the effective viscosity (to be discussed in following section) is a characteristic value for the entire mixing system. A number of non-Newtonian fluids encountered in the mixing processes show a decrease of the viscosity with increasing shear rate, which is the so called *shear-thinning* property. Various

rheological models, which are empirical expressions of the viscosity curves, have been proposed. Of those, the "*power law*" model is frequently used, e.g.

$$\eta = m\,\dot{\gamma}^{n-1} \tag{1}$$

where n is the so called *flow index* (or *flow behaviour index* by some authors), m is material consistency. For $n<1$, $n>1$ and $n=1$ the properties are shear-thinning, shear-thickening, and Newtonian respectively. The values of n of the fluids dealt with in this work are smaller than or equal to one.

At relatively lower shear rate, the low-shear-rate viscosity plateau may be observed for many fluids. For these fluids, the Carreau's model (Carreau, 1972) was proposed to represent the viscosity, e.g.

$$\frac{\eta}{\eta_0} = \left[1 + (t_1\dot{\gamma})^2\right]^{\frac{n-1}{2}} \tag{2}$$

Where η_0 is the zero-shear viscosity, t_1 is the characteristic time, and n is flow index. Carreau's model may be rearranged to be in the form of the Ellis model (see Ulbrecht and Carreau, 1985). Carreau's model can give quite satisfied predictions of viscosity for the fluids with relatively rapid transition in the viscosity curve from the power law regime to the low shear rate viscosity plateau. The Cross model may be used in the circumstance where the transition regime is less abrupt. The Cross model is expressed as

$$\eta = \frac{\eta_0}{1 + (t_1\dot{\gamma})^{n-1}} \tag{3}$$

In contrast to the zero shear rate viscosity, a viscosity of plateau may occur at high shear rates for some fluids. Thus, the following expression can be used

$$\eta = m\,\dot{\gamma}^{n-1} + \eta_s \tag{4}$$

Where η_s is the solvent viscosity.

The elastic properties of fluids are caused by the stretching of long molecular chains of high molecular weight polymer solutions experienced a shear deformation (Bird et al. 1987), where the molecular chains tend to retain their original spacial positions. Under simple shear deformation, the primary and secondary normal stress differences are frequently used to describe the fluid's elastic behaviour,

$$N_1 = \tau_{11} - \tau_{22} = \frac{\psi_1}{\dot{\gamma}^2} \tag{5}$$

$$N_2 = \tau_{22} - \tau_{33} = \frac{\psi_2}{\dot{\gamma}^2} \tag{6}$$

where ψ_1 and ψ_2 are the primary and secondary normal stress difference coefficients, respectively. Practically, the secondary normal stress difference is difficult to measure (Bird et al.1987 and Carreau, 1991). Fortunately, in most cases, the secondary normal stress is quite small compared with primary normal stress difference (about 10% of N_1) and can be neglected.

The primary normal stress difference is usually expressed as a power term of shear rate, e.g.

$$N_1 = m'\,\dot{\gamma}^{n'} \quad or \quad \psi_1 = m'\,\dot{\gamma}^{n'-2} \tag{7}$$

Where *m'* is a material consistency and *n'* is a power index and is larger than 0.

The fluids are classified as viscoelastic fluids when they exhibit elasticity. In general, they show both a non-Newtonian viscosity (shear dependent viscosity) and elasticity. Boger and Binnington (1977) dissolved a trace quantity of polyacrylamide (PAA) into a corn syrup solution and obtained an elastic but shear independent

viscosity solutions, so called Boger fluids. The primary normal stress difference, N_1, for Boger fluids is proportional to the shear rate at the power of 2, e.g. $N_1 \propto \dot{\gamma}^2$. In other words, ψ_1 is independent of shear rate and we classify these fluids as *second order* fluids.

Another characteristic elastic time λ, which is defined from the modified Maxwell model by Metzner (1964), has also been used to describe fluid's elasticity,

$$\lambda = \frac{N_1}{2\tau_{21}\dot{\gamma}_{21}} \tag{8}$$

For a second order fluid, λ is independent of shear rate. For most viscoelastic fluids, it decreases with increasing shear rate.

The Weissenberg number is the most frequently used elastic parameter for mixing systems. One form of Weissenberg number is expressed as

$$Wi = \frac{\psi_1 N_1}{\eta_e} \tag{9}$$

Attention should be drawn when one compares data from literature since there are several different forms for the Weissenberg number used by authors. In some occasions, an elastic number, as a ratio of the Weissenberg number over the Reynolds number, has also been used, given by:

$$El = \frac{Wi}{Re} \tag{10}$$

All rheological aspects discussed above are for homogeneous fluids without aeration. Dealing with aerated mixing systems, the frequently used rheological parameters, to our knowledge, are all obtained from ungassed conditions. This classical approach is still widely accepted, which is quite questionable. Obviously, the reason why the classical approach remains unchanged is mainly due to technical difficulties dealing with gassed rheological behaviour. Hopefully, experimental work will be carried out

to explore this highly interesting area.

2-2. Effective Deformation Rate

The need for an effective viscosity in mixing systems emerges as we calculate the generalized Reynolds number, Re_g. In this work, we prefer to use the word "*effective deformation rate*" rather than effective shear rate since three dimensional flow in a mixing reservoir is not only a simple shear flow but also contains a non negligible extensional flow. The effective deformation rate is reviewed in a separate section from the power consumption, though it is related to the power requirement. Over the years, the effective deformation rate has been emerging as a sole subject of high interest. Before the detailed review is being dealt with, the most often seen geometrical parameters for the helical ribbon agitators should be listed hereby for the reader's convenience (a sketch of helical ribbon agitator system is shown in Fig.1). They are

c - clearance between the impeller blade's tip to the vessel inner wall,
$=(D-d)/2$
d - impeller diameter
D - vessel diameter
H - liquid's height
h_c - bottom clearance
l - length of impeller blade
n_b - number of blade
p - impeller pitch
w - impeller width

A significant method was proposed by Metzner and Otto (1957) and has been widely used in mixing processing over the several decades. The concept of Metzner-Otto method is that the effective viscosity, η_e, can be estimated from the effective deformation rate, $\dot{\gamma}_e$, which was found to be proportional to the impeller rotational

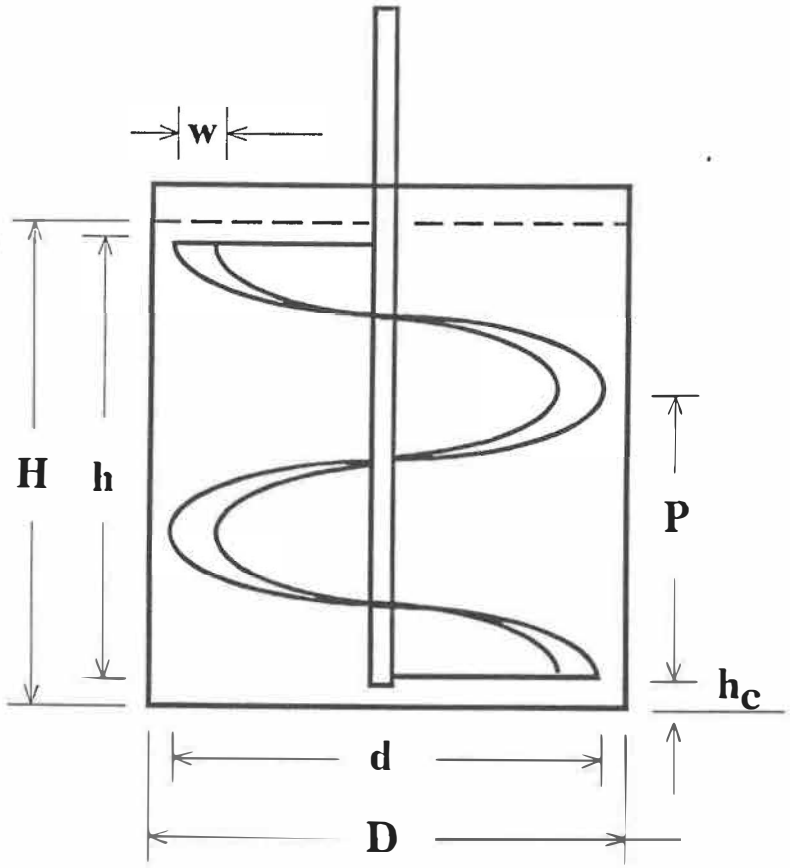

Figure 1 Helical Ribbon Agitator System

speed, *N*, in the laminar flow regime

$$\dot{\gamma}_e = k_s N \tag{11}$$

where k_s is the effective shear rate constant.

The following section demonstrates the detailed procedure to evaluate the effective shear rate, $\dot{\gamma}_e$ (an illustration of this procedure is shown in Fig.1).

1) The power requirement in the Newtonian fluids is measured in a mixer of given geometry (namely, a given vessel, impeller, position of impeller and fluid's height inside the vessel). The results are plotted as the power number, *Np,* versus the Reynolds number, *Re* (see Fig. 1a), where the power number and Reynolds number

are defined as

$$Np = \frac{P}{d^5 N^3 \rho} \tag{12}$$

$$Re = \frac{d^2 N \rho}{\mu} \tag{13}$$

At laminar flow regime, the power number *Np*, is inversely proportional to the Reynolds number, *Re*, e.g.

$$Np = K_p \, Re^{-1} \tag{14}$$

2) Then the power consumption in a non-Newtonian fluid is measured in a mixer of the same geometry used for Newtonian fluids. The non-Newtonian power number, Np_{nN}, can be directly calculated from the experimental data via Eq.12. Thus, the corresponding generalized Reynolds number, Re_g, can be obtained using the Newtonian power curve measured before (see Fig.1b). It means that, according to Metzner-Otto's concept, the same effective viscosity for different fluids should result in the same power input at a given mixer at the same rotational speed.

3) Consequently, the effective viscosity η_e can be obtained from the generalized Reynolds number, Re_g, e.g., $\eta_e = d^2 N \rho / Re_g$.

4) Finally, the effective shear rate $\dot{\gamma}_e$, can be obtained for the non-Newtonian fluid, using the curve of viscosity vs shear rate for non-Newtonian fluids (see Fig.1c), or using the rheometers or using rheology models, for instance, for the power law fluids:

$$\dot{\gamma}_e = \left(\eta_e / m\right)^{\frac{1}{(n-1)}} \tag{15}$$

5). The effective shear rate obtained from this manner can be plotted against the rotational speed. In the laminar flow regime, the relationship between $\dot{\gamma}_e$ and *N* is a linear function passing through the origin, that is the well known Metzner-Otto's

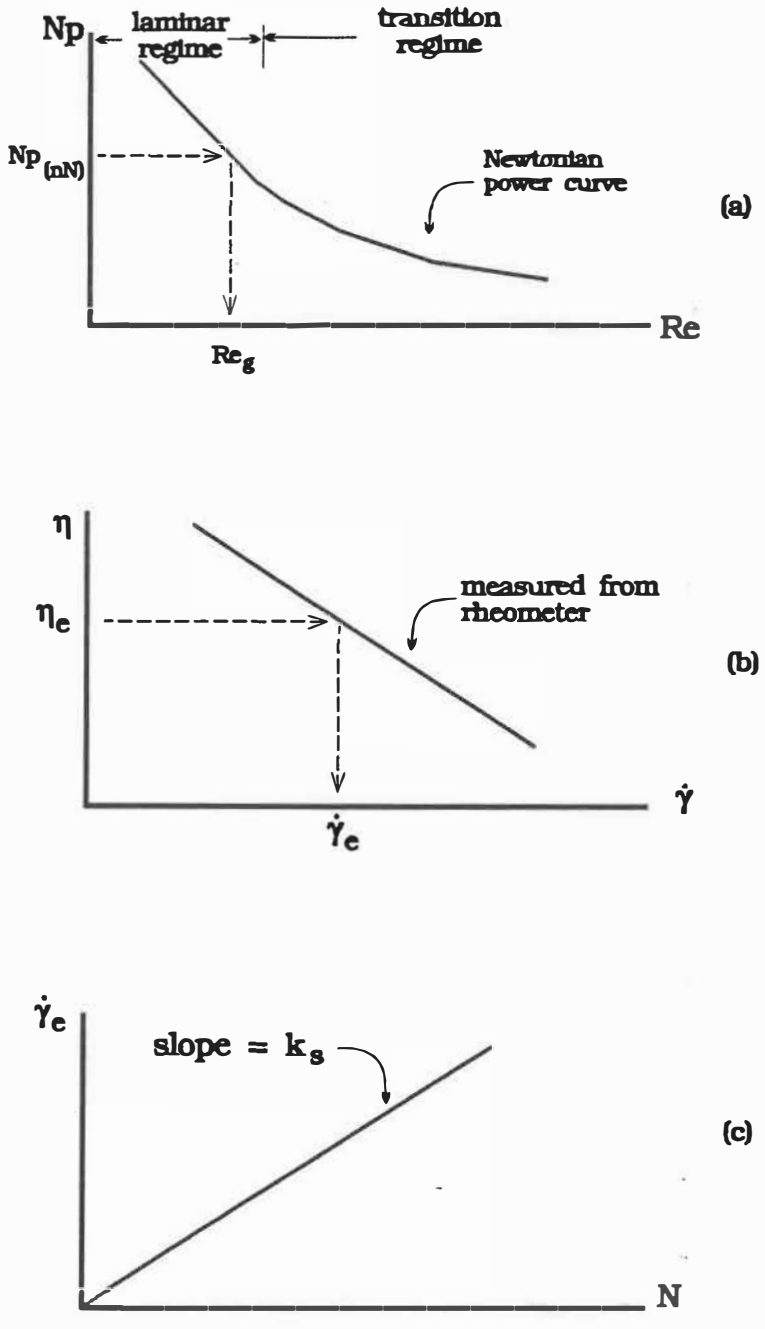

Figure 2. Illustration of the procedure to calculate the effective shear rate from power data using Metzner-Otto's method.

equation (Eq.1). The slope of this line is the effective shear rate constant, k_s.

Hall and Golfrey (1970) and Nagata et al.(1971) found that the values of k_s were almost constant for fluids agitated by helical ribbon impellers, with values of 27 and 30 by former and later authors, respectively.

2-2-1. Geometry influence on k_s

The dependence of k_s on the geometry of mixers has been found as follows. The k_s values have been found to be mainly dependent on the impeller pitch, width and clearance between the impeller tip to the vessel wall and often, expressed in terms of the dimensionless ratios (over impeller or vessel diameter).

Takahash et al.(1984) proposed the following correlation for k_s

$$k_s = 11.4 \left(\frac{C}{D}\right)^{-0.441} \left(\frac{p}{D}\right)^{-0.361} \left(\frac{w}{D}\right)^{0.164} \quad (16)$$

This correlation shows the general dependence, that is the k_s value decreases with increasing the clearance *C/D* and pitch *p/D*, increases with increasing the width *w/D* (which is relatively a weak dependence comparing with other two parameters, *C/D* and *p/D)*. Shamlou and Edwards (1985) focused on the clearance effects by using six different clearance values and found

$$k_s = 34 - 114 \left(\frac{C}{d}\right) \quad (17)$$

Yap et al.(1979) proposed a correlation using the length of the impeller blades as one of the key geometrical parameter for helical ribbon impellers, e.g.

$$k_s = 4^{1/n} \left(\frac{D}{d}\right)^2 \left(\frac{l}{D}\right) \quad (18)$$

the l is a length of the impeller.

Merquiol and Choplin (1988) obtained relatively higher values of k_s for helical screw impellers and found k_s to be only dependent on the ratio of the impeller pitch over the vessel diameter. Their expression is

$$k_s = 60 \left(\frac{p}{D}\right)^{0.65} \tag{19}$$

Hereby, another approach to evaluate k_s was proposed by Rieger and Novak (1973) which is also based on the Metzner-Otto definition. k_s is obtained via the following expression

$$B\ k_s = Np\ Re \tag{20}$$

The k_s values for a helical ribbon impeller in a draft tube and a off centre helical screw impeller were given by Rieger and Novak. However, no geometrical influence on k_s was taken into account.

2-2-2. Flow index influence on k_s

Beyond the geometrical effects, k_s is also found to be dependent on the flow index, n. With the close examination of Yap et al.(1979), the k_s value was found to increase with increasing the flow index value (e.g. less shear-thinning), as seen in Eq.18. The range of n values of the test fluids in their work is relatively narrow but it shows a definite trend. Brito et al.(1992) reported a similar trend, for one helical ribbon impeller in a relatively extended flow index range. They examined closely the Rieger and Novak's approach and indicated that k_s is to be independent to the flow index if the Metzner-Otto's method is applied. They verified Rieger and Novak's approach and proposed an expression to include the flow index effects, that is:

$$k_s = \left[\frac{K_p(n)}{K_p}\right]^{1/(n-1)} \tag{21}$$

2-2-3. Flow regime influence on k_s

It was first noticed by Metzner et al.(1961) that the proportionality between the effective shear rate and the rotational speed is no longer valid beyond the laminar flow regime. They found k_s to be almost proportional to the square of the rotational speed in the transition flow regime for both shear-thickening and shear-thinning fluids agitated by blade turbine impellers. A similar trend was found for shear-thinning fluids by Pollard and Kantyka (1969) and for shear-thinning suspensions by Bourne et al(1980, 1981), all with anchor agitators. Exponents equal to 3.75 and 2, with which the effective deformation rate varies with rotational speed, were found by Bourne et al. and Pollard and Kentyka respectively. Other available experimental evidences that the non-Newtonian power number is lower than the corresponding Newtonian one, have been reported by Nagata et al.(1971), Höcker et al.(1981), Forschner et al.(1991) for shear-thinning fluids, and Metzner et al.(1961), Calderbank and Moo Young (1959) for shear-thickening liquids.

However, few efforts have been devoted to elucidate this subject. Carreau (Ulbrecht and Carreau, 1985) proposed a semi-theoretical correlation based on an analysis of the equivalent Couette flow, using the Newtonian power information in both the laminar and transition flow regimes (see Eq.26 in Chapter 5). The predictions were compared with the data of Bourne et al.(1981) and the agreement is quite good in case of small scale of the mixer. The elaboration and validation of this model will be discussed in Chapter 5.

Another attempt has been made more recently by Forschner et al.(1991), as they dealt with the industrial scale-up in the transition flow regime. They found an overestimation of the effective viscosity using the methods of Metzner-Otto (1957) and of Rieger and Novak (1973), compared to their experimental data which is shown in Figure 2. They proposed an empirical correlation extending Rieger-Novak's method into the transition flow regime (see Eq.27 in Chapter 5). Unfortunately, they

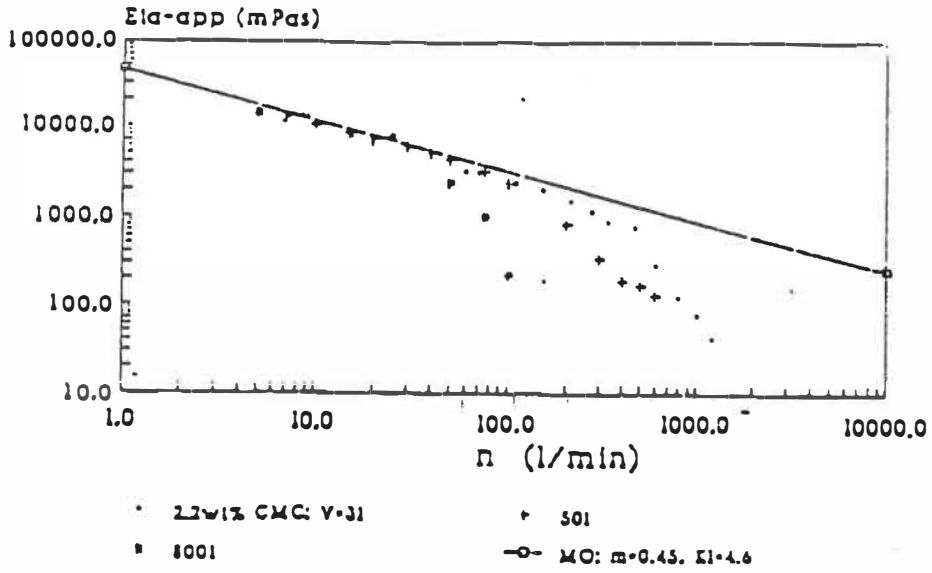

Figure 3. Experimental data of the effective viscosity in the transition flow regime for an aqueous CMC solution (*from Forschner et al., 1991)*

did not specify the value for a key parameter ($k_{2,\,trans.}$ in Eq.27 of Chapter 5), and how to evaluate this parameter due to their commercial concerns. Hopefully, more elaboration will be coming out by them soon. As seen from the literature, a full investigation of the effective deformation rate for the transition regime is still needed.

2-2-3. Aeration influence on k_s

The validity of the k_s values obtained from unaerated conditions for gassed reservoirs is quite questionable, since there should be additional deformation caused by bubbles' presence and bubbles stretching the liquid. No attempt has been ever made to explore this unknown field due to the complexity of the gassed mixing systems.

Available information about the effective deformation rate for gas-liquid reactors, namely bubble columns, may be helpful to understand how bubbles cause

deformation. It can be argued that shear deformation in the bubble columns is comparable to shear deformation caused by bubbles in aerated agitated vessels, although, the total deformation in an aerated agitated vessel may not be a simple sum of the deformation in the bubble column and in the ungassed agitated mixer. Interaction between these two modes should be expected. Nakahashi et al.(1967) applied the Metzner-Otto's definition of the effective viscosity for the heat transfer processes in bubble columns and obtained the effective shear rate being proportional to the gas superficial velocity, that is:

$$\dot{\gamma} = 5000\ v_g \qquad (22)$$

The validity of the Metzner-Otto's concept for the heat transfer process is questionable. Other information such as gas hold-up, superficial area, etc, should be taken into account (Chisti and Moo-Young, 1988, Kawase and Moo-Young, 1990). Nevertheless, Nakahashi et al.'s method has been frequently used for bubble column systems due to its simplicity. Henzler (1970) found that the proportional constant in Eq.22 to be 1500, instead of 5000. The following works by Schumpe and Deckwer (1987), Zaidi et al.(1987)confirm the constant value's range of Henzler's work. Merchuk and Ben-Zvi-Yona (1992) proposed a semi-empirical equation to give the acceptable predictions but some extra information such as pressure drop, superficial area, etc, is required.

2-3. Power Consumption

Power consumption in agitated reservoirs has long been a subject of considerable research interest. It goes back to the year of 1880 when Unwin handed over a first scientific report about the power in a mixing vessel in front of the British Royal Society of Science (Unwin, 1880). As pointed by Ulbrecht and Carreau (1985), the power requirement is not only an important design and economic concerning

parameter, but also reflects changes in the flow patterns within the mixing reservoir.

The power consumption can be evaluated through several approaches (Tatterson, 1991). One of them is to use the energy dispersion equation or the power input is the energy transformed through the impeller in to the fluid per time. The power consumption is given

$$P = \int \Phi \, dV \tag{23}$$

Where ϕ is a specific energy dissipation rate and V is volume. It is difficult to evaluate this integration using experimental data at the present stage and may be solved partially by the a dimensional computation (Tatterson, 1991).

2-3-1 Dimensional analysis

In the literature, the power consumption data are often reported in terms of a dimensionless number, the so called power number, *Np,* which is obtained from a dimensional analysis. The dimensional analysis method is always an useful way to examine how variables could affect behaviour of a complicated systems like mixing. Skelland (1983) reviewed the application of this method for mixing systems. Hereby, it is still worthwhile to summarize the approach of dimensional analysis. The reader is referred to the book of MaCabe et al. (1985) for the basic principles of the dimensional analysis.

The power consumption can be expressed as functions of typical mixer geometrical parameters and fluid material properties. It should be noticed that, in the dimensional analysis illustrated here, we are only concerned with the effects of the flow behaviour and fluids properties on the power input at a given mixer. Geometrical effects are not taken into account. We prefer the following relation for the power

$$P = f(\rho, N, Q_g, d, \eta, N_1) \tag{24}$$

Hereby, the general cases include an elastic effect (N_1) and aeration effects (Q_g). The basic units involved in the above equation are the mass [kg], time [s], and length [m]. It should be mentioned that the acceleration of gravity, g, is neglected from the above expression because the energy dissipation caused by the inertial force is much smaller than that caused by the viscous force. A simple expression of the function in the right hand of Eq.25 is in power terms, e.g.

$$P = a_1 \rho^{a_2} N^{a_3} Q^{a_4} d^{a_5} \eta^{a_6} N_1^{a_7} \tag{25}$$

Applying the dimensions into the above equation, we have

$$\left[\frac{kg\ m^2}{s^3}\right] = \left[\frac{kg}{m^3}\right]^{a_2} \left[\frac{1}{s}\right]^{a_3} \left[\frac{m^3}{s}\right]^{a_4} [m]^{a_5} \left[\frac{kg}{m^3}\right]^{a_6} \left[\frac{kg}{ms^2}\right]^{a_7} \tag{26}$$

The relations among the exponent indexes $a_2 \sim a_7$ can be obtained from Eq.26,

$$1 = a_2 + a_6 + a_7 \tag{27}$$

$$2 = -3a_2 + 3a_4 + a_5 - a_6 - a_7 \tag{28}$$

$$-3 = -a_3 - a_4 - a_6 - 2a_7 \tag{29}$$

These are three equations containing 6 unknowns, so three unknowns have to be fixed in order to solve these equations. We choose a_4, a_6 and a_7 as pre-fixed values so that a_2, a_3 and a_5 can be expressed in terms of a_4, a_6 and a_7, e.g.

$$a_2 = 1 - a_6 - a_7 \tag{30}$$

$$a_3 = 3 - a_4 - a_6 - 2a_7 \tag{31}$$

$$a_5 = 5 - 3a_4 - 2a_6 - 2a_7 \tag{32}$$

Eq.25 can be rearranged by substitution of Eq.30 ~ Eq.32,

$$\frac{P}{d^5N^3\rho} = a_1 \left(\frac{d^2N\rho}{\eta}\right)^{-a_6} \left(\frac{Q_g}{Nd^3}\right)^{a_4} \left(\frac{N_1}{d^2N^2\rho}\right)^{a_7} \tag{33}$$

where the first dimensionless group in right hand of Eq.33, $d^2N\rho/\eta$, is the so called Reynolds number, *Re*; second term Q_g/Nd^3, is called the aeration number, *Na*; while the third one, $N_1/d^2N^2\rho$, is the elastic number, *El*, as mentioned before. In circumstances where elastic effects can be neglected, and without aeration, Eq.33 reduces to

$$Np = a_1 \, Re^{-a_6} \tag{34}$$

a_1 is dependent of the mixer geometry. At laminar flow regime, a_6 is equal to 1 and Eq.14 is one of the forms derived from Eq.34.

2-3-2 Power correlations

The power number constant, K_p (=*NpRe*), has been found to be dependent on the mixer geometry. Gray (1963) found K_p = 300 for a helical ribbon impeller. In a subsequent work, Hall and Godfrey (1970) investigated geometrical effects for helical ribbon agitators and proposed a correlation:

$$K_p = 66 \, n_R \left(\frac{p}{d}\right)^{-0.73} \left(\frac{H}{d}\right) \left(\frac{w}{d}\right)^{0.5} \left(\frac{C}{d}\right)^{-0.6} \tag{35}$$

This correlation illustrates the general dependence of K_p on the mixer geometry: the K_p value increases with increasing impeller width and liquid height, but decreases with increasing the impeller pitch and clearance. It also increases with increasing the blade number. Hall and Godfrey (1970) found no significant scale effect. They compared

with the literature data from seven authors and their work, and found differences ranging from -10.0 to 26.7%.

Kappel (1979) proposed the following correlation after a study of twelve different geometries of helical ribbon impellers:

$$K_p = 60\ (n_R)^{0.8} \left(\frac{p}{d}\right)^{-0.5} \left(\frac{C}{d}\right)^{-0.3} \tag{36}$$

Kappel reviewed the available data in the literature and noticed that the power data reported in the literature are in good agreement with each other in the tanks with larger clearance and are in big differences in the mixers with small clearance.

Following Bourne and Butler (1969), Chavan and Ulbrecht (1973, 1974) developed a semi-empirical correlation based on the equivalent Couette flow for power-law inelastic fluids agitated by helical ribbon impellers:

$$Np = 2.5A\pi\left(\frac{d_e}{d}\right)\left(\frac{D}{d_e}\right)^2 \left(\frac{4\pi}{n\left[(D/d_e)^{2/n} - 1\right]}\right)^n \left(\frac{d^2N^{2-n}\rho}{m}\right)^{-1} \tag{37}$$

where d_e is an equivalent diameter calculated using impeller geometry via following equation:

$$\frac{d_e}{D} = \frac{D_t}{D} - 2\frac{W}{d} \Big/ \ln\left(\frac{(D/d) - 1 + 2(W/d)}{(D/d) - 1}\right) \tag{38}$$

and A is given by

$$A = \frac{(h/d)(p/d)}{3\pi}\left[\pi\frac{\sqrt{(p/d)^2+\pi^2}}{(p/d)^2} + \ln\left(\frac{\pi}{(p/d)} + \frac{\sqrt{(p/d)^2+\pi^2}}{(p/d)}\right)\right](1-[1-2(w/d)]^2) \tag{39}$$

The power should be doubled if the impeller has two ribbons.

Nagata (1975) proposed a correlation for double helical ribbon agitators, e.g.:

$$N_p = 74.3 \left(\frac{2C}{d}\right)^{-0.5} \left(\frac{s}{d}\right)^{-0.5} Re_g^{-1} \quad (40)$$

Yap et al.(1979) based on the analysis of the drag force exerted on the impeller's blades and developed a model for Newtonian fluids, and then extended their result to the non-Newtonian fluids:

$$N_p = 24\, n_b \left[Re_g^{0.93} \left(\frac{D}{d}\right)^{0.91} \left(\frac{d}{l}\right)^{1.23} \right]^{-1} \quad (41)$$

where the blade length, l, was first introduced as one of the characteristics of the impeller geometry. Yap et al.(1979) and Shamlou and Edwards (1985) compared these semi-theoretical or empirical correlations for the power number and found the correlation of Yap et al.(1979) to be most successful. They also found that the Chavan and Ulbrecht's correlation could give quite good predictions.

Shamlou and Edwards (1985) studied mixers of different scales and presented the following empirical power correlation

$$K_p = 150\, n_b^{0.5} \left(\frac{l}{d}\right) \left(\frac{p}{d}\right)^{-0.5} \left(\frac{C}{w}\right)^{-0.33} \quad (42)$$

They also used the impeller blades' length as one of the mixer geometrical characteristics. The differences between the predictions and the data reported in the literature range from -57 % to +40 %. They intensively examined the influence of the impeller wall clearance on the power consumptions in terms of K_p using five different ratios of D/d. They also reviewed the predictions of power correlations in the literature and found that the K_p value increases much sharply as the wall clearance approaching small values.

2-3-3. Influence of non-Newtonian properties and flow regime on power input

The reader may is probably aware that the power prediction for the non-Newtonian inelastic fluids is obtained using the correlations for Newtonian liquids, replacing the Reynolds number by the generalized Reynolds number. The generalized Reynolds number is evaluated from the effective viscosity which is discussed in the previous section.

Elastic effects on the power input are usually neglected in the laminar flow regime. It is expected that the viscous energy dispersion overshadows the energy to overcome the elastic force resistance in the laminar regime due to the relative lower rotational speeds. However, more recently Prud'homme and Shaqfeh (1984) and Brito et al.(1991) employed Boger fluids and second order fluids with high elastic levels and found quite a pronounced effect of elasticity on the power requirement. A marked increase of the power requirement for elastic fluids was found in the laminar regime in terms of a dimensionless torque. The power number for elastic fluids may expressed as functions of the Reynolds number and Weissenberg number for a given mixer (Kale et al., 1973, 1974), that is

$$Np = f\left(Re_g\ ,\ Wi\right) \tag{43}$$

More work is needed to elucidate the effects of the non-Newtonian properties (especially elasticity) on power consumption.

In the transition flow regime, the power number is no longer inversely proportional to the Reynolds number. The power number decreases more moderately than in the laminar regime. For non-Newtonian inelastic fluids, Metzner et al.(1961) were the first to observe the lower power number compared with the corresponding Newtonian one for blade turbine agitators. However, Nagata et al.(1971) found no differences of between non-Newtonian and Newtonian power numbers for moderately shear-thinning CMC and PAA aqueous solutions agitated by a helical ribbon impeller

up to the turbulent flow regime. Brito et al. (1992) found a lower power number for highly shear-thinning xanthan aqueous solution mixed with a helical ribbon agitator, compared with the corresponding Newtonian one. Obviously, the non-Newtonian behaviour (both shear-thinning and elasticity) could considerably affect the power consumption.

Before we close this section, another aspect which should be stressed is the power requirement for gassed systems. Gassed power consumption has been barely investigated in the case of the helical ribbon agitator. The only available data in the literature are for Newtonian fluids or for moderately shear-thinning inelastic xanthan aqueous solutions (Termote, 1991). Available information obtained from other types of impellers such as blade turbine can be helpful to understand how the energy is dispersed under gassed conditions. The correlation for the gassed power proposed by Michel and Miller (1962) has been found to be quite successful, that is

$$P_g = C\left(\frac{P_0^2 N D^3}{Q^{0.56}}\right)^{0.45} \qquad (44)$$

This correlation was originally proposed for Newtonian fluids. It has been extended to the non-Newtonian systems in subsequent work by others. However, no geometrical effects are taken into account. An attempt has been made to apply the correlation to helical ribbon mixers for both Newtonian and non-Newtonian fluids. The results are not too satisfactory (Termote, 1991). More sophisticated correlations for gassed power requirement should be developed, especially for the helical ribbon agitators.

2-4. Mixing and Circulation Times

Power consumption is one of the important mixing characteristics which reflects the mixing behaviour. However, it is not enough to describe the mixing performance

in a reservoir. Therefore, mixing and circulation times have been used as additional criteria. Mixing time is defined as the time necessary to attain a given degree of homogeneity in the agitated fluids. A number of methods such as conductivity, thermal, decoloration methods, etc, have been used to measure the mixing time. Voncken (1965), Hoodendoorn and den Hartog (1967) and Ford et al. (1972) have presented excellent reviews of the merits and de-merits of the most used methods reported in the literature. By using a thermal method, the test fluids can be repeatedly used to run a number of experiments, but one has to verify that there is no effect on the fluids' rheological properties in the range of temperature at which the experiments are being carried out. The electrical conductivity method is similar to the thermal method, but the number of experimental runs is limited to the point at which the fluid is conductively saturated. Obviously, there should be no influence of salts on the rheological properties of the test fluids within the experimental range. Compared to conductivity and thermal methods, one of the advantages of the decoloration method is to allow one to observe the flow patterns and mixing behaviour when the measurement of mixing time is being conducted. As pointed by Ford et al. (1972), it is difficult to determine the final stage and this method is somewhat subjective. A radioactive tracer technique has been also used in the measurements of the mixing and corculation times and used in the observation of flow patterns (Ford et al., 1972). One of the advantages of this method is to measure the mixing time and circulation time at the same time. The main disadvantage, as pointed by Ford et al.(1972), is its implementation.

It should be stressed that the mixing time is very useful criterion only when it is used to compare with other data obtained using the same technique and the same scheme. Otherwise, comparing mixing times bases on different techniques can be totally misleading. The early work of Nagata et al. (1956), of Grey (1963) and of Johnson (1967) have shown that the helical ribbon agitator is highly efficient for

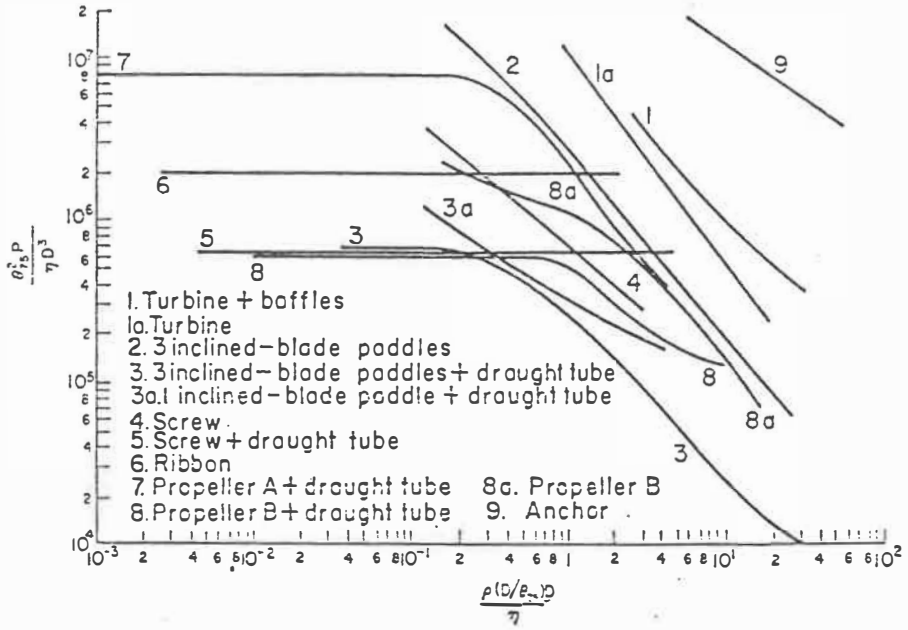

Figure 4 Mixing time data in terms of $t_m^2\rho/\mu D^3$ (*From Hoogendoorn and den Hartog, 1967)*

blending highly viscous, especially viscoelastic fluids. Mixing time is frequently reported in terms of a dimensionless mixing time, Nt_m. In the laminar flow regime, the dimensionless mixing time is almost independent of the Reynolds number, e.g.:

$$Nt_m = k_m \tag{45}$$

where k_m is dependent of the mixer geometry for Newtonian fluids. For instance, k_m valuewas reported to be 65 for Newtonian fluids mixed by a helical ribbon impellers by Hoogendoorn and den Hartog (1967). Novak and Reiger (1969) found a value of k_m close to that reported by Hoogendoorn and den Hartog (1967). Nagata et al. (1972) studied various geometries of helical ribbon impellers and obtained k_m for single helical ribbon, double helical ribbon and helical ribbon screw impellers equal to, 100 ~ 150, 40, 30 ~ 57, respectively. In the transition regime, the dimensionless mixing time decreases with increasing the Reynolds number. A typical mixing time

data in terms of $t_m^2\rho/\mu D^3$ from the work of Hoogendoorn and den Hartog (1967) is shown in Figure 3. The value of $t_m^2\rho/\mu D^3$ is independent of the Reynolds number in the laminar regime and decreases with increasing Reynolds number in the transition flow regime, as seen in this figure.

Mixing time is considerably affected by non-Newtonian properties, especially elasticity, in the laminar flow regime. Chavan et al.(1975a) and Ford and Ulbrecht (1976) reported no significant effects of the shear-thinning character for the inelastic fluids on the mixing time, whereas the mixing times for blending viscoelastic PAA and PAA in glycerol were found to much larger than mixing times obtained for Newtonian fluids. The dimensionless mixing time increases with increasing Weissenberg number (Ford and Ulbrecht, 1976). Carreau et al. (1976) found the mixing times for a 2% CMC aqueous solution to be several fold high than that for glycerol. They confirmed that in an elastic 1% Separan solution the mixing time was considerably higher than for shear-thinning inelastic fluids.

Circulation time is related to the impeller pumping capacity, or the intensity of the macro-flow (Ulbrecht and Carreau, 1985). Mixing time is taken as the time necessary for a free suspended a particle reflecting a fluid element complete a closed loop. Like mixing time, the circulation time is also expressed in terms of a dimensional circulation time, Nt_m. The dimensionless circulation time has also been found to be independent of the Reynolds number for the Newtonian fluids in the laminar flow regime, that is:

$$Nt_c = k_c \tag{46}$$

Investigations on the circulation time has been conducted by Holmes (1964), Gray (1966) and Coyle et al. (1970). Chavan and Ulbrecht were the first to introduce a circulation number which is also related to the impeller pumping capacity. It is defined as:

$$Ci = \frac{q}{Nd^3} \approx \frac{V}{t_c Nd^3} \qquad (47)$$

Chavan et al.(1975b) found lower circulation numbers for viscoelastic fluids that for corn syrup in the laminar flow regime. Similar trends were reported by Guérin et al. (1984). In the transition flow regime, the dimensionless circulation time decreases with increasing Reynolds number.

Guérin et al. (1984) found quite broad and bimodal distributions of the circulation time for glycerol and a 1% CMC aqueous solution. However, the distribution for a 2% CMC was relatively narrower since there may be a segregation between the high deformation zone and the almost stagnant zone. Carreau et al. (1976) measured the axial and tangential velocities' distributions and found that the axial velocity for a viscoelastic 1% Separan solution is much smaller than that for glycerol and for a shear-thinning 2% CMC aqueous solution. This finding confirmed a similar trend observed by Chavan et al. (1975a, 1975b) from the measurements of the axial circulation times. Meanwhile, Carreau et al. (1976) found that the maximum axial velocity is about 15% of the maximum tangential velocity at laminar flow regime for helical ribbon agitators. The influence of the elastic properties on the mixing and circulation times, especially in the transition flow regime still need to be investigated intensively.

2-5. References

Bird, R.B., R.C. Armstrong and O. Hassager, *Dynamics of Polymeric Liquids,* Vol.1, Fluid Mechanics, Weiley, New York (1977).

Bourne, J.R., and H. Bulter, "Power Consumption of Helical Ribbon Impellers in Inelastic Non-Newtonian Liquids", *Chem. Eng. J.* **47**, 263-270(1969).

Bourne, J.R., M. Buerli and W. Regenass, "Power and Heat Transfer to Agitated

Suspensions: Use of Heat Flow Calorimetry", *Chem. Eng. Sci.,* **36**, 782-784 (1981).

Boger D.V. and R. Binnington, "Separation of Elastic and Shear Thinning Effects in Capillary Rheometer", *Trans. Soc. Rheol.,* **21**, 511-534(1977).

Brito E., J.C. Leuliet, L. Choplin and P.A. Tanguy, "On the Role of Elasticity on Mixing with a Helical Ribbon Impeller", *Trans. IChemE.* **69,** 324-331(1991).

Brito E., "Mixing of Rheological Complex Fluids with Helical Ribbon and Helical Ribbon Screw Impellers", *Ph.D. Thesis*, Univ. Laval, (1992).

Calderbank, P.H. and M.B. Moo Young, "The Prediction of Power Consumption in the Agitation of non-Newtonian Fluids," *Trans. IChemE.* **37**, 26-(1959).

Carreau, P.J., "Rheological Equations from Molecular Network Theories", *Trans. Soc. Rheol.*, **16**, 99(1972).

Carreau, P.J., W.I. Patterson and C.Y. Yap, "Mixing of Viscoelastic Fluids with Helical Ribbon Agitators, I - Mixing Time and Flow Patterns", *Can. J. Chem. Eng.,* **54**, 135-142(1976)

Carreau, P.J., J. Paris and P. Guérin, "Mixing of Newtonian and Non-Newtonian Liquids: Screw Agitator and Draft Coil System", *Can. J. Chem. Eng.,* **70**, 1071-1082(1992)

Chavan, V.V., and J.J. Ulbrecht, "Internal Circulation in Vessels Agitated by Screw Impellers", *Chem. Eng. J.*, **6**, 213-223(1973).

Chavan, V.V. and J.J Ulbrecht, "Power Correlation for Close-Clearance Helical Impellers in Non-Newtonian Liquids", *Ind. Eng. Chem. Proc. Des. Dev.*, **12.** 472 (1974).

Chavan V.V., M. Arumugam and J. Ulbrecht, "On the influence of Liquid Elasticity on Mixing in a Vessel Agitated by a Combined Ribbon-Screw Impeller", *AIChE J.* **21**, 613-615(1975a).

Chavan V.V., D.E. Ford and M. Arumugam, "Influence of Fluid Rheology on Circulation, Mixing and Blending", *Can. J. Chem. Eng.* **53,** 628-635(1975b).

Chisti Y. and M. Moo-Young, "Gas Hold-up Behaviour in Fermentation Broths and Other Non-Newtonian Fluids in Pneumatically Agitated Reactors", *Chem. Eng. J.*, **39**, B31-B36(1988).

Coyle, C.K., H.E. Hirschland, B.J. Michel and J.Y. Oldshue, "Mixing in Viscous Liquids", *AIChE J.*, **16,** 903-905 (1970).

Ford, D.E., R.A. Mashelkon and J. Ulbrecht, "Mixing Times in Newtonian and Non-Newtonian Fluids", *Proc. Tech. Int.,* **17**, 803-806 (1972).

Ford, D.E., and J. Ulbrecht, "Blending of Polymer Solutions with Different Rheological Properties", *AIChE J.,* **21,** 1230-1233(1975).

Ford, D.E., and J. Ulbrecht, "Influence of Rheological Properties of Polymer Solutions upon Mixing and Circulation Times", *Ind. Eng. Chem. Proc. Des. Dev.* **15**, 321-326 (1976).

Forschner, P., R. Krebs and T. Schneider, "Scale-up Procedures for Power Consumption of Mixing in Non-Newtonian Fluids, *7th European Cong. on Mixing,* Brugge, Belgium, 161-165(1991),

Gray, J.B., "Batch Mixing of Viscous Liquids", *Chem. Eng. Prog.,* **59,** 55-59 (1963).

Guérin P., P.J. Carreau, W.I. Patterson and J. Paris, "Characterization of Helical Impellers by Circulation Times", *Can. J. Chem. Eng.,* **62**, 301-309(1984)

Hall, K.R. and J.C. Golfrey, "Power Consumption by Helical Ribbon Impellers", *Trans. IChemE.*, **48**, 201-209(1970).

Henzler, M., "Begasen Höherviskoser Flüssigkeiten", *Chem. Ing. Tech.,* **52.** 643-652 (1980).

Höcker, H., G. Langer and U. Werner, "Power Consumption of Stirrers in Non-Newtonian Liquids", *Ger. Chem. Eng.,* **4**, 113-123(1981).

Hoogendoorn, C.J. and A.P. Den Hartog, "Model Studies on Mixers in Viscous Flow Region", *Chem. Eng. Sci.*, **22**, 1689-1699 (1976).

Johnson, R.T., "Batch Mixing of Viscous Liquids", *Ind. Eng. Chem. Proc. Des. DEv.*

6, 340-345(1967).

Kappel, M., "Development and Application of a Method for Measuring the Mixture Quality of Miscible Liquids, III. Application of New Method for Highly Viscous Newtonian Liquids", *Int. Chem. Eng.,* **4.** 571-590(1979).

Kawase Y. and M. Moo-Young, "Mathematical Models for Design of Bioreactors: Applications of Kolmogoroff's Theory of Isotropic Turbulence", *Chem. Eng. J.*, **43**, B19-B41(1990).

MaCabe, W., J.C. Smith and P. Harriott, Unit Operations of Chemical Engineering, *4th Ed.*, McGraw-Hill, Ney York(1985).

Merchuk, J.C. and S. Ben-Zvi(Yona), "A Novel Approach to the Correlation of Mass Transfer Rates in Bubble Columns with Non-Newtonian Liquids", *Chem. Eng. Sci.*, **47**, 3517-3523(1992).

Merquiol, T. and L. Choplin, "Mixing of Viscoelastic Fermentation Broth with Helical Ribbon-Screw (HRS) Impeller", *6th Europ. Cong. on Mixing*, Pavia, Italy, 465-472 (1988).

Metzner, A.B. and R.E. Otto, "Agitation of Non-Newtonian Fluids", *AIChE J.,* **3.** 3-10 (1957).

Metzner, A.B., R.H. Feehs, H. Lopez Ramos and J.D. Tuthill, "Agitation of Viscous Newtonian and Non-Newtonian Fluids", *AIChE J.*, **7**, 3-9 (1961).

Michel, B.J. and S.A. Miller, "Power Requirement of gas-Liquid Agitated Systems", *AIChE J.*, **8**, 262-266(1962).

Nagata, S., T. Yanagimoto and T. Yokoyama, "A Study of the Mixing of High Viscosity", *Mem, Fac., Eng. Kyoto Univ.* **18.** 444-454(1956)

Nagata, S., M. Nishikawa, H. Tada and S. Gotoh, "Power Consumption of Mixing Impellers in Pseudoplastic Liquids", *J. Chem. Eng. Japan,* **4,** 72-76 (1971).

Nagata, S., Mixing: Principles and Applications, Kodansha, Wiley, Tokyo (1975).

Nishikawa, M., H. Kato and K. Hashimoto, "Heat Transfer in Aerated Tower Filled

with Non-Newtonian Liquid", *Ind. Eng. Chem. Proc. Des. Dev*. **16**. 133-137(1977).

Pollard, J. and T.A. Kantyka, "Heat Transfer to Agitated non-Newtonian Fluids", *Trans. IChemE J.,* **47,** T21-T27 (1969).

Prud'homme, R.K. and E. Shaqfreh, " Effect of Elasticity on Mixing Torque Requirement for Rushton Turbine Impellers", *AIChE J.* **30.** 485-486(1984).

Rieger, F. and V. Novak, "Power Consumption of Agitators in Highly Viscous Non-Newtonian Liquids", *Trans. IChemE.*, **51**, 105-111 (1973).

Schumper, A. and W.D. Deckwer, "Viscous Media in Tower Bioreactors: Hydrodynamic Characteristics and Mass Transfer Properties", *Bioproc. Eng.*, **2**, 79-94(1987).

Shamlou, P.A. and M.F. Eduards, "Power Consumption of Helical Ribbon Mixers in Viscous Newtonian and Non-Newtonian Fluids", *Chem. Eng. Sci.*, **40**, 1773-1781 (1985).

Skelland, A.H.P., Mixing and Agitation of Non-Newtonian Fluids, *in Handbook of Fluids in Motion* (Eds: N.P. Cheremisinoff and R. Gupta), Ann Arbor Science, New York, (1983).

Smith, J.M., "Industrial Needs for Mixing Research", *Trans. IChemE.*, **68**, 3-6 (1990).

Takahashi, K., M. Iwoki, T. Yokota and H. Konno, "Circulation Time for Pseudoplastic Liquids in a Vessel Equipped with a Variety of Helical Ribbon Impellers", *J. Chem. Eng. Japan,* **22,** 413-418(1989).

Tatterson, G.B., Fluid Mixing and Gas Dispersion in Agitated Tanks, McGraw-Hill, New York (1991).

Termote, A., "Comortement Hydrodynamique et Transfert de Matière dans des Réacteurs Agités Mécaniquement", M.Sc. Memory, Ecole Polytechnique, (1991).

Vorcken, R.M., "Homogenization of miscible liquids", *British Chem. Eng.,* **10**, 12-18 (1965).

Ulbrecht, J.J., "Comments on Sawinsky et al.", *Chem. Eng. Sci.,* **35,** 2372-2373(1980)

Ulbrecht, J.J. and P.J. Carreau, Mixing of Viscous Non-Newtonian Liquids, *in Mixing of Liquids by Mechanical Agitation,* (Eds: Ulbrecht J.J. and Patterson G.K.), Gordon and Breach, New York (1985).

Unwin, W.C., *Proc. Roy. Soc.,* **A31**, 54(1880).

Yap, C.Y., W.I. Patterson and P.J. Carreau, "Mixing with Helical Ribbon Agitators: III. Non-Newtonian Fluids", *AIChE J.*, **25**, 516-521(1979).

Zaidi, A., H. Bourziza and L. Echihabi, "Warmeubergang und Effetives Schergefalle in Blasensaulen-Bioreaktoren mit Xanthan-Losungen", *Chem. Ing. Tech.*, **59**, 748-749(1987).

Chapter 3 POWER REQUIREMENT

Effect of Rheological Properties on Power Consumption with Helical Ribbon Impellers

P.J. CARREAU*, R.P. CHHABRA and J. CHENG

Centre de recherche appliquée sur les polymères, CRASP
Department of Chemical Engineering
Ecole Polytechnique
C.P. 6079, Succursale A
Montreal, Quebec, Canada H3C 3A7

* Author for correspondence

published in *AIChE Journal,* September Vol. **39**, No. **9**, 1421-1430 (1993)

3-1. SUMMARY

The influence of shear thinning and viscoelasticity on the power required for the mixing of viscous liquids using six different helical ribbon agitators has been investigated. Four Newtonian and twelve non-Newtonian fluids prepared using several polymers dissolved in varying concentrations in different solvents cover a wide range of rheological properties. By a careful choice of test media, the specific as well as combined effects of shear thinning and viscoelasticity on the power requirement have been examined. Simple models are proposed to predict the effective shear rate in the tank from the knowledge of the torque or the power number. The effective shear rate predictions are compared with the effective shear rate estimated using the scheme of Metzner and Otto (1957). It is shown to be slightly dependent upon the shear thinning properties. The fluid's elasticity is shown to increase appreciably the power requirement and departures from the generalized Newtonian power curve in the laminar regime are observed at smaller Reynolds numbers for viscoelastic fluids. Bottom wall resistance of the mixing vessel is shown to make a negligible contribution to the power consumption.

3-2. INTRODUCTION

Mixing of liquids by mechanical agitation is a commonly encountered operation in chemical and polymer processing applications. Notwithstanding the importance of flow patterns and mixing time etc., it is widely recognized that the power consumption is possibly the most important design parameter in these applications. Over the years, a wealth of information has accumulated on the power consumption for low viscosity liquids for a variety of geometrical configurations of agitator-tank combinations.

Consequently, satisfactory methods are now available which permit the estimation of the power consumption for the mixing of low viscosity and purely viscous Newtonian and non-Newtonian systems under most conditions of practical interest. Excellent review articles are available on this subject (Oldshue, 1983; Ulbrecht and Carreau, 1985; Tatterson, 1991).

In contrast to this, the mixing of viscous non-Newtonian and rheologically complex media has received much less attention. The available scant literature on this subject has been reviewed by Ulbrecht and Carreau (1985) and Harnby et al. (1992). An examination of these reviews clearly suggests that the conventional impellers employed for the agitation of low viscosity liquids are not at all satisfactory for the applications involving high viscosity liquids. It is now readily agreed that the close clearance type impellers (such as helical ribbon or screw) result in much better mixing and circulation. Detailed discussions concerning the relative merits and de-merits of various impellers are also available in the literature (Tatterson, 1991). Among the different impeller geometries available, the helical ribbon agitator is considered to be more efficient for the agitation of highly viscous liquids. Whence this paper is concerned with the mixing of viscous Newtonian and non-Newtonian systems using a helical ribbon type agitator.

The power consumption is known to be strongly dependent upon the system geometry, type of agitator, the rheological characteristics of the liquid including shear thinning and viscoelasticity and the kinematic conditions prevailing in the tank. Owing to the high viscosity of liquids being considered herein the flow regime rarely exceeds beyond the transition zone between laminar and turbulent flows. It is well known that strong interactions take place between the geometry and the viscoelasticity and it is therefore not at all possible to extrapolate the role of viscoelasticity from one geometry to another, even qualitatively (Ulbrecht and Carreau, 1985). It is, therefore, not at all surprising that conflicting conclusions have been reached by different investigators regarding the possible role of fluid viscoelasticity on power consumption. Admittedly

detailed discussions concerning the influence of rheological complexities on power consumption are available in the literature (e.g., Harnby et al., 1992), the salient features of the previous pertinent studies are re-capitulated herein.

3-2-1. PREVIOUS WORK

Chavan and Ulbrecht (1973) developed a semi-theoretical model for the prediction of power for a helical screw in the laminar flow ($Re<10$) by assuming the flow to be Couette type and by replacing the helical screw by an equivalent cylinder exerting the same torque. Their predictions for power law fluids are in agreement with the experimentally measured power data. Subsequently, Patterson et al. (1979) used the concept of drag flow about an inclined blade to predict the power and the resulting expression was modified to include viscoelastic fluids (Yap et al., 1979). The Couette analogy approach has also been used to develop a theoretical framework for the prediction of the effective shear rate in the vessel (Ulbrecht and Carreau, 1985), albeit the predictions have not been validated thoroughly. Admittedly, some attempts have also been made at elucidating the effect of viscoelasticity on power consumption but conflicting conclusions have been reported in the literature. For instance, both Chavan and Ulbrecht (1973) and Yap et al. (1979) concluded that the shear thinning effects completely overshadowed viscoelastic effects for helical ribbon impellers. Whereas Nienow et al. (1983) reported a slight increase in power consumption for turbine impellers in viscoelastic xanthan gum solutions. In most of the aforementioned studies, aqueous polymer solutions (exhibiting both shear dependent viscosity as well as varying levels of viscoelasticity) have been used as model test fluids. It is thus not clear whether the observed changes in power consumption are due to the shear thinning or due to the viscoelastic behaviour or due to both. Subsequently, Prud'homme and Shaqfeh (1984) have used non shear thinning but highly elastic fluids (Boger and Binnington, 1977) and reported a large increase in power consumption for turbine

impellers. Similarly, very little is known about the influence of various geometric parameters such as the scale of equipment, bottom clearance etc. on power consumption with helical ribbon agitators. Most of the previous work is limited to the so called laminar flow regime and as far as known to us, no prior results on the mixing of viscoelastic systems with helical ribbon agitators in the transition zone are available in the literature. The present study aims to bridge this gap in our currently available body of knowledge.

In particular, this investigation sets out to elucidate the influence of fluid viscoelasticity and shear thinning on the effective shear rate and power consumption by using suitable and well characterized experimental fluids. Six helical ribbon-tank combinations have been used to demonstrate the effect of the equipment geometry on the power consumption. The experimental results reported herein embrace wide ranges of physical and kinematic conditions.

3-3. CONCEPTS

As suggested by Ulbrecht and Carreau (1985), the variation of power consumption with Reynolds number reflects the overall flow pattern and the in-situ rheology of the mixed liquid in a mixing system. Dimensional analysis suggests that for purely viscous (that is, time independent) fluids and in the absence of vortex formation the power number is a unique function of Reynolds number as

$$Np = \frac{P}{\rho N^3 d^5} = f(Re) \qquad (1)$$

While for Newtonian systems, the Reynolds number is defined unambiguously, considerable confusion exists regarding the appropriate choice of an effective viscosity for non-Newtonian fluids, since the deformation rate in a mixing vessel is neither

constant nor is known a priori. This difficulty was circumvented by Metzner and Otto (1957) who introduced the concept of the effective shear rate, viz.,

$$\dot{\gamma}_e = k_s N \tag{2}$$

where k_s is an experimentally determined constant and it is a function of geometry (see for example Takahashi et al.,1984). Though originally postulated to be independent of the liquid rheology, recent work, however, suggests that for shear thinning fluids its value also depends upon the power law index (Beckner and Smith, 1966; Yap et al., 1979; Brito et al., 1991). While Eq. 2 provides a convenient method for the estimation of power consumption for time independent fluids, virtually no attempt has been made to delineate the variation of k_s with the power law index n and geometry. In the following section, simplified models are presented which do provide useful guidelines for calculating the effective shear rate for helical ribbon agitators operating in the laminar flow regime.

3-3-1. Prediction of Effective Shear Rate

A schematic representation of a helical ribbon agitator is shown in Figure 1. Following Bourne and Butler (1969), Chavan and Ulbrecht (1973), and Ulbrecht and Carreau (1985), the fluid motion caused by the rotating helical ribbon agitator is approximated here by an equivalent flow produced in a coaxial cylinder configuration with the inner cylinder rotating. The helical ribbon impeller is replaced by a cylinder of an equivalent diameter d_e which is rotating with a constant angular velocity Ω. For steady and fully developed Couette flow and in the absence of end effects, one can postulate:

$$v_r = v_z = 0, \quad v_\theta = v_\theta(r) \tag{3}$$

The θ-component of the motion equation simplifies to

$$\tau_{rz} = \tau_{\theta z} = 0, \quad \tau_{r\theta} = f(r) \tag{4}$$

$$\frac{\partial}{\partial r}\left(r^2 \tau_{r\theta}\right) = 0 \tag{5}$$

For power law fluids, the rθ-component of the extra stress tensor may be expressed as

$$\tau_{r\theta} = -m\,\dot{\gamma}_{r\theta}^{n} = -m\left[r\frac{\partial}{\partial r}\left(\frac{v_\theta}{r}\right)\right]^n \tag{6}$$

Substituting Eq. 6 into Eq. 5 and integrating the resulting equation with respect to r and with the boundary conditions $v_\theta = \Omega(d_e/2)$ at $r = d_e/2$ and $v_\theta = 0$ at $r = D/2$ yields the following expression for the velocity profile:

$$\frac{v_\theta}{r} = \frac{\Omega}{\left[(D/d_e)^{2/n} - 1\right]}\left[\left(\frac{R}{r}\right)^{2/n} - 1\right] \tag{7}$$

Then from Eq. 6 the shear stress, $\tau_{r\theta}$, is given by

$$\tau_{r\theta} = m\left[\frac{2\Omega}{n\left[(D/d_e)^{2/n} - 1\right]}\right]^n \left(\frac{R}{r}\right)^2 \tag{8}$$

The torque acting on the inner surface of outer cylinder is obtained from the wall shear stress

$$\Gamma = (2\pi RH)(-\tau_{r\theta})\big|_{r=R}\, R \tag{9}$$

and the power required for mixing is

$$P = 2\ \pi\ \Gamma\ N \tag{10}$$

Then, combining Eqs. 8 to 10, the power number is expressed as:

$$Np = \frac{m\pi^2 D^2 H}{d^5 N^2 \rho}\left[\frac{2\Omega}{n\left[(D/d_e)^{2/n}-1\right]}\right]^n \tag{11}$$

In the laminar regime, the power number - Reynolds number relation can be expressed by

$$Np = K_p\ Re_g^{-1} = K_p\ \frac{\eta_e}{dN^2\rho} \tag{12}$$

Where η_e is an effective viscosity. For power law fluids, $\eta_e = m\,|\,\dot{\gamma}_e\,|^{n-1}$ and Eqs. 11 and 12 can be re-arranged to yield the following expression for the effective shear rate:

$$\frac{\dot{\gamma}_e}{N} = k_s = \left[\frac{K_p d^3}{\pi^2 D^2 H}\right]^{\frac{1}{1-n}}\left[\frac{n\left[(D/d_e)^{2/n}-1\right]}{4\pi}\right]^{\frac{n}{1-n}} \tag{13}$$

Eq. 13 thus elucidates the functional dependence of k_s on the flow behaviour index n and geometry via d_e.

Alternately, one can re-arrange Eq. 9 together with Eq. 6 to obtain the following expression for the shear rate at the outer cylinder, i.e., $\dot{\gamma}_{r\theta,wall}$ as

$$\dot{\gamma}_{r\theta,\ wall} = \left[\frac{2\Gamma}{\pi m D^2 H}\right]^{1/n} \tag{14}$$

It can be argued that the effective shear rate $\dot{\gamma}_e$ (estimated by using Eq. 13) and the shear rate at the wall $\dot{\gamma}_{r\theta,wall}$ (calculated via Eq. 14) should be inter-related as both involve the knowledge of torque or power. The torque acting on the vessel wall can be represented as a function of the effective viscosity by combining Eqs. 10 and 12:

$$\Gamma_{wall} = \frac{K_p d^3 N}{2\pi} \eta_e \tag{15}$$

The wall shear rate is also assumed to be proportional to the rotational speed

$$\dot{\gamma}_{r\theta,wall} = k_s' N \tag{16}$$

where k_s' is a constant to be determined via the experimental results. For the power law fluids, $\eta_e = m (k_s N)^{n-1}$, and from Eqs. 14 to 16, k_s can be expressed as a function of k_s':

$$k_s = \left[\frac{\pi^2}{K_p}\left(\frac{D}{d}\right)^2\left(\frac{H}{d}\right)\right]^{\frac{1}{n-1}} k_s'^{\frac{n}{n-1}} \tag{17}$$

In contrast to Eq. 13, Eq. 17 can be used to predict k_s from k_s' without making use of the equivalent diameter, d_e.

3-4. EXPERIMENTAL

The mixing system employed in this work consisted of a cylindrical plexiglas vessel fitted with a helical ribbon agitator together with an automated data acquisition system. In order to ascertain the effect of geometric parameters on power consumption two cylindrical vessels (0.292 m and 0.40 m diameter) together with six different helical ribbon agitators have been used; the major dimensions of the various tank/agitator combinations employed herein are defined in Figure 1 and their values are presented in Table 1. The torque acting on the agitator shaft was measured using a torquemeter whereas the rotational speed was measured using a tachometer. More detailed descriptions of the experimental setup and procedure are available elsewhere (Carreau et al., 1976; Yap et al., 1979). Suffice it to add here that each power data point

represents an average of several repeated measurements in order to minimize the experimental uncertainty; the torque measurement is believed to be reproducible within 2.0%.

3-4-1. Test Fluids

In order to encompass a wide range of the rheological characteristics, several Newtonian and non-Newtonian test fluids have been used in this work. Steady shear stress and primary normal stress differences were measured using a R-18 Weissenberg rheogoniometer at the same temperature as that encountered in the mixing experiments. Aqueous solutions of corn syrup (Bee Hive, Best Foods) and glycerol (G-177, American Chemicals) of different concentrations were used as Newtonian liquids whereas the non-Newtonian fluids used herein can be further divided into different types depending upon whether these fluids exhibited any measurable primary normal stress difference or shear dependent viscosity or both. Thus, the aqueous solutions of xanthan, XTN, (28602-8, Aldrich) and carboxyl methylcellulose, CMC, (CMC-70-F, Aqualon) and gellan (4900-1890, Scott) dissolved in a Newtonian corn syrup did not exhibit measurable primary normal stress differences and hence were classified as inelastic shear thinning fluids. On the other hand, solutions of xanthan and CMC in mixtures containing 85 mass % glycerol and 15 mass % water were found to be shear thinning as well as viscoelastic. Finally, the influence of viscoelasticity in the absence of shear thinning was examined by using two Boger fluids (Boger and Binnington, 1977). The first fluid was a 0.35% polyisobutylene, PIB, (M_w = 2.5×10^6 kg/kmol, Vistanex MM, Exxon) dissolved in a mixture containing 77 mass % of polybutene, PB, (Parapol 1300, Exxon) and 23 mass % kerosene, and the second fluid was a solution of 800 ppm of polyacrylamide, PAA, (Separan AP30, Dow Chemical) in corn syrup. This last fluid was slightly shear thinning.

Only steady state shear viscosity and primary normal stress difference data

were used to characterize the fluids. Owing to the qualitatively different behaviours, it was not possible to use a single rheological model even for their shear viscosity behaviour. For instance, the usual two parameter power law model provides a satisfactory fit of the viscosity data for the aqueous solutions of xanthan and CMC as well as for the 0.7% gellan in corn syrup solutions. The more concentrated (1-3%) solutions of CMC, on the other hand, displayed a rather broad transition zone between the zero shear viscosity and power law regime. The Cross model was used to represent their shear viscosity - shear rate behaviour:

$$\eta = \frac{\eta_0}{1+(t_1\dot{\gamma})^{n-1}} \tag{18}$$

For the solution of xanthan in the glycerol/water mixture, it was necessary to modify the power law by incorporating the solvent viscosity as follows

$$\eta - \eta_s = m \mid \dot{\gamma} \mid^{n-1} \tag{19}$$

The resulting values obtained by non-linear regression of power law constants (n and m), Cross model parameters(η_0, n and t_1) and the solvent viscosity η_s are given in Table 2 where a wide range of rheological conditions, especially the value of n (0.18 to 1.00), is seen to be covered. The solid curves in Figure 2 represent the fits obtained with the viscosity models.

The primary normal stresses data are shown in Figure 3 to be adequately represented by the following power law type expression

$$N_1 = -(\tau_{11} - \tau_{22}) = \Psi_1\dot{\gamma}^2 = m'\dot{\gamma}^{n'} \tag{20}$$

and the experimental values of m′ and n′ are also included in Table 2. Attention is drawn to the fact that, as expected, n′ is generally greater than the corresponding value of n and that the N_1 data for the Boger fluids seem to approach the expected

second order limit and under these conditions, their viscoelastic behaviour can be described in terms of a characteristic elastic time defined by

$$\lambda = N_1/2\tau_{r\theta}\dot{\gamma}_{r\theta} \qquad (21)$$

Figure 4 supports this contention whereas for all other fluids used herein, the characteristic elastic time decreases with increasing shear rate.

Thus, in this work, altogether 16 fluids exhibiting a wide range of rheological properties have been employed to delineate the effects of non-Newtonian characteristics on the power consumption and these are presented and discussed in the next section.

3-5. RESULTS AND DISCUSSION

The power consumption was measured as a function of the system geometry, rheological properties of fluids and kinematic variables, namely, speed. It is customary to present these results in a dimensionless form in terms of the power number as a function of the Reynolds number. It is desirable and instructive to begin with the results for Newtonian fluids, as it provides a convenient basis for the analysis of the results for non-Newtonian systems (presented in subsequent sections.)

3-5-1. Newtonian Liquids

The power consumption for Newtonian fluids has been measured using the six different agitators up to Re = 4500, albeit our primary concern here is in the viscous and transition flow regimes. Depending upon the specific geometry of the agitator, the laminar flow regime (NpRe = constant = K_p) is observed to persist up to about Re $\approx$ 30 ~ 70, as shown by Figure 5. The critical value of the Reynolds number up to which the laminar flow prevails is seen to vary somewhat with the system geometry.

The resulting mean values of K_p for all geometries are listed in Table 3. Also included in the same table are the calculated value of K_p using the semi-analytical methods due to Chavan and Ulbrecht (1973), Yap et al. (1979) and the empirical correlation proposed by Shamlou and Edwards (1985). While the agreement between the predicted and experimental values of K_p is seen to be moderately good for the models proposed by Chavan and Ulbrecht (1973) and by Yap et al. (1979), the correspondence with the results of Shamlou and Edwards (1985) is rather poor. Further examination of this table shows that the value of K_p increases with the decreasing agitator pitch and with the increasing blade width, albeit the latter is a rather small effect. These observations are consistent with the findings of Hall et al. (1970), Chavan and Ulbrecht (1973) and Yap et al. (1979), etc.

3-5-2. Non-Newtonian Fluids

Typical experimental results on power consumption in non-Newtonian systems are shown in Figures 6 and 7 for several test fluids but one geometry HR3 thereby elucidating the effects of shear thinning and viscoelastic behaviour. Qualitatively similar trends were observed with the other geometrical arrangements investigated in this work. The generalized Reynolds number in these figures has been defined using the effective viscosity calculated using the method of Metzner and Otto (1957), i.e., Eq. 2 using the Newtonian power curve in the laminar regime as a reference.

A detailed examination of the results shown in Figures 6 and 7 as well as of those not presented herein suggests that, in the absence of viscoelastic effects, laminar flow for highly shear thinning fluids persists up to somewhat larger values of the generalized Reynolds number than that for the Newtonian fluids. Therefore, a smaller torque is needed to mix shear thinning liquids in the transition regime than that for Newtonian fluids. The smaller the value of n is, the higher is the value of the Reynolds number marking the onset of the transition flow. The results obtained with the highly shear

thinning and relatively inelastic 2.5% xanthan aqueous solution corroborate these assertions. Similar results have been also reported by Brito et al.(1991). For mildly shear thinning and inelastic fluids, the present results are virtually indistinguishable from the Newtonian power curve in the transition regime. This observation is also consistent with the finding of previous studies (Harnby et al., 1992).

For the mixing of viscoelastic liquids, the values of power number are in line with the Newtonian curve only for low values of the Reynolds number. For these low values, the corresponding values for the Weissenberg number ($Wi=(\Psi_1/\eta_e)N$) are small and it is expected to show little effect on the power consumption. With an increase in the velocity (hence Re and Wi), the viscoelastic effects become more and more pronounced and the more elastic the fluid is, the sooner is the departure from the Newtonian curve. In other words much greater power is required to mix highly viscoelastic systems than Newtonian fluids of comparable viscosity and with increasing elasticity of the fluids smaller is the value of the Reynolds number up to which the laminar flow is seen to exist. These results are in line with the findings of Prud'homme and Shaqfeh (1984) and Carreau et al. (1992) for impellers of different types, and with the observations of Brito et al. (1991) for similar agitators. In this context, the results obtained with the two Boger (nearly shear independent elastic) fluids are particularly informative which illustrate the aforementioned phenomena unequivocally.

Figure 8 shows the effect of the Weissenberg number on the power number. Note the qualitatively similar behaviour exhibited by different types of fluids. Bearing in mind the opposing effects of shear thinning and viscoelasticity, the results for the Boger fluids (0.35 % PIB and 800 ppm PAA) are seen to deviate at rather small values of the Weissenberg number. The fact that the results for the highly shear thinning and viscoelastic xanthan solution in glycerol conform the Newtonian behaviour up to rather large values of the Weissenberg number (~ 0.1) suggests that shear thinning delays the onset of viscoelastic effects. Qualitatively similar trends have been documented by

Brito et al. (1991) for a helical ribbon agitator and by Nienow et al.(1983) for a Rushton type agitator. However, there does not appear to be a simple method of predicting a priori the onset of departure from the Newtonian curve in this complex flow configuration. It should be mentioned here that the point at which the results begin to veer away from the Newtonian curve also coincides with that at which the rod climbing phenomenon is observed in mixing experiments. Obviously the fluid's elasticity is responsible for changes in the flow patterns, as discussed by Ulbrecht and Carreau (1985). To quantitatively describe the effects of flow pattern changes on the power consomption in such a complex flow system is, however, impossible without a detailled investigation of the flow field. Qualitatively, we suggest that more energy is required to mix viscoelastic fluids because the flow in a mixing vessel is highly transient and partly extensional. Viscoelastic fluids are known to exhibit large stress overshoots in transient experiments and their extensional viscosity could be quite large compared to their shear viscosity (see Bird et al., 1987).

In view of the opposing effects of shear thinning and viscoelastic behaviour on power, it is conceivable that under appropriate circumstances, the results for a shear thinning viscoelastic liquid may not deviate from the corresponding Newtonian curve. This expectation is borne out by the results obtained with the highly shear thinning and viscoelastic 0.5% xanthan solution in glycerol. Only at sufficiently high values of the Reynolds number (and thus Weissenberg number) do the results begin to veer away from the Newtonian curve. Finally, Figure 9 shows that the clearance between the impeller and the bottom of the vessel exerts virtually no influence on the power consumption for a series of Newtonian and non-Newtonian fluids using the impeller HR3. One would intuitively expect similar results for other geometries too.

3-5-3. Predicted and Experimental Effective Shear rate

Figures 10 and 11 show representative results of k_s (calculated using the method of

Metzner and Otto (1957)) as a function of the generalized Reynolds number Re_g for one agitator geometry (HR3). The k_s value is found to be constant only in the laminar flow regime for purely viscous (i.e. inelastic) fluids and for very low Reynolds numbers in the case of the viscoelastic liquids, i.e. before the departure from the laminar regime. For the 0.4% CMC in glycerol/water, no constant k_s could be obtained within the experimental range.

Beyond the laminar flow and/or beyond the point of departure, the relationship between k_s and Re_g seems to be strongly dependent upon the rheological characteristics of the liquid. Broadly speaking, k_s calculated using the Metzner-Otto (1957) method is strongly dependent on the generalized Reynolds number Re_g. For highly shear thinning fluids the increase of k_s at high Reynolds number is due to the extension of the laminar regime. For viscoelastic fluids, on the contrary, the decrease is caused by early departure from the generalized Newtonian power curve. As expected, k_s is somewhat dependent on the agitator geometry. Figure 12 reports the values of k_s for the non-Newtonian fluids used in this work determined in the laminar regime, for only three geometries to avoid overcrowding of the figure. It is obvious that in addition to geometry, k_s is quite dependent on the flow behaviour index, n. This last finding is also consistent with the conclusions reached by other investigators (e.g. Beckner and Smith, 1966; Yap et al., 1979; Brito et al., 1991). The increase of k_s with n is not predicted by Eq. 13 using the power constant, K_p, determined for Newtonian fluids. This will be discussed below.

Alternately, one can also predict k_s using Eq. 17, via the wall shear rate constant k_s'. The constant of proportionality k_s' is also plotted against the power law index n in Figure 12, for three geometrical configurations only. The other systems show a similar behaviour. The predictions of k_s and the values calculated from the Metzner-Otto (1957) method are in close agreement. For high values of n, the predictions are quite sensitive to the K_p values and become undetermined for $n = 1$. These results

provide a theoretical justification for the empirical approach of Metzner and Otto (1957).

The power and applicability of the approach developed herein is also demonstrated by predicting the equivalent diameter d_e using the power measurements via Eq. 13. The results are shown in Figure 13 where it is clearly seen that the value of d_e is somewhat influenced by the extent of shear thinning behaviour. Although the reasons for the dependence of D/d_e on n are not immediately obvious, this can be attributed in part to the changes in flow patterns for highly shear thinning fluids as observed by Carreau et al.(1976) and recently computed by Tanguy et al.(1991). However, in spite of the slight dependence of D/d_e on n, it can be argued that the calculation of power is not very sensitive to the variation of D/d_e with n. For engineering calculations, it is quite adequate to use the value of (D/d_e) from Newtonian fluids, listed in Table 1, together with the k_s determined from Eq. 13. Figure 14 confirms this expectation: the deviations between the predicted values using the equivalent diameter for Newtonian fluids and the power data for impeller HR3 are barely noticeable. The predictions for 2.5% XTN solution coincide almost exactly with the experimental data, so that the differences in the figure cannot be seen. For this solution, k_s is exactly predicted by Eq. 13. The results for the other geometries would be comparable. We stress that, with this approach, power consumption for mixing inelastic non-Newtonian fluids can be predicted from the Newtonian power constant, K_p.

3-6. CONCLUSIONS

In this work, the influence of the shear thinning and viscoelastic characteristics on the power requirement for the mixing of liquids with helical ribbon agitators have been investigated. For mildly to fairly high shear thinning inelastic liquids ($n \geq 0.25$), the power consumption does not deviate from the corresponding Newtonian curve in the

laminar as well as in the early transition flow regime. For highly shear thinning inelastic fluids ($n < 0.2$) the power number shows an extended laminar flow regime, i.e. the onset of the transition regime is somewhat delayed. The viscoelastic behaviour exerts an exactly opposite effect, i.e., the power number for shear independent viscoelastic (Boger) fluids is well represented by the Newtonian curve only for very low values of the Reynolds number (and Weissenberg number). With increasing Re, viscoelastic effects become more pronounced and the power number is much larger than for Newtonian fluids. Conversely, these fluids exhibit a much shorter laminar flow regime than Newtonian fluids. For fluids which exhibit both shear thinning as well as viscoelastic properties, the effect of elasticity (or Weissenberg number) is less pronounced and the departures of the power number from the Newtonian curve is observed for higher Reynolds number than for the shear independent viscoelastic fluids.

Based on the analysis of Couette flow, simple semi-theoretical models have also been outlined for the laminar regime herein, which in conjunction with the experimental torque values enable us to predict the effective shear rate. The functional dependence of the wall shear rate and of the effective shear rate on the flow behaviour index and geometry is reported and discussed. The wall shear rate is linked with the effective shear rate in the tank estimated using the concept introduced by Metzner and Otto (1957). The proposed models can be used to predict the effective shear rate and predict the power consumption for the mixing of inelastic non-Newtonian fluids with close clearance impellers in the laminar regime. Finally, the present experimental results also suggest that the clearance between the agitator and bottom does not influence the power consumption to an appreciable extent.

3-7. Acknowledgement

We wish to express our thanks to Professor L. Choplin and Dr. E. Brito for most

appreciated suggestions and discussion. During the course of this work, R.P.Chhabra was supported by an International Exchange Visitor grant provided by NSERC (to P.J. Carreau). Also, the financial support received from the FCAR Program of the Province of Quebec is gratefully acknowledged.

3-8. References

Beckner J. L. and J. M. Smith, "Anchor-Agitated Systems: Power Input with Newtonian and Pseudoplastic Fluids," *Trans. Inst. Chem. Eng.,* **44,** 224(1966)

Bird R. B., R.C. Armstrong and O. Hassager, *Dynamics of Polymeric Liquids*, Vol.1, Fluid Mechanics, Second Edition, Wiley, New York (1987)

Boger D. V. and R. Binnington, "Separation of Elastic and Shear Thinning Effects in the Capillary Rheometer," *Trans. Soc. Rheol.,* **21**, 515(1977)

Bourne J. R. and H. Butler, "Power Consumption of Helical Ribbon Impellers in Inelastic Non-Newtonian Liquids," *Chem. Eng. J.,* **47**, 263(1969)

Brito E., J. C. Leuliet, L. Choplin and P. A. Tanguy, "On the Effect of Shear-Thinning Behaviour on Mixing with a Helical Ribbon Impeller," *Chem. Eng. Res. & Des.,* **69,** 324(1991)

Carreau P. J., I. Patterson and C. Y. Yap, "Mixing of Viscoelastic Fluids with Helical-Ribbon Agitators-I-Mixing Time and Flow Patterns," *Can. J. Chem. Eng.,* **54,** 135(1976)

Carreau P. J., J. Paris and P. Guérin, "Mixing of Newtonian and Non-Newtonian Liquids: Screw Agitator and Draft Coil System," *Can. J. Chem. Eng.*, in press (1992)

Chavan V. V. and J. J. Ulbrecht, "Power Correlations for Close-Clearance Helical Impellers in Inelastic non-Newtonian Liquids," *Chem. Eng. J.,* **3**, 308(1972)

Hall K. L. and J. C. Godfrey, "Power Consumption by Helical Ribbon Impellers," *Trans Inst. Chem. Eng.,* **48**, T201(1970)

Harnby N., M. F. Edwards and A. W. Nienow, *Mixing in the Process Industries,*

Butterworths, London(1992)

Metzner A. B. and J. C. Otto, "Agitation of Non-Newtonian Fluids," *AIChE J*, **3**, 3(1957)

Nienow A. W., D. J. Wisdom and J. Solomon, "The Effect of Rheological Complexities on Power Consumption in an Aerated Agitated Vessel," *Chem. Eng Commun.,* **19**, 273(1983)

Oldshue, J. Y., *Fluid Mixing Technology,* McGraw Hill, New York (1983)

Patterson I., P. J. Carreau and C. Y. Yap, "Mixing with Helical Ribbon Agitators,Part II- Newtonian Fluids," *AIChE J.,* **25**, 516(1979)

Prud'homme R. A. and E. G. Shaqfeh, "Effect of Elasticity on Mixing Torque Requirements for Rushton Turbines," *AIChE J.,* **30**, 485(1984)

Shamlou P. A. and M. F. Edwards, "Power Consumption of Helical Ribbon Mixers in Viscous Newtonian and Non-Newtonian Fluids," *Chem. Eng. Sci.*, **40**, 1773(1985)

Takahashi K., T. Yokota and H. Konno, "Power Consumption of Helical Ribbon Agitators in Highly Viscous Pseudoplastic Liquids", *J. Chem. Eng. Japan*, **17**, 657(1984)

Tanguy P. A., R. Lacroix, F. Bertrand, L. Choplin and E. Brito, Mixing of Rheologically Complex Fluids with an Helical Ribbon Impeller: Experimental and 3-D Numerical Studies, *7th European Cong. on Mixing,* Brugge, Belgium, 507(1991).

Tatterson G. B., *Fluid Mixing and Gas Dispersion in Agitated Tank,* McGraw-Hill, New York(1991)

Ulbrecht J. J. and P. J. Carreau, "Mixing of Viscous non-Newtonian Fluids," p93, Chapter 4, in *Mixing of Liquids by Mechanical Agitation,* (Eds: J. J. Ulbrecht and G. K. Patterson), Gordon and Breach, New York(1985)

Yap Y. C., W. I. Patterson and P. J. Carreau, "Mixing with Helical Ribbon Agitators, Part III - Non-Newtonian Fluids," *AIChE J.*, **25** 516(1979)

Table 1 Agitator's Goemetries

Geometry	d(m)	D/d	h/d	p/d	w/d	D/d_e*
HR1	0.263	1.11	1.05	0.695	0.097	1.42
HR2	0.263	1.11	1.05	0.850	0.133	1.50
HR3	0.263	1.11	1.05	0.695	0.133	1.37
HR4	0.360	1.11	1.03	0.686	0.083	1.45
HR5	0.360	1.11	1.03	1.028	0.133	1.57
HR6	0.360	1.11	1.03	0.686	0.133	1.43

* d_e calculated from Eq. 13 for Newtonian fluids ($n = 1$).

Table 2. Rheological Parameters of the Fluids

Fluids	n	m	t_1	η_0	η_s	n′	m′	ρ
	-	$Pa \cdot s^n$	s	Pa·s	Pa·s	-	$Pa \cdot s^{n'}$	kg/m^3
Dilute corn syrup #1	1	12.0						1440
Dilute corn syrup #1	1	4.16						1360
Dilute glycerol #1	1	0.470						1140
Dilute glycerol #2	1	0.067						1100
2.5% XTN	0.183	22.4						1080
0.5% XTN (gly./H_2O)	0.199	4.13			0.19	0.782	7.85	1200
1.8% XTN	0.200	11.8						1080
0.8% XTN	0.240	2.31						1050
0.5% XTN	0.250	1.84						1030
3% CMC	0.299		7.83	469				1060
1% CMC	0.409		0.110	1.57				1040
0.4% CMC (gly./H_2O)	0.530	9.75				0.740	18.0	1200
0.1% CMC (gly./H_2O)	0.701	1.20				1.12	0.140	1200
0.7%gellan (corn syrup)	0.910	0.750						1300
800 ppm PAA (corn syrup)	0.940	1.03				1.67	0.150	1350
0.35% PIB (PB+Kerosene)	1	8.19				2.00	1.29	1100

Table 3 Conparison of Experimental Data of Kp with Literature

Agitators	Experimental (This Work)	Chanvan and Ulbrech (1973)	Yap et al (1979)	Shamlou and Edwards (1985)
HR1	164.1	180.9	136.2	226.7
HR2	132.2	176.7	103.0	229.5
HR3	192.2	206.8	129.8	253.9
HR4	160.5	165.5	136.2	213.2
HR5	120.1	150.9	80.4	203.9
HR6	176.8	204.6	127.9	249.6

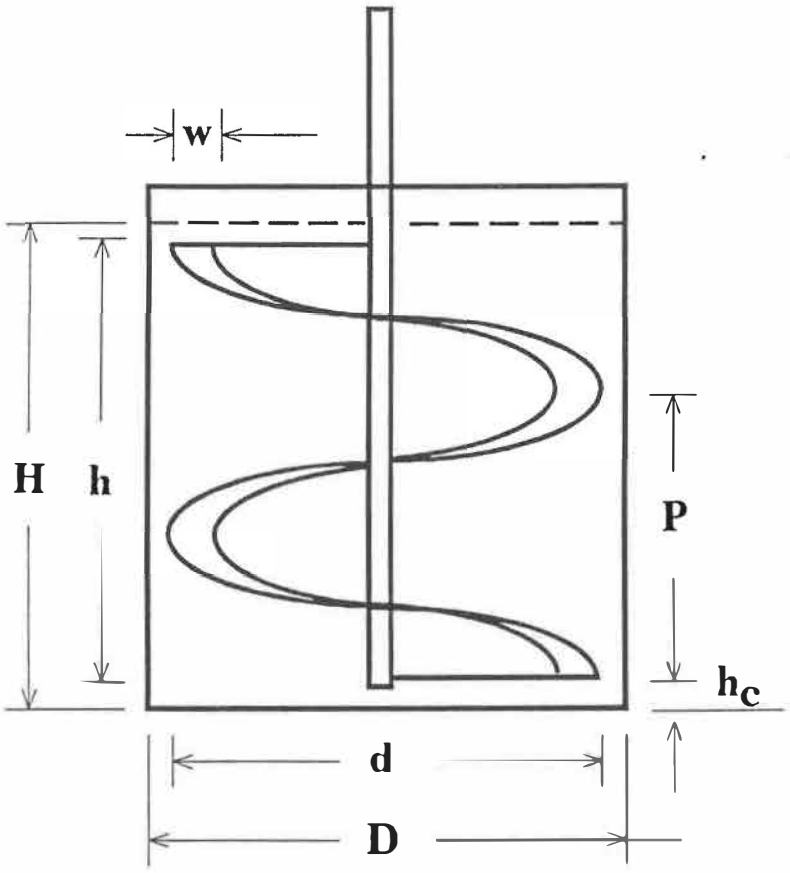

Figure 1 Sketch of helical ribbon agitator system

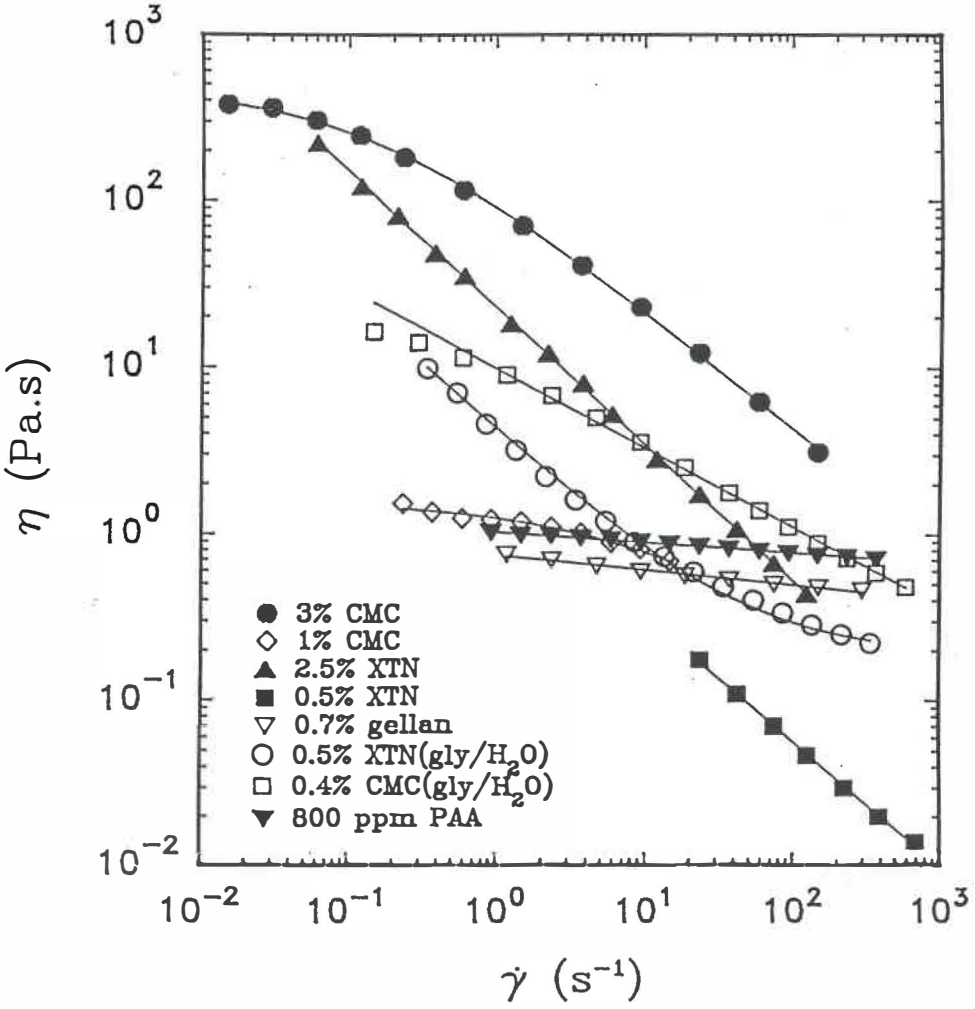

Figure 2 Shear viscosity data for eight polymer solutions

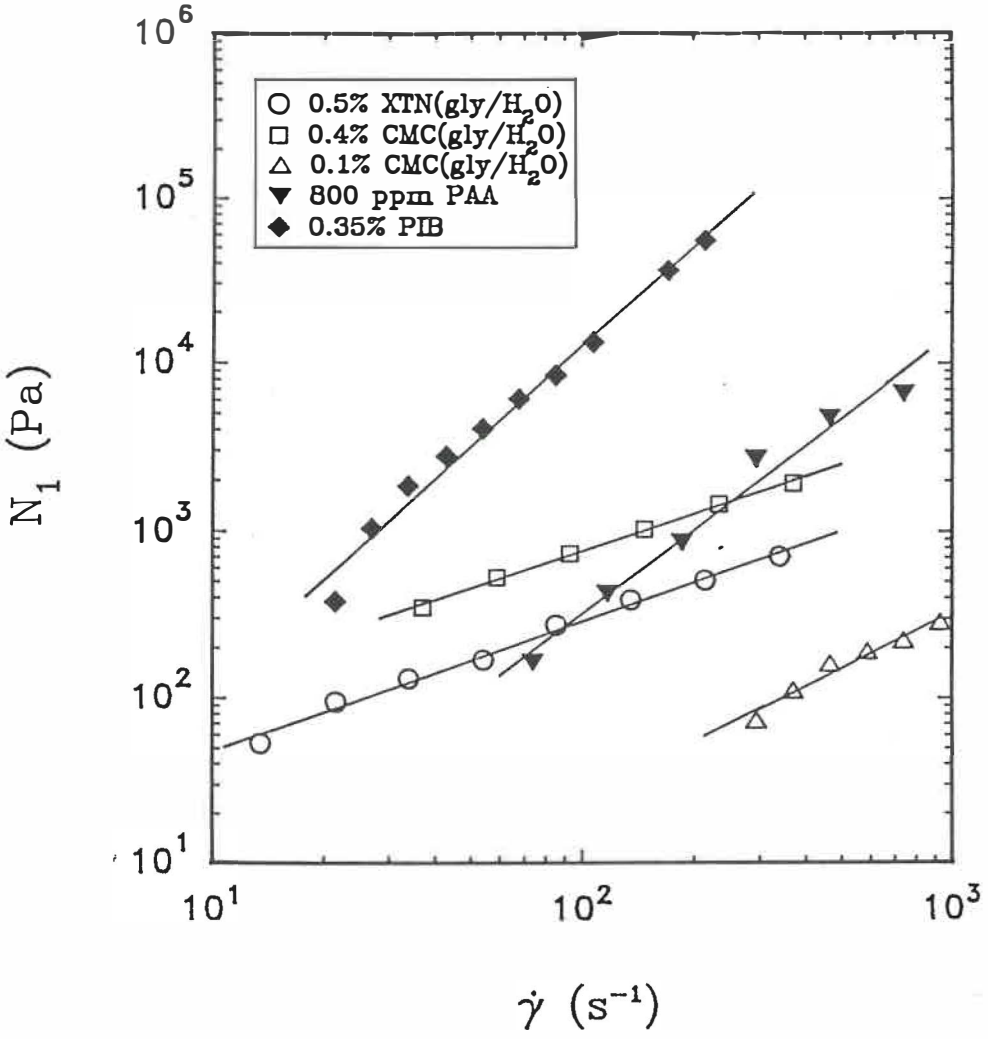

Figure 3 Primary normal stress difference data for five polymer solutions

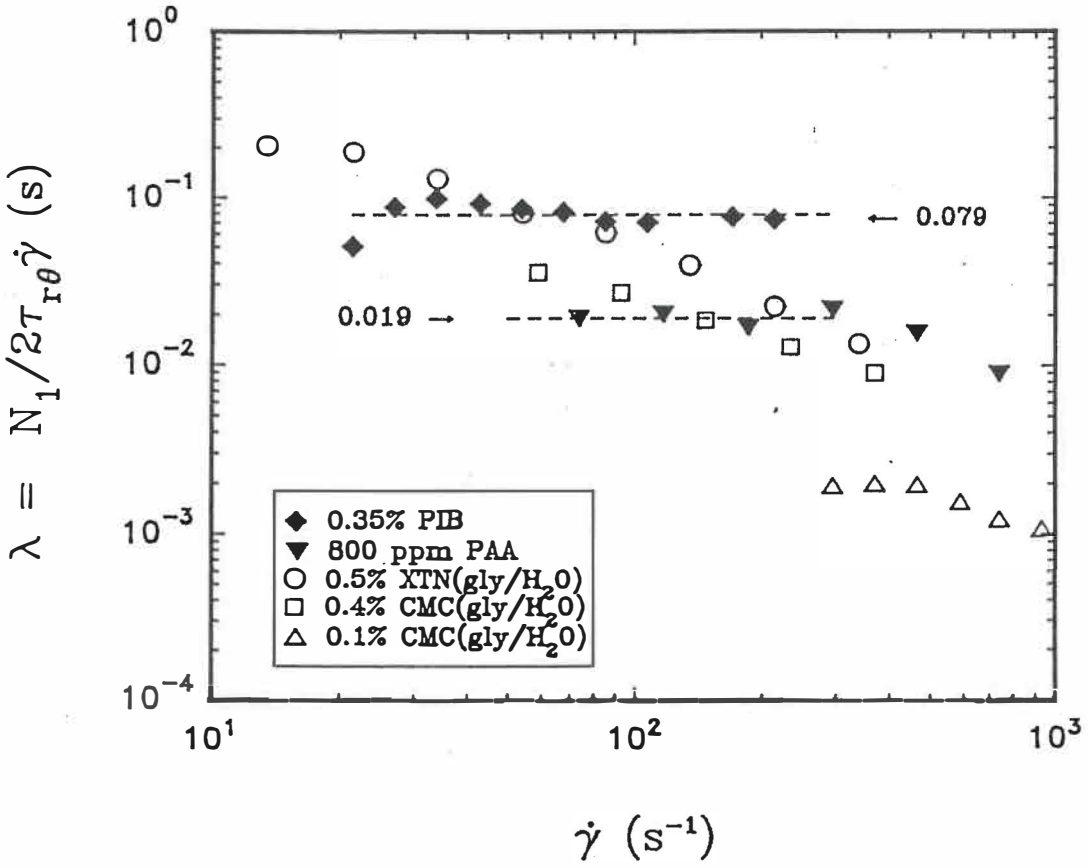

Figure 4 Variation of elastic time constant with shear rate for five polymer solutions

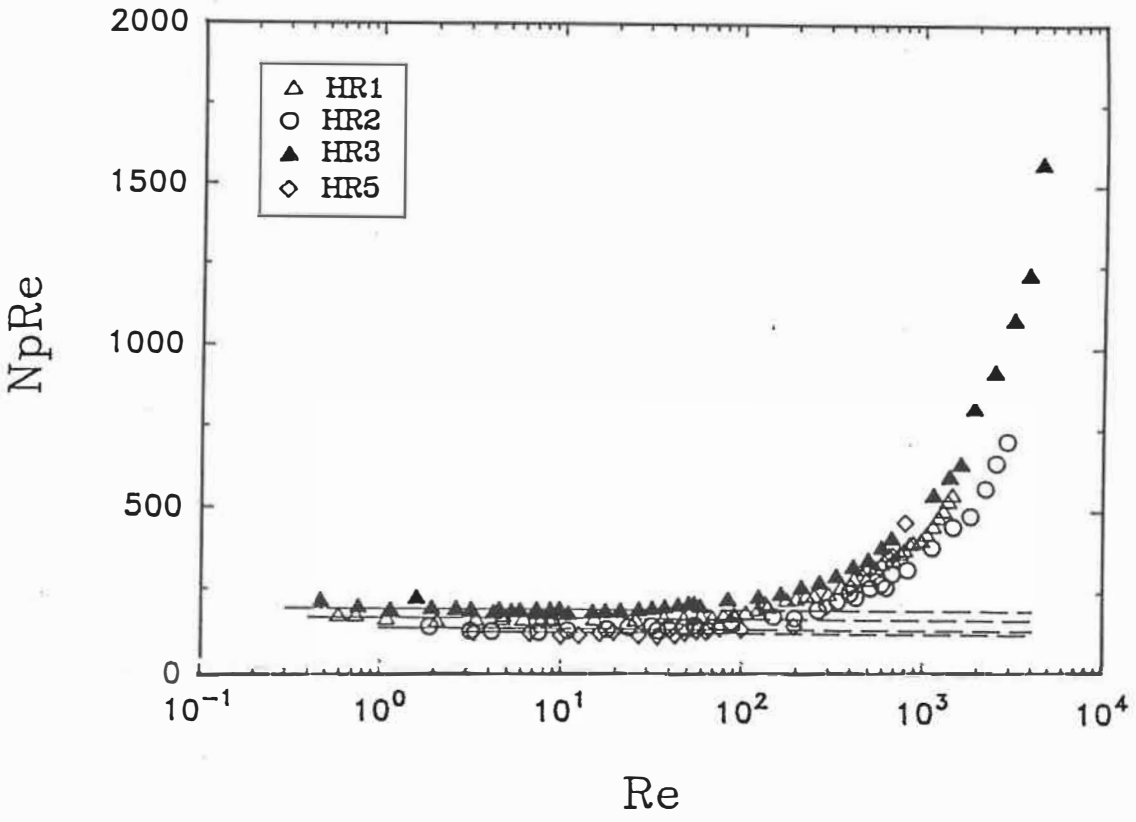

Figure 5 Variation of *NpRe* with Reynolds number for Newtonian fluids

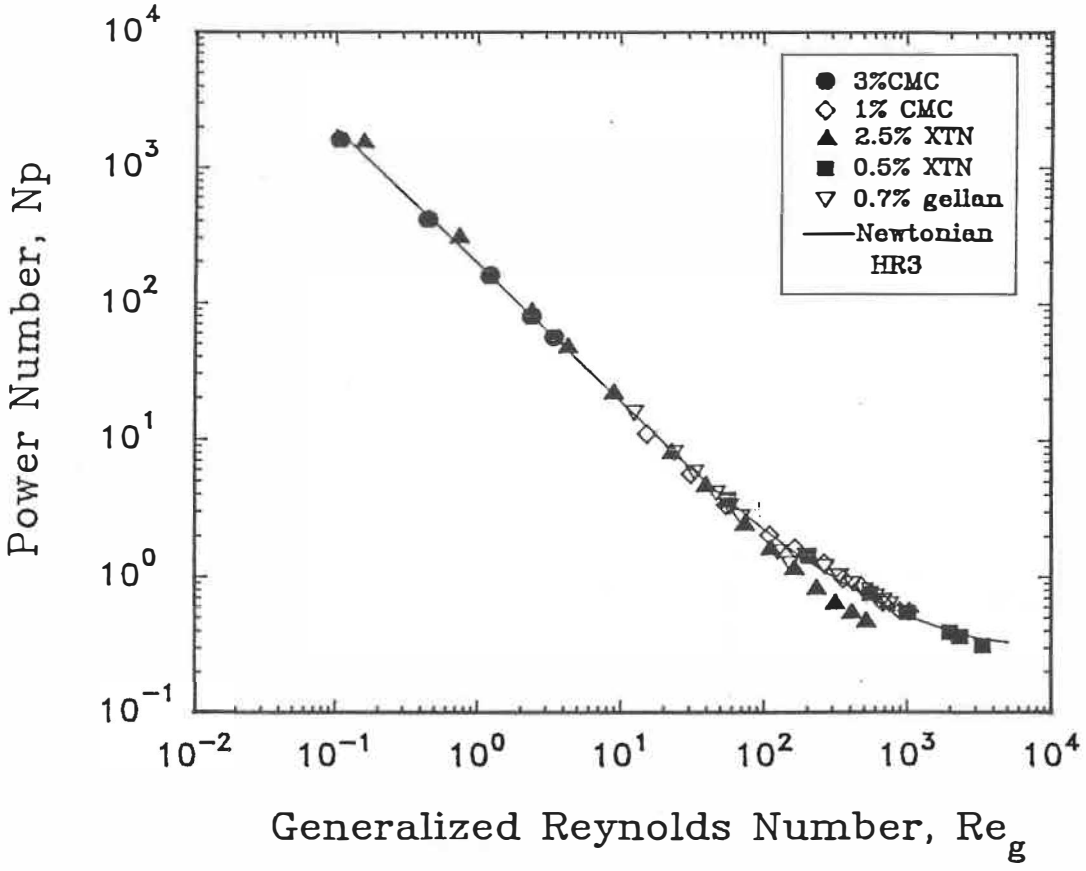

Figure 6 Power data for shear-shinning inelastic fluids

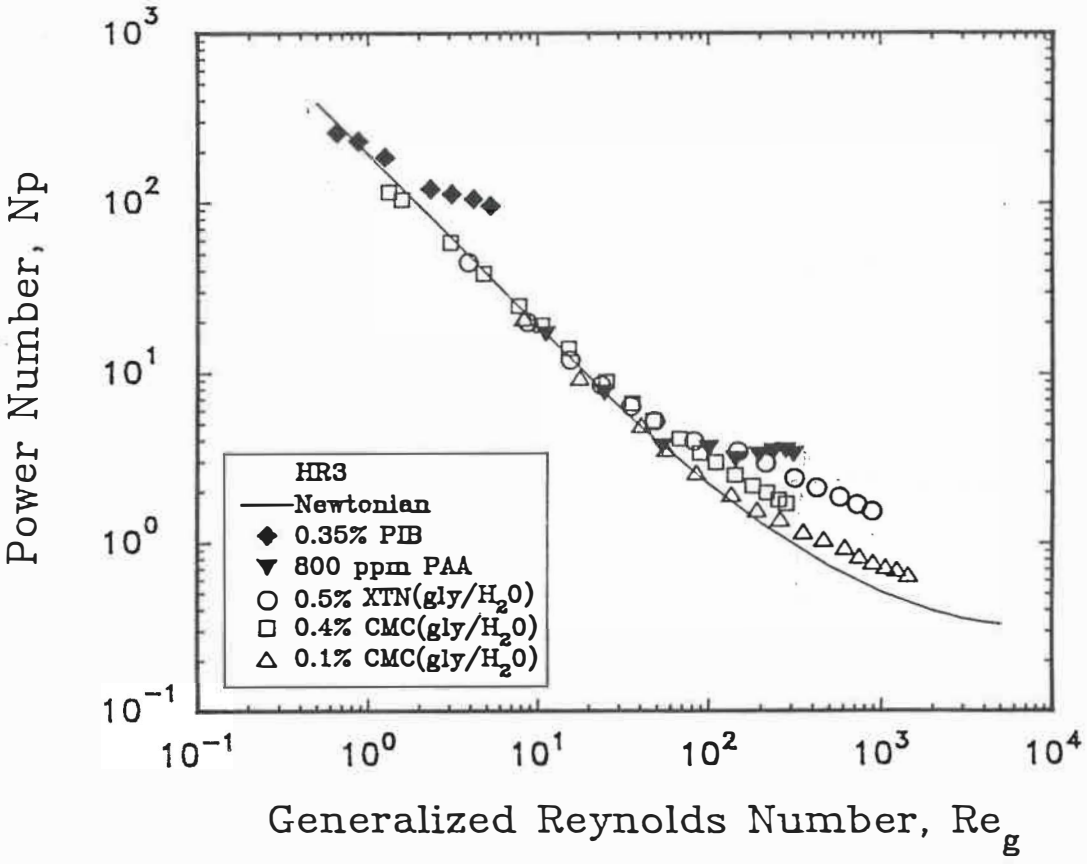

Figure 7 Power data for viscoelastic fluids

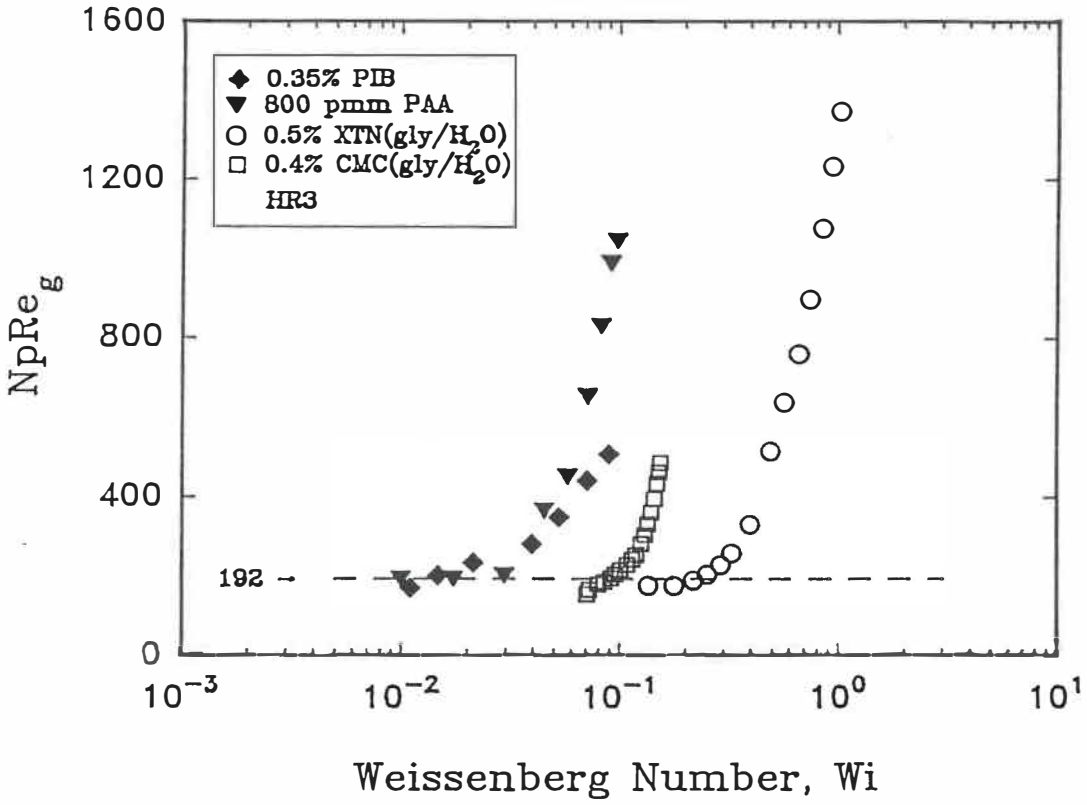

Figure 8 Variation of $NpRe_g$ with Weissenberg number

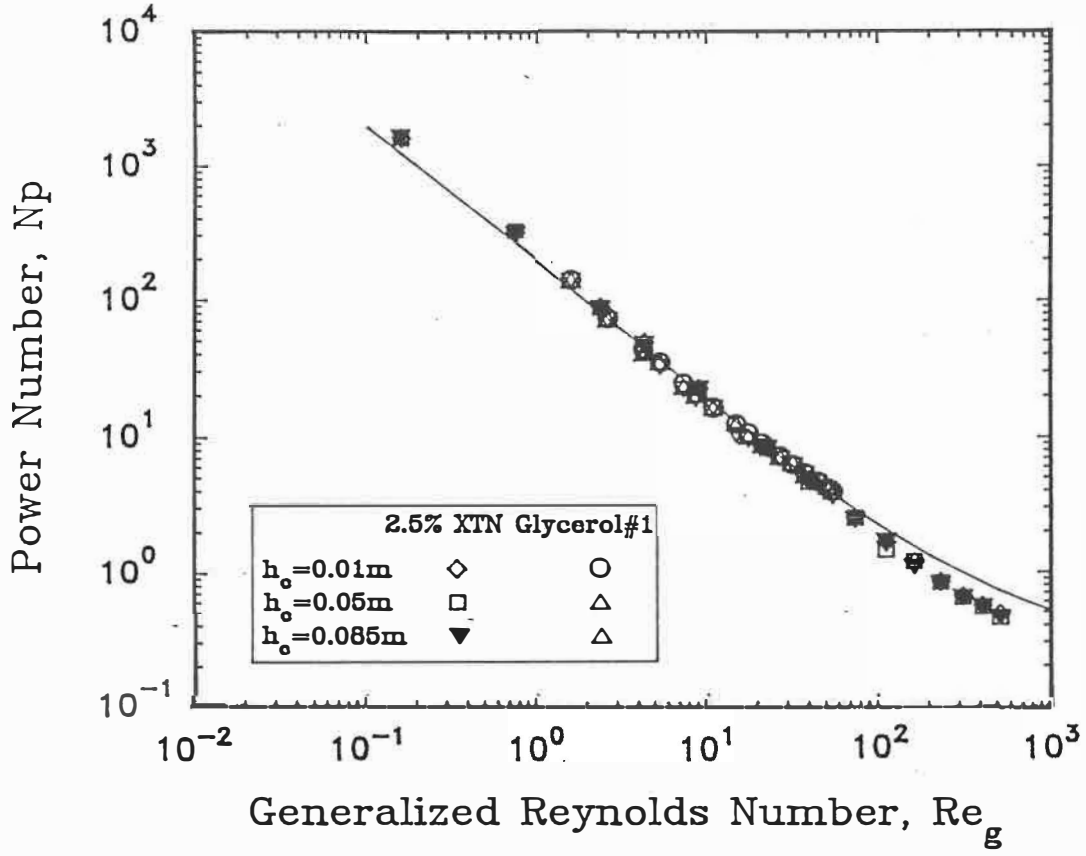

Figure 9 Bottom effect on the power consumption

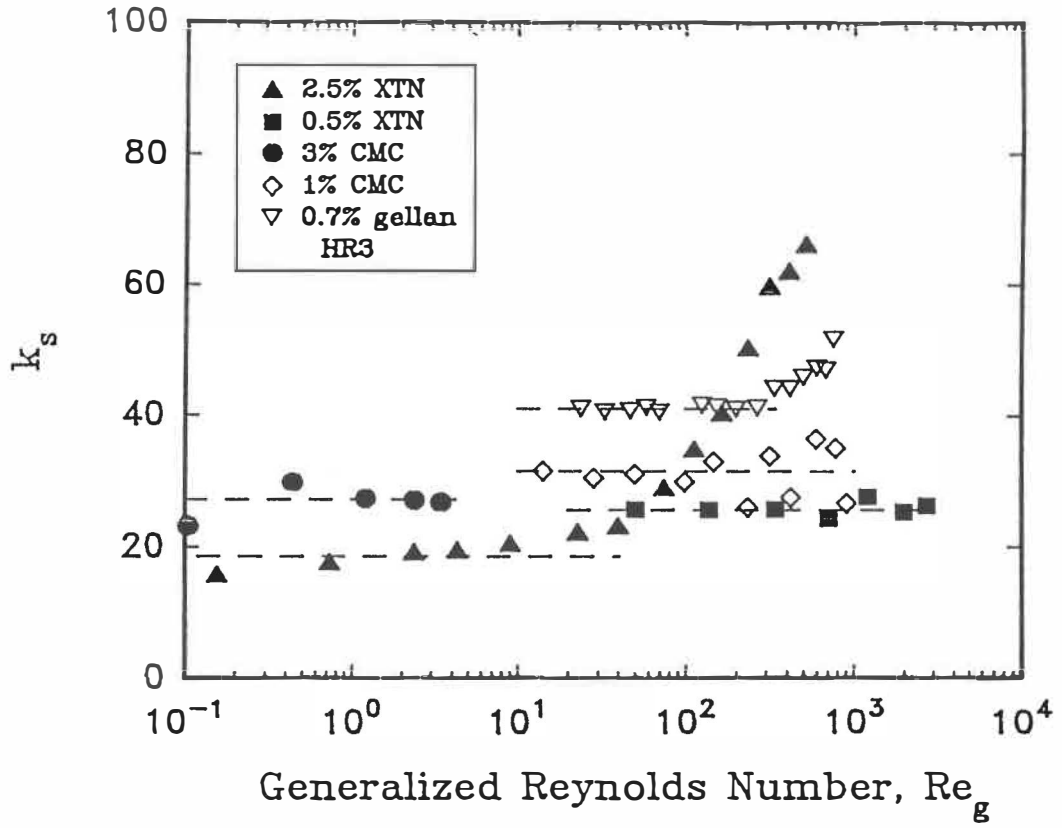

Figure 10 Variation of k_s with generalized Reynolds number for the shear-thinning inelastic fluids

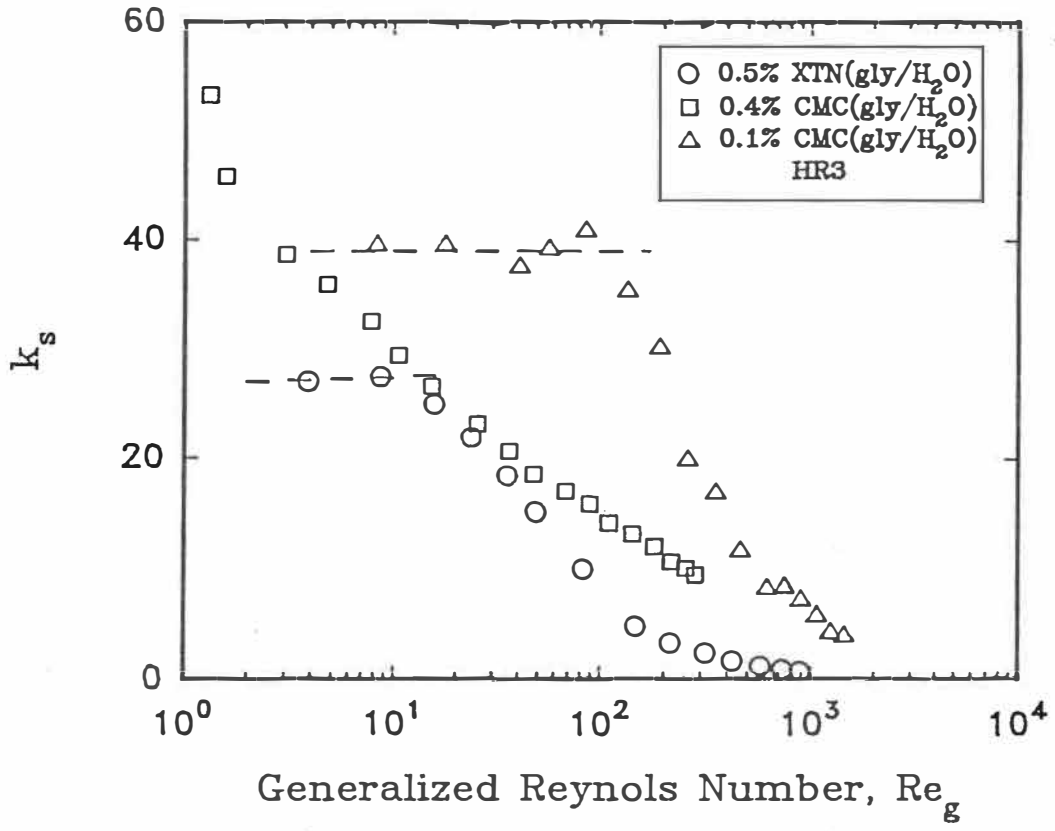

Figure 11 Variation of k_s with generalized Reynolds number for viscoelastic fluids

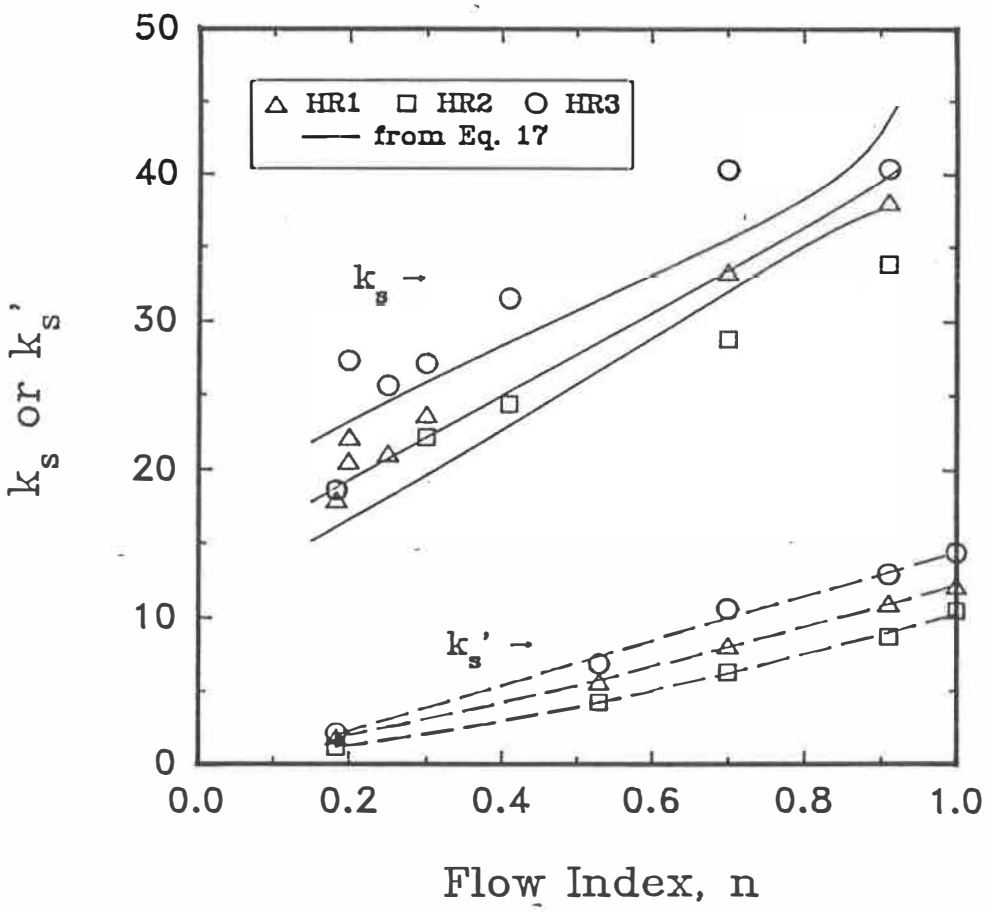

Figure 12 Dependence of k_s or k_s' on the flow index n

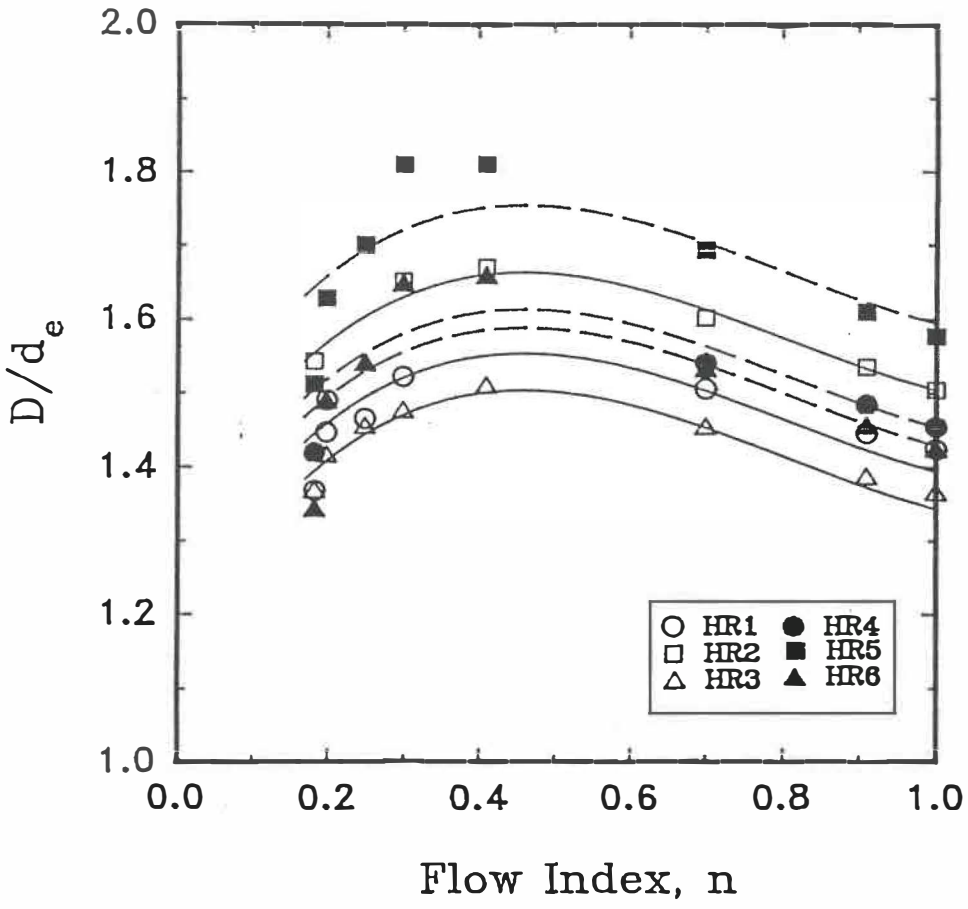

Figure 13 Dependence of D/d_e on the flow index n

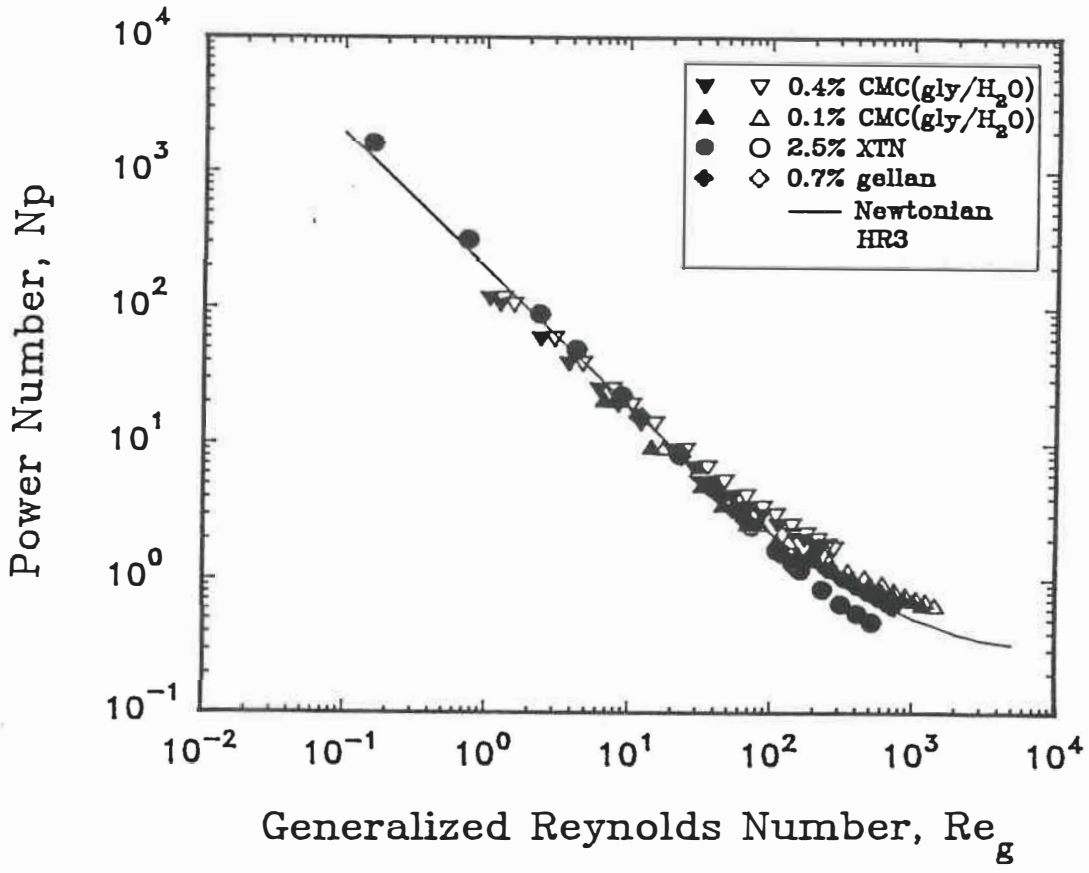

Figure 14 Power predictions using d_e from Newtonian data (value reported in Table 1). Open symbols: experimental; solid symbols: predictions

Chapter 4 AERATED MIXING

Aerated Mixing of Viscoelastic Fluids with Helical Ribbon Impellers

Jianya CHENG and Pierre J. CARREAU*

Centre de recherche appliquée sur les polymères, CRASP
Department of Chemical Engineering
Ecole Polytechnique
C.P. 6079, Succursale A
Montreal, Quebec, Canada H3C 3A7

* Author for correspondence

submitted to *Chem. Engng. Sci.*

4-1. ABSTRACT

Aerated mixing of shear thinning and elastic fluids with helical ribbon impellers in the laminar and transition flow regimes has been investigated. Various Newtonian, shear-thinning inelastic, viscoelastic and non shear-thinning elastic fluids have been chosen to assess the influence of complex rheological properties on the power requirement. For the first time, the power requirement in non shear-thinning elastic fluids is shown to be larger in gassed systems than in ungassed fluids, while a decrease of power is observed for the shear-thinning inelastic fluids. The gassed power is also dependent on the gas flow rate and Reynolds number. Two correlations are proposed in the laminar and transition flow regimes respectively to predict the power consumption as functions of the Reynolds number defined for aerated non-Newtonian fluids, the aeration and Weissenberg numbers. Gas hold-up, bubble size and bubble behaviour have also been studied.

4-2. INTRODUCTION

Aerated mixing of liquids in mechanically agitated vessels is involved in many chemical processes. Gas dispersion is a dominating step controlling the process in most gas-liquid chemical reactions. The evolution of research in this field has been since carried out mainly for disk turbine type impellers, but focused in water like solutions and low viscous fluids. Excellent reviews of gas dispersion in agitated tanks are available (Nagata 1975, Oldshue 1983, Smith 1985, Nienow and Ulbrecht 1985, Tatterson 1991). Difficulties arise for gas-liquid systems especially for rheological complex fluids (Smith, 1990). Alone with gas distribution, mass transfer etc, the power consumption has been a topic of high interest. The power input is not only an

important design parameter but also reflects the flow pattern changes and the rheological properties in such complicated systems (Ulbrecht and Carreau, 1985). Some of those rheological properties cannot be determined in a simple or direct way and/or method. Of those is the apparent primary normal stress difference of the dispersion. The whole picture of gas dispersion, even for disk style turbine impellers, is far from being clarified. Further more, gas dispersion in agitated systems with helical ribbon impellers has barely investigated, although its applications have been widely used in biochemical fermentation and polymerization etc, where the media encountered are frequently viscoelastic fluids. It can be misleading to extrapolate the results obtained from disk turbine type impellers to helical ribbon impellers. There is a quite pronounced gap between the current available knowledge and the requirements for design and scale-up of gas-liquid agitators with helical ribbon impellers, for both low viscous fluids in general and non-Newtonian viscoelastic fluids in particular. This work was carried out in an attempt to fill part of this gap. The effects of the fluid's complex rheological properties, gas distribution, gas flow rate and flow pattern on the power consumption in the reservoirs agitated by helical ribbon impellers has been investigated.

4-3. EXPERIMENTAL

The experimental set-up is schematically shown in Figure 1. The gas was introduced through a 200 mm diameter circular tube sparger with 20 holes of 2 mm diameter placed in the bottom of vessel. The gas flow rate was measured by a pre-calibrated rotameter. The reader is referred to Carreau et al.(1993) for a detailed description of equipment and methods for torque measurement, ungassed rheological property measurement in steady state and test fluids used in this work. The geometrical ratios of D/d, w/d, p/d, h/d of the typical helical ribbon impeller reported in this work are

respectively 1.11, 0.133, 0.695, 1.05 (geometry HR3 in Carreau et al., 1993)

Gas hold-up was measured by measuring the change of the fluid's level in the tank in absence of vortex. The measurement of the apparent viscosity of the dispersion was carried out using a Bohlin portable rheometer (Visco 88, Bohlin). Fluid samples for different gas hold-up were quickly withdrawn from the well mixed system, then injected into the cylinder cup of the Bohlin rheometer to measure the variation of the apparent viscosity with time under a given shear rate. The sizes of the small bubbles for samples tested in the Bohlin rheometer were measured using a microscope (American Optical Company, MOD 569, 0.7 to 3.0X). The reader is also referred to Carreau et al(1993) for the ungassed rheological properties and parameters of test fluids used in this work. The test fluids can be classified into two types: inelastic shear-thinning fluids and elastic fluids. The 2.5% xanthan (XTN) and the 1% and 3% CMC aqueous solutions belong to the inelastic shear- thinning fluids, while the 800 ppm polyacrylamide (PAA) in corn syrup solution, the 0.35% polyisobutylene (PIB) dissolved in 23% kerosene and 77% polybutene (PB) and the 0.5% xanthan in 15% water and 85% glycerol solution show elastic properties.

4-4. RESULTS AND DISCUSSION

The variations of the apparent viscosity of the dispersion with time were measured at different gas hold-up at given shear rates for the elastic 800 ppm PAA solution in corn syrup and the inelastic shear thinning 2.5% xanthan and 1% CMC aqueous solutions. The results are shown in Figures 2 and 3 respectively (where ε_0 is the initial value for the gas hold-up of the tested sample). Surprisingly for the elastic fluids, the apparent viscosity of the dispersion is found to be much higher than for the ungassed fluids. As seen in Figure 2, it is almost 2 fold higher for high gas hold-up level and it increases with gas hold-up. As far as we are aware, this behaviour has never been

reported before. For the inelastic shear-thinning 2.5% xanthan and 1% CMC solutions, a slight enhancement of the apparent viscosity of the dispersion is observed (shown in Figure 3). It can be argued that the bubbles inside the elastic fluids may behave as solid spheres to enhance the apparent viscosity. The increased viscosity for gassed Boger fluids may be also explained by interactions between the high deformable particles and the viscoelastic fluids. Nevertheless, the finding of this work is surprising and this information is helpful for a better understanding of the power requirement for dispersions.

In an attempt to understand the mechanism for the increase on the apparent viscosity of the dispersions, the sizes of the small bubble of the fluid samples tested in Bohlin Rheometer were measured. The sizes for the 0.5% xanthan, 2.5% xanthan aqueous solutions and 800 ppm PAA corn syrup solution are 0.25 ~ 0.35 mm, 0.60 ~ 0.75 and 1.0 ~ 1.4 mm, respectively. Gas flow rate in the mixing vessel appears not to affect the bubble dimensions. The gas hold-up of the tested samples for such small bubbles are 6.2 ~ 7.0% for the 800 ppm PAA in corn syrup solution and 3.5 ~ 4.1% for the xanthan aqueous solution. We notice that the gas hold-up of small bubbles is higher for elastic fluids than for inelastic shear-thinning fluids.

4-4-1. MIXING WITH AERATION

The power number and the generalized Reynolds number in the mixing system are defined respectively as

$$Np = P/d^5 N^3 \rho \qquad (1)$$

$$Re_g = d^2 N\rho/\eta_e \qquad (2)$$

where P is the power input in the mixing system, η_e is the effective viscosity and is

evaluated from Metzner-Otto's (1957) method assuming that the effective shear rate is proportional to the impeller rotational speed in the laminar flow regime, i.e.

$$\dot{\gamma}_e = k_s N \tag{3}$$

The reader is referred to Carreau et al.(1993) for values of k_s obtained in this manner under ungassed conditions (the typical geometry used here is HR3 in the work of Carreau et al., 1993).

In the procedure to develop a more suitable power correlation for non-Newtonian fluids, the need of a corrected effective shear rate under aerated conditions has emerged. The effective shear rate of fluids under aerated conditions is expected to be different from that without aeration, due to additional deformation caused by the presence of bubbles and bubble stretching in the liquid. A simple approach consists of combining the shear deformation caused by bubbles' passage and deformation caused by the impeller blades. Hence, we define here an aerated effective deformation rate as

$$\dot{\gamma}_a = \sqrt{\dot{\gamma}_b^2 + \dot{\gamma}_e^2} \tag{4}$$

where $\dot{\gamma}_e$ is the deformation rate caused by the mechanical agitation and is calculated by the Metzner-Otto method under ungassed conditions (via Eq.3), $\dot{\gamma}_b$ is the additional deformation rate due to bubbles' flow. Due to the lack of a detailed flow field for gassed fluids, the additional deformation rate is estimated using the concept of Hashikawa et al.(1977), which was initially proposed for gas-liquid bubble columns, i.e.

$$\dot{\gamma}_b = 1500\ v_g \tag{5}$$

where v_g is the superficial gas velocity and the proportionality constant value of *1500* (m^{-1}) as used by Henzler (1980) is retained here. Obviously, the value for the Reynolds number under aerated conditions, Re_a, evaluated from the aerated deformation rate

$\dot{\gamma}_{a,}$ is higher than the unaerated one for shear-thinning fluids and increases with increasing gas flow rate. For easier comparison of gassed results with ungassed ones, the generalized Reynolds number Re_g calculated via Eq.2 is still used in parts in the next section, while the aerated Reynolds number Re_a will be used for the power correlations.

4-4-2. Newtonian and inelastic fluids

The power consumption for Newtonian and inelastic shear-thinning fluids with different aerated levels is plotted as a ratio of gassed over ungassed power, P_g/P_o, versus the generalized Reynolds number, Re_g, and the results are shown in Figures 4 and 5. The power ratio for the Newtonian glycerol solution (μ = 0.47 Pa.s) in the range of Re_g from 28 to 440 is found to be almost constant and independent of gas flow rate.

For the shear-thinning fluids, the power input decreases as gas is sparged at low Reynolds number values, then the ratio P_g/P_o increases with increasing Reynolds number, and eventually levels off. There is no comparable literature data available for helical ribbon impellers. The gassed power input decreases as gas flow rate is increased. This finding is different from the previous observations made by Nienow et al.(1983) who found the gassed power input to be independent of gas flow rate for turbine impellers in shear-thinning CMC fluids. Also similar trend were found by Özecan et al.(1988) for Newtonian fluids and by Ranada and Ulbrecht (1977) for shear-thinning PAA aqueous. The difference with our observations may be due to the low level of gas sparging rates used by the other authors and more properly due to the different mechanisms for gassed power in systems agitated by helical ribbon impellers compared to disk turbine type impellers. Carpenter (1986) found that P_g/P_o initially decreased as gas was sparged and then climbed up as the gas flow rate increased above 0.5 $\times 10^{-3}$ m^3/s.

There is a minimum ratio of P_g/P_o for the 3% CMC aqueous solution as seen in Figure 4. The power reduction in the highly shear-thinning 2.5% xanthan aqueous solution is much more pronounced than that for the fairly shear-thinning 1% and 3% CMC aqueous solutions under the same gas flow rate and Reynolds number. But the differences in power reduction between these two kinds of fluids level off at larger Re_g values. At lower rotational speeds, large size bubbles are formed and then pass through the liquid; the break-up of bubbles rarely occurs and the bubbles appear to follow the impeller blade over a certain period, then exit the fluid through the free surface. It may be argued that those large bubbles behind the impeller blades can somewhat reduce the shear stress exerted on the blade's surface, and hence lead to the reduction of the power requirement. With increasing rotational speed, the bubbles are broken down to form a much finer dispersion then the power consumption possibly increases

4-4-3. Elastic Fluids

Gassed power consumption for the elastic 800 ppm PAA in corn syrup and 0.35% PIB solution dramatically increases, in contrast to the results obtained for the inelastic shear-thinning fluids discussed above. As shown in Figure 6, the gassed power input increases with increasing gas flow rate, at lower Reynolds numbers and it is almost 3 time higher than the ungassed power at the same rotational speed. This somewhat coincides with the enhancement of the apparent viscosity of the dispersion (2 fold higher, as seen in Figure 2). As far as we know, this sharp enhancement of gassed power has not been reported before. Such highly elastic constant viscosity fluids (so called Boger fluids, Boger and Binnington, 1977) have never been studied in gassed agitated systems. Although viscoelastic fluids have been investigated before, they are usually shear-thinning and their shear-thinning properties may somewhat overshadow the elastic effects. The different flow patterns generated by helical ribbon impellers

compared to patterns generated by disk turbine type impellers, and under different flow regimes, may lead to different mechanisms for gas dispersion, then marked differences in the power requirement. The power data, P_g, reported in Figure 6, does not include the power required to inject air in the mixing vessel. The sparging power is about 20% or less of the mechanical power consumption under aerated conditions (see Guy and Carreau, 1986, for detailed description of calculation of the sparging power). However, the sparging power to the mechanical power will not change much the power ratios, reported in Figure 6.

At low impeller rotational speeds, very large size bubbles were observed, and the break-up of such large bubbles in highly elastic fluids appears to be very difficult at low speed. The impeller blades stretch the bubbles as they pass near the blade surface. The extensional energy required to break up such bubbles due to the fluid's elastic memory effect could be quite large. This may partially explain the high power input at low Reynolds number (e.g. low rotational speed). On the other hand, the higher apparent viscosity of the dispersion for elastic fluids may also lead to increases in the power requirement. With increasing rotational speed, the bubbles are broken-up right after emerging from the orifices of the sparger. Some unbroken bubbles move up rapidly via the central area. The power ratio eventually reduces to 1, but this is higher then for values obtained for the inelastic fluids.

The overall gas hold-up for the elastic 800 ppm PAA in corn syrup is considerably higher than that for the Newtonian glycerol solution and the inelastic shear-thinning fluids (2.5% and 0.5%xanthan aqueous solutions) at the same gas flow rate and rotational speed, as shown in Figure 7. These hold-up results obtained for the main vessel should be compared with the gas hold-up results for the fluids samples containing only small bubbles (mentioned before for the rheological measurements). The hold-up for the highly shear-thinning 2.5% xanthan solution is lower compared to that for the fairly shear-thinning 0.5% xanthan solution which has almost the same

hold-up level as the glycerol solution of comparable viscosity. Bubble coalescence in elastic fluids is more difficult than in shear-thinning inelastic fluids, as observed by Dekee et al.(1986). A special gas ascension phenomenon was observed for elastic fluids at high gas flow rates and low rotational speeds. Under such circumstances, a layer of bubbles is formed and move up without being deformed by the blade action. There is a critical impeller speed needed to achieve a good dispersion in highly elastic fluids. Unfortunately, no photograph of the gas dispersion for the elastic fluids used in this work could be taken due to the fluid's opacity.

4-4-4. Gassed Power Correlation

Various correlations for gassed power have been proposed by a number of investigators from Calderbank (1958) to the recent work of Murugesan and Degaleesan (1992). Of those, the Michel and Miller (1962) correlation is found to be fit most gassed power data, although this correlation originally was proposed for Newtonian water like liquids. The correlation is

$$P_g = C\left(\frac{P_o^2 N D^3}{Q^{0.56}}\right)^{0.45} \tag{6}$$

where Q is gas flow rate and C is constant. However, the non-Newtonian effects on gassed power onset is not accounted in Michel and Miller's correlation. Furthermore, the dimensions of the quantities of this correlation are not appropriate for generalization. We prefer to use a dimensionless analysis. The gassed power for no-Newtonian fluids can be expressed as a function of the aerated Reynolds number, Re_a, aeration number, $Na\ (Q/Nd^3)$, and Weissenberg number, $Wi\ (\psi_1 N/\eta_a)$, i.e.

$$Np = C_1\, Re_a^{C_2}\, Na^{C_3}\,(1 + c_4 Wi^{c_5}) \tag{7}$$

Where ψ_1 is the primary normal stress difference coefficient and η_a is the aerated

effective viscosity evaluated from the aerated effective deformation rate, $\dot{\gamma}_a$.

An attempt has been made to correlate the gassed power data for the Newtonian, inelastic shear thinning fluids, and viscoelastic fluids for all the conditions. A single correlation could not obtained. However, two successful correlations are proposed for the laminar and transition flow regime respectively:

Laminar flow regime, $0.28 \leq Re_a \leq 70$ ($0.028 \leq Na \leq 0.87$, $0.0044 \leq Wi \leq 0.060$):

$$Np = 1030\ Re_a^{-0.942}\ Na^{0.604}\ (1 + 724 Wi^{2.15}) \qquad (8)$$

Transition flow regime, $70 \leq Re_a \leq 2600$ ($0.0087 \leq Na \leq 0.63$, $0.013 \leq Wi \leq 0.96$):

$$Np = 40.3\ Re_a^{-0.623}\ Na^{0.06}\ (1 + 3.79 Wi^{0.057}) \qquad (9)$$

Figure 8 shows that the correlations fit very well the data. Ta the transition point, $Re_a = 70$, a single value of Np of the correlations is obtained and we notice that for the laminar regime without aeration, Eq.8 reduces to the classical results for Newtonian fluids ($Wi = 0$). In the transition flow regime, aeration number Na has very slight effect on the gassed power while the power number increases with increasing Na with power of 0.604 in the laminar regime. There is no conflict between the experimental evidences that power decreases with increasing gas flow rate, and this correlation. The power decrease due to the increase of gas flow rate is already accounted by using the aerated generalized Reynolds number, Re_a. Weissenberg number, Wi, has larger effect (with power of 2.15) on the gassed power in the laminar regime than in transition regime.

4-5. CONCLUSION

This work investigates the aerated mixing of shear thinning and elastic fluids with helical ribbon impellers in the laminar and transition flow regimes. For the first time, the gassed power consumption in no shear-thinning elastic fluids was found to be much larger than that in ungassed fluids. It is more than 3 fold higher at high gas flow rates and low Reynolds number values, which somewhat coincides with increases of the apparent viscosity of the dispersion. The decrease of the ratio of gassed over ungassed power was observed for Newtonian and inelastic shear thinning fluids and this power ratio levels off at high Reynolds number. Larger bubble size and gas hold-up were observed for elastic fluids than for inelastic fluids and rather poor dispersion occurred at low rotational speeds. Two power correlations for the laminar and transition flow regimes are proposed as functions of the aerated Reynolds number, aeration number and Weissenberg number.

4-6. Acknowledgement

The financial support received from FCAR Program of the Province of Quebec is gratefully acknowledged.

4-7. REFERENCES

Boger D.V. and Binnington R., 1977, Separation of Elastic and Shear Thinning Effects in Capillary Rheometer, *Trans. Sco. Rheol.,* **21**, 515-534.

Calderbank, P.H., 1958, Physical Rate Processes in Industrial Fermentations, *Trans. Inst. Chem. Engng.,* **36** 517.

Carpenter K.J., 1986, Fluids Processing in Agitated Vessels, *Chem. Engng. Res. Des.,* **64**, 3-10.

Carreau P.J., Chhabra R.P. and Cheng J., 1993, Effect of Rheological Properties on Power Consumption with Helical Ribbon Agitators, *AIChE J.,* in press.

Dekee D., Carreau P.J. and Mordanski J., 1986, Bubble Velocity and Coalescence in Viscoelastic Fluids. *Chem. Engng. Sci.* **41**, 2273-2283.

Henzler, 1980, Begasen Höherviskoser Flüssigkeiten, *Chem. Ing. Tech.,* **52,** 643-652.

Machon V. Vlcek J. Nienow A.W. and Solomon J., 1980, Some Effects of Pseudoplasticity on Hold-up in Aerated, Agitated Vessels, *Chem. Engng. J.,* **19**, 67-74.

Metzner A.B. and Otto R.E., 1957, Agitation of Non-Newtonian Fluids, *AIChE J.,* **3**. 3-10.

Michel B.J. and Miller S.A., 1962, Power Requirements of Gas-Liquid Agitated Systems, *AIChE J.* **8,** 262-266.

Murugesan T. and Degaleesan T.E., 1992, Holdup, Interfacial Area and Power Requirement in Turbine Agitated Gas-Liquid Contactors, *Chem. Engng. Commun.,* **117**, 263-278.

Nagata S., 1975, Mixing: Principles and Applications, Halstead, New York.

Nienow A.W., Wisdom D. J., Solomon J. Machon V. and Vlcek J., 1983, The Effect of Rheological Complexities on Power Consumption in An Aerated Agitated Vessel, *Chem. Engng. Commun.,* **19**, 273-293.

Nienow A.W. and Ulbrecht J.J., 1985, Gas-Liquid Mixing and Mass Transfer in High Viscosity Liquids, *in Mixing of Liquids by Mechanical Agitation,* (Eds: Ulbrecht J.J. and Patterson G.K.), Gordon and Breach, New York.

Nishikawa M., Kato H. and Hashimoto K., 1977, Heat Transfer in Aerated Tower Filled with Non-Newtonian Liquid, *Ind. Engng. Chem. Proc. Des. Dev.,* **16**. 133-137.

Özecan G., Decloux M. and Bruxelmane M., 1990, Effect of Viscosity on Cavity Formation and Power Characteristics of an Agitated Aerated Newtonian Fluid, *Trans, IChemE,* **68**, Part A, 63-68.

Ranada, V.R. and Ulbrecht J.J., 1977, Gas Dispersion in Agitated Viscous Inelastic and Viscoelastic Liquids, *Proc. 2nd European Mixing Conf.,* BHRA Fluid Eng., Cambridge, England, F6-83 to F6-89.

Smith J.M., 1985, Dispersion of Gases in Liquids: The Hydrodynamics of Gas Dispersion in Low Viscosity Liquids, *in Mixing of Liquids by Mechanical Agitation,* (Eds: Ulbrecht J.J. and Patterson G.K.), Gordon and Breach, New York.

Smith J.M., 1990, Industrial Needs for Mixing Research, *Trans, IChemE,* **68,** 3-6.

Tatterson G.B., 1991, Fluid Mixing and Gas Dispersion in Agitated Tanks, McGraw-Hill, New York.

Ulbrecht J.J. and Carreau P.J., 1985, Mixing of Viscous Non-Newtonian Liquids, *in Mixing of Liquids by Mechanical Agitation,* (Eds: Ulbrecht J.J. and Patterson G.K.), Gordon and Breach, New York.

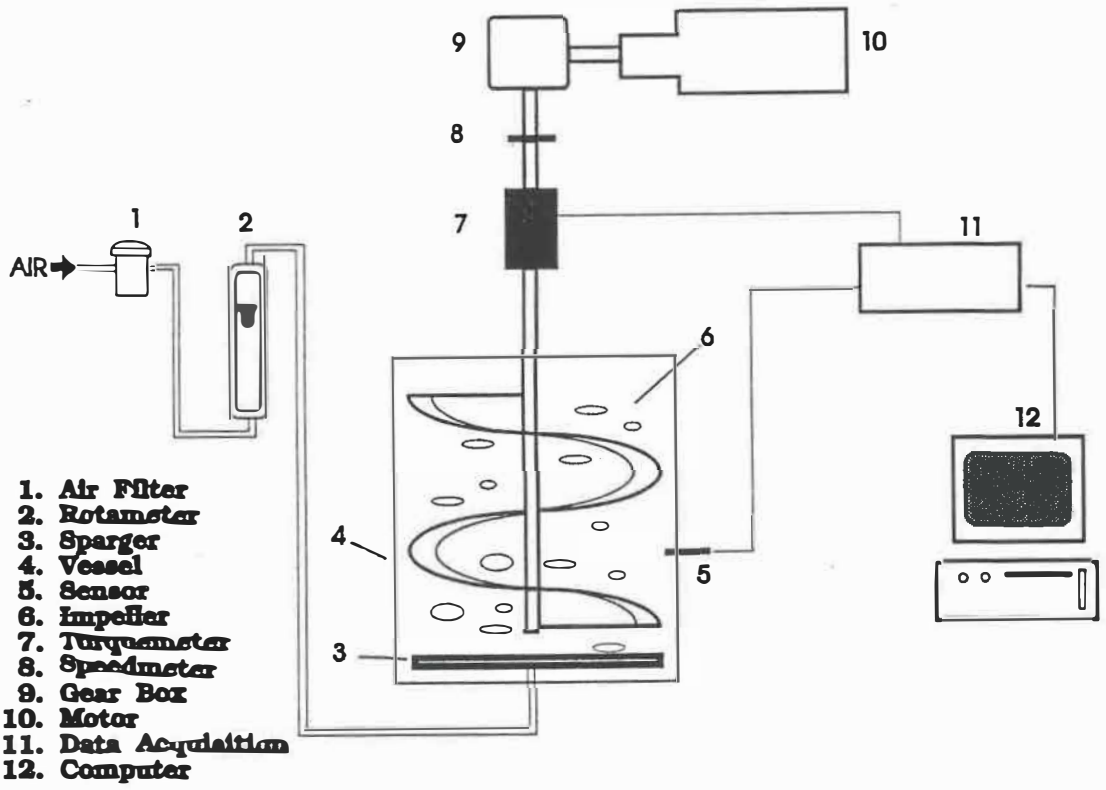

Figure 1 Sketch of experimental equipment

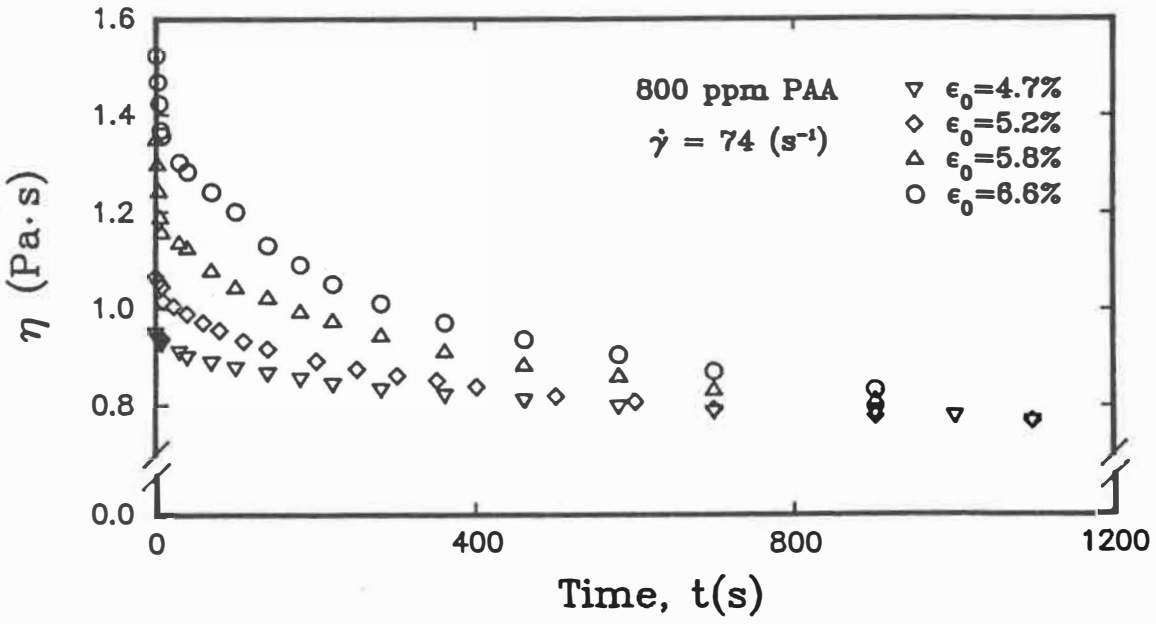

Figure 2 Variation of the apparent viscosity of dispersion with time for the elastic 800 ppm PAA solution

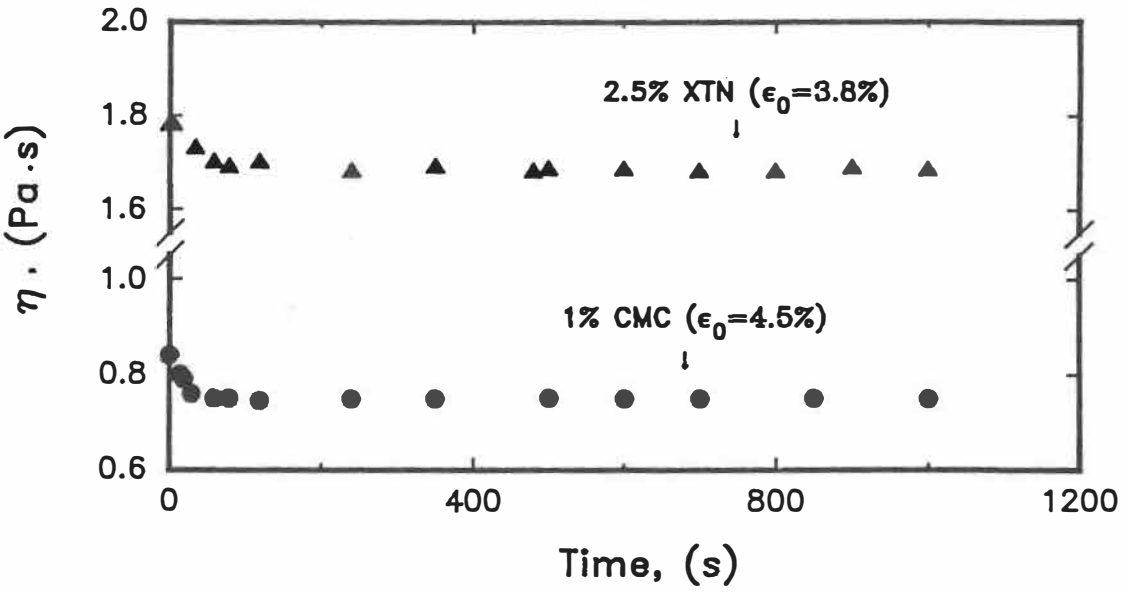

Figure 3 Variation of the apparent viscosity of dispersion with time for the shear-thinning inelastic xanthan and 1% CMC aqueous solutions ($\dot{\gamma}$ = 42 s^{-1})

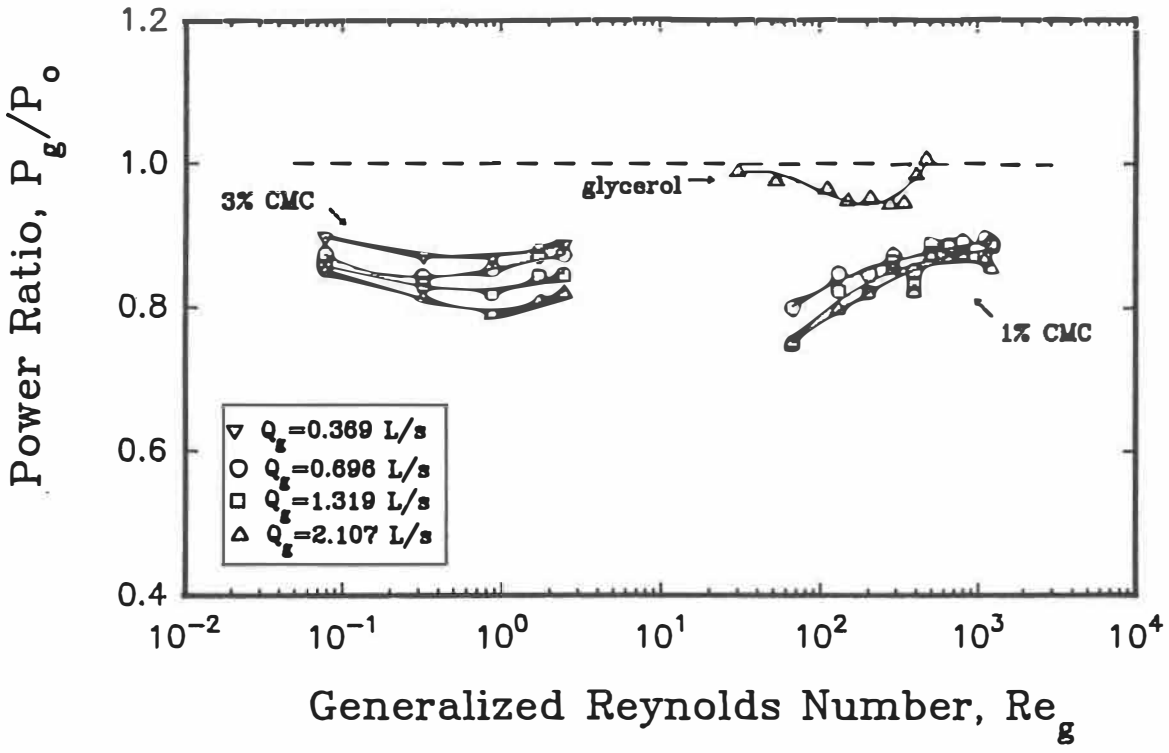

Figure 4 Gassed power data for Newtonian and shear-thinning fluids

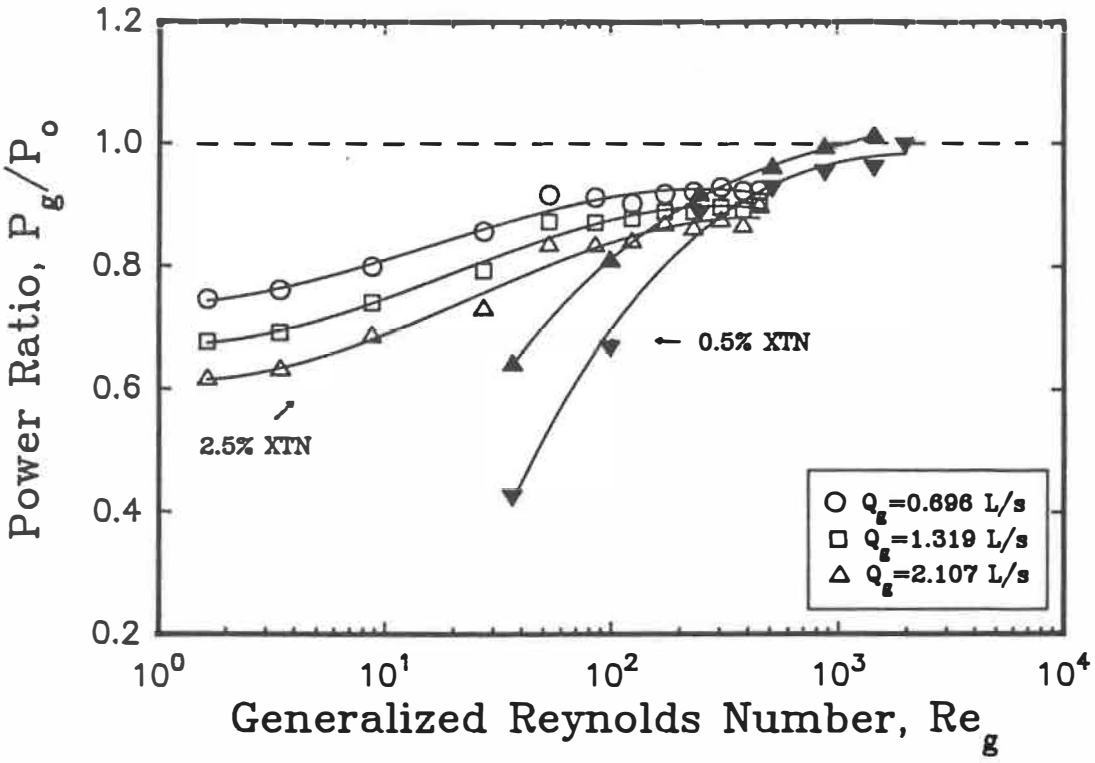

Figure 5 Gassed power data for shear-thinning fluids (△ □ ○: 2.5% xanthan, ▲ ▼: 0.5% xanthan)

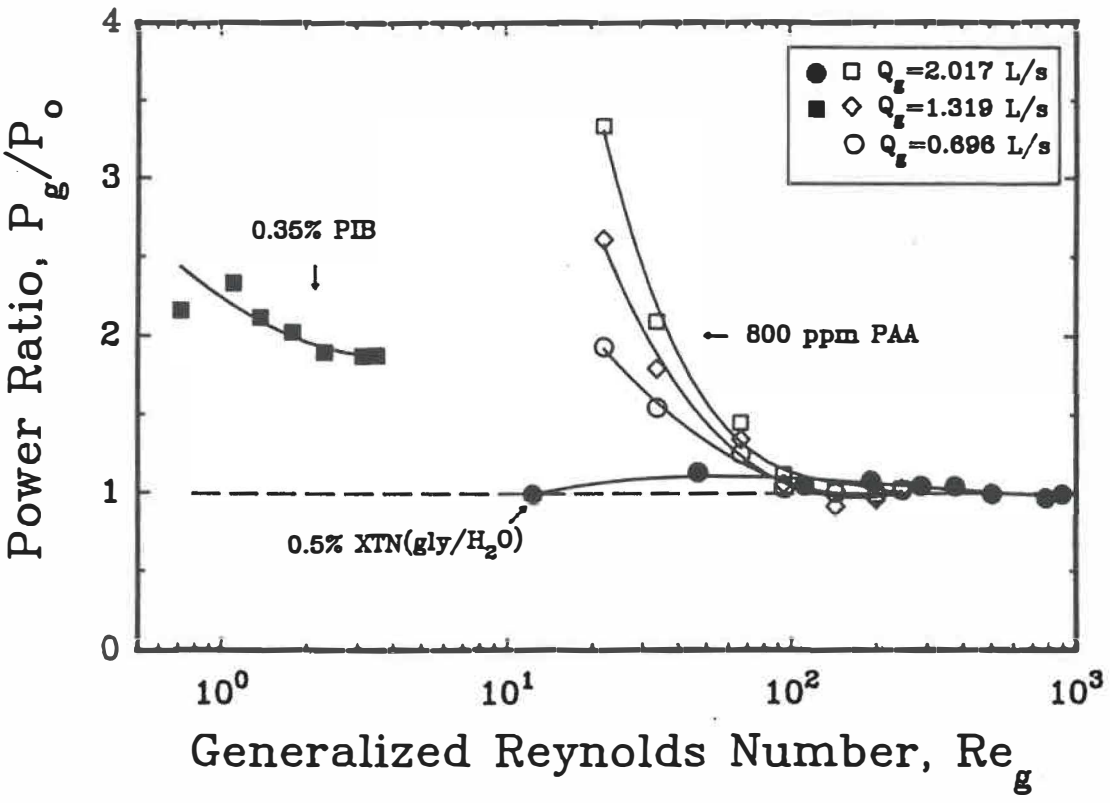

Figure 6 Gassed power data for elastic fluids (□ ◇ ○: 800 ppm PAA, ■: 0.35% PIB, ●: 0.5% xanthan (gly/H_2O))

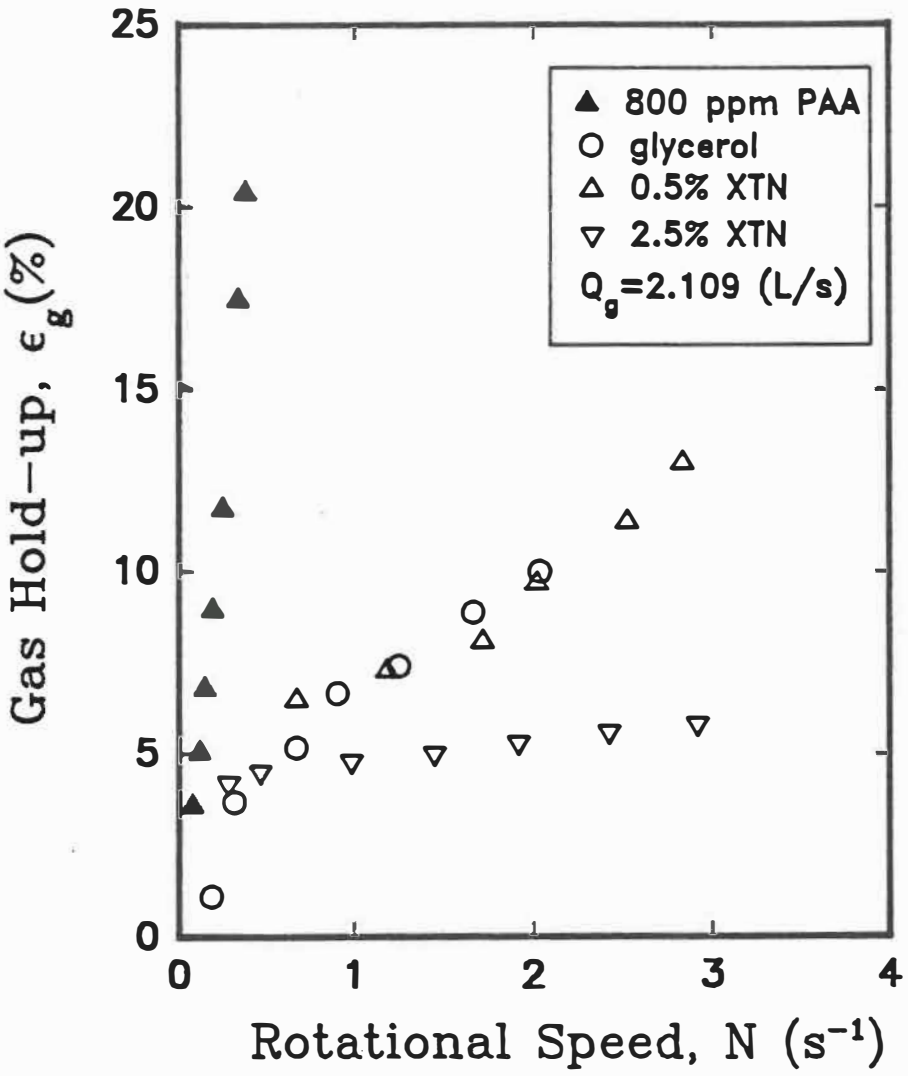

Figure 7 Variation of gas hold-up with impeller rotational speed

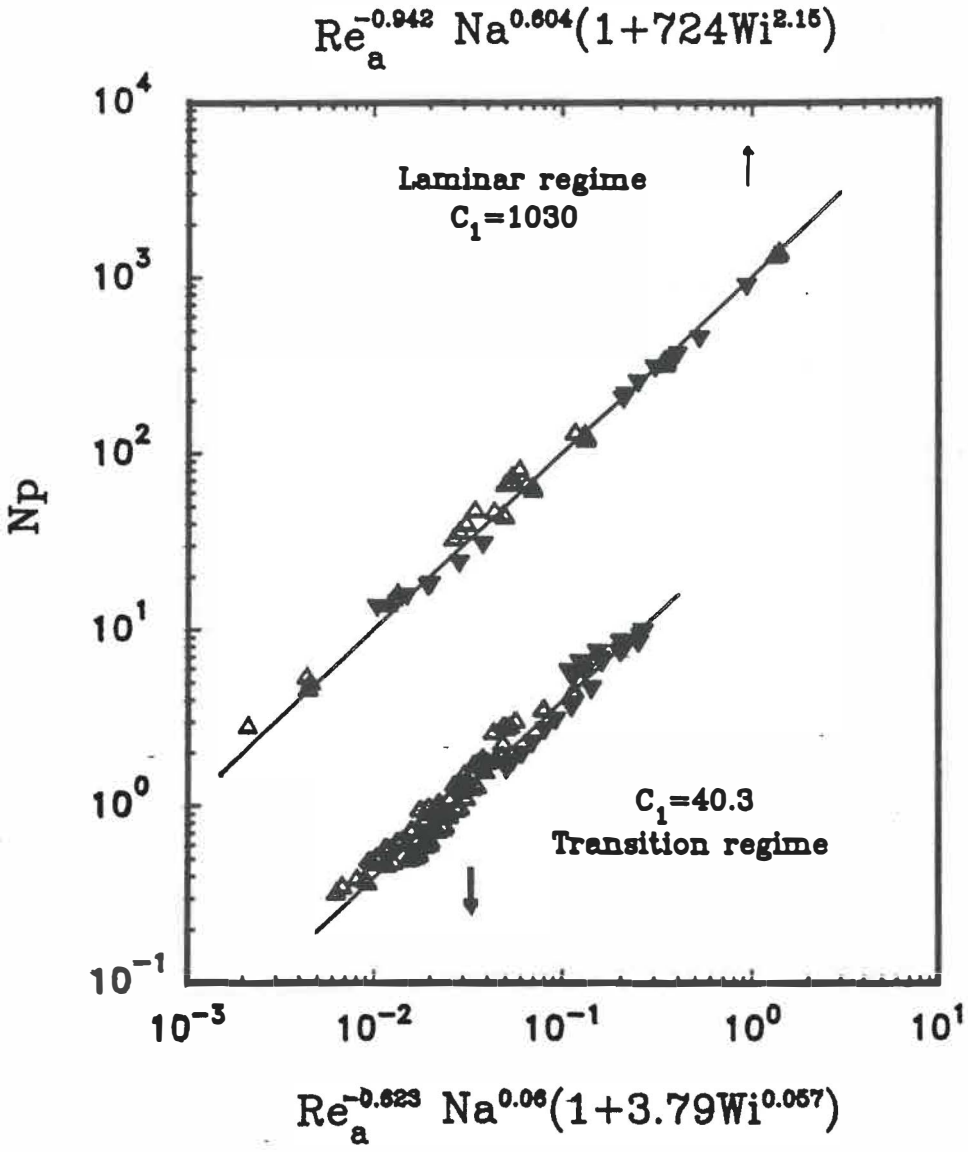

Figure 8 Power correlations (△: Newtonian and inelastic shear-thinning fluids, ▲: elastic fluids)

Chapter 5 MIXING IN TRANSITION FLOW REGIME

Mixing in the Transition Flow Regime with Helical Ribbon Agitators

Jianya CHENG and Pierre J. CARREAU*,

Centre de recherche appliquée sur les polymères, CRASP
Department of Chemical Engineering
Ecole Polytechnique
C.P. 6079, Succusale A
Montreal, Quebec, Canada H3C 3A7

* Author for Correspondence

submitted to *Can. J. Chem. Eng.* (1993)

5-1. ABSTRACT

The effects of the non-Newtonian properties on the effective deformation rate, mixing and circulation times and flow behaviour have been investigated in the transition flow regime of mixing systems. Based on the equivalent Couette flow, three models are proposed and are shown to predict similar and drastic increases of the effective deformation rate with the impeller rotational speed in the transition regime. The predictions are shown to fit very well data obtained for various non-Newtonian fluids mixed with helical ribbon agitators, and with literature data for anchor, blade turbine and flat disc agitators. The elasticity along with shear-thinning properties appear to have slight effect on the dimensionless mixing and circulation times in the transition regime whereas their effects in the laminar regime are quite drastic, as reported by others.

5-2. RÉSUMÉ

L'influence des propriétés non newtoniennes sur la vitesse de déformation effective, les temps de mélanges et de circulation et sur les patrons d'écoulement a été étudiée pour le mélange dans un réservoir en régime transitoire. Utilisant sur l'analogie avec l'écoulement couette, on a proposé trois modèles, qui prédisent de façon semblable des augmentations très marquées de la vitesse de déformation effective en fonction de la vitesse de l'agitateur en régime transitoire. Les modèles décrivent très bien les résultats obtenus pour plusieurs fluides non newtoniens mélangés par des agitateurs à lames hélicoïdales et les résultats de la littérature pour des agitateurs de type ancre, turbine à lames et disque plat. Les propriétés élastiques ainsi que la rhéofluidifiance ont peu d'effet sur les temps adimensionnels de mélange

et de circulation en régime transitoire alors que leurs effets en régime laminaire sont très marqués, tel que rapporté par d'autres auteurs.

Key Words:
Mixing, Transition regime, Effective shear rate, Non-Newtonian fluids.

5-3. INTRODUCTION

Mixing of low viscosity liquids is normally achieved in turbulent flow to take advantages of the rapid transfer and reaction rates, which could be an order of magnitude larger than the rates in laminar flow. However, for many industrial materials, such as viscoelastic polymeric liquids, suspensions, etc, it is impossible or impractical to operate under turbulent mixing. One then has to proceed in the laminar or at best in the transition flow regime. Due to the complexities and uncertainties of mixing in the transition regime, it makes it difficult to predict mixing performances and power requirement for rheological complex non-Newtonian fluids, especially for scaling up (Ulbrecht and Carreau, 1985, Smith, 1990). The influence of the complex non-Newtonian properties (in particular, viscoelasticity), secondary flow pattern and flow irregularity is expected to be more and more pronounced, as the inertial forces become more and more important. This area of research is still in an early exploring stage although some work has been carried out in this filed. Available data obtained from the laminar regime has been used to design and scale up mixing operations in the transition regime due to lack of information in the transition regime. This could, however, lead to considerably misleading results and totally wrong designs. Modelling using numerical methods, rather than empirical methods, for the transition flow regime, has been highlighted to be likely much successful (Smith, 1990).

The effective shear or deformation rate, to evaluate the effective viscosity, is a very important design parameter (we prefer to use the word "*effective deformation rate*"

since the complex three dimensional flow in a mixing vessel is not only simple shear flow, but contains a non negligible extensional part). The significant method suggested by Metzner and Otto (1957) to evaluate the effective deformation rate is limited in the laminar flow regime and is no longer valid in the transition regime (Metzner et al. 1961, Polard and Kantyka, 1969, 1971, Bourne et al., 1980, Forschner et al. 1991, and Carreau et al. 1993). It was pointed by Ulbrecht and Carreau (1985) that use of the Metzner-Otto method could lead to very large errors for scale-up in the transition flow regime. Forschner et al. (1991) mentioned that the power input for non-Newtonian fluids in the transition flow regime is significantly overestimated by using the Metzner-Otto and the Rieger-Novak (1965) methods, due to additional shear caused by increasing fluctuating velocities. Experimental evidences have shown that shear thinning appears to increase the effective shear rate (Metzner et al. 1961, Polard and Kantyka, 1969, Nagata et al.,1971, Bourne et al., 1981, Höcker et al., 1981, Forschner et al. 1991, and Carreau et al. 1993) while elasticity tends to decrease it (Carreau et al, 1993). Very few efforts (Ulbrecht and Carreau, 1985 and Forschner et al., 1991) have been devoted to elucidate this obvious unmapped domain.

Power consumption is not enough to describe the complex flow behaviour within an agitated reservoir. Mixing time as well as circulation time are frequently employed to ascertain the mixing performance. Mixing time is defined as the time to achieve a certain degree of homogeneity. It is quite useful information but it should be compared with data obtained from same technique scheme (Ulbrecht and Carreau, 1985). Voncken (1965), Hoogendoorn and den Hartog (1967) and Ford et al.(1972) have presented overall reviews of the merits and de-merits of the different methods used to measure the mixing time. The impeller pumping capacity, or the intensity of the macro-flow, is characterized by a circulation time, defined as the time to complete a closed loop for a free suspended particle reflecting a fluid element. Mixing and circulation times have been intensively studied for the laminar flow regime. Some work has been devoted to the transition regime but mainly for Newtonian fluids (Nagata,

1956, Gray, 1963, Hoogendoorn and dan Hartog, 1967). The influence of non-Newtonian behaviour, either shear-thinning or elasticity accompanied with shear-thinning properties, has been investigated for the transition flow regime (Ford and Ulbrecht, 1975, 1976, Chavan et al., 1975b, Guérin et al., 1984, and Carreau et al., 1992), but elastic constant viscosity Boger fluids (Boger and Binnington, 1977) have not been used as test liquids to assess the elastic effects.

The main objective of this work is to develop models to correctly predict the effective deformation rate in transition flow regime in agitated mixing systems. The effects of non-Newtonian properties, including inelastic shear-thinning, elastic constant viscosity and shear-thinning viscoelastic, on mixing time, circulation time and flow patterns, etc, are also reported.

5-4. CONCEPTS

5-4-1. Effective Deformation Rate

Metzner and Otto (1957) proposed a significant method to calculate the effective viscosity of non-Newtonian fluids in terms of the effective deformation rate in mixing vessels, which is proportional to the impeller rotational speed:

$$\dot{\gamma}_e = k_s N \qquad (1)$$

This linear relation is valid only in the laminar flow regime.

The Couette flow analysis is used to simplify the flow behaviour in an agitated vessel following the early work of Bourne and Butler (1969). The fluid motion within a reservoir is approximated by that generated in the gap between two coaxial cylinders, with the inner cylinder of equivalent diameter d_e rotating. The readers are referred for more elaboration to Carreau et al.(1993) who proposed a simple model to predict the effective deformation rate in the agitated tank for the laminar flow regime. Two dimensional helical flow of non-Newtonian fluids in an annular gap has been studied

using analytical solutions by Coleman and Noll (1959), Dierckes and Schowalter (1967), Bird et al.(1987) and using numerical solutions by Dostal et al.(1993). However, such two dimensional analysis has not been applied to characterize mixing systems. In the following sections, three approaches based on one or two dimensional analysis of the equivalent Couette flow to evaluate the effective deformation rate will be presented.

5-4-1-1. Approach 1

Bourne et al. (1981) have presented a simple analysis to show that the effective deformation rate is no longer proportional to the impeller rotational speed in the transition flow regime. However, their approach is based on the use of a constant k_s, which is in contradiction with their findings. Here, we propose a slightly different approach. The power number in the transition regime is no longer inversely proportional to the Reynolds number, and can be empirically expressed as:

$$Np = K_p' \, Re^{-a} \tag{2}$$

where a < 1. For power-law fluids, Eq.2 can be written as:

$$N_p = \frac{K_p'}{Re_g{}^a} = K_p' \left(\frac{D^2 N \rho}{m |\dot{\gamma}_e|^{n-1}} \right)^{-a} \tag{3}$$

The power consumption is related to the torque exerted on the inner cylinder of equivalent diameter d_e, and the shear stress on the inner cylinder is related to the effective deformation rate by the following equation:

$$P = 2\pi N \, \Gamma = \pi N \left[\tau_{r\theta}|_{r=d_e/2} (\pi d_e H) d_e \right] \tag{4}$$

This equation defines the equivalent diameter of the impeller. We assume that the shear stress $\tau_{r\theta}\big|_{r=de/2}$ is related to the effective deformation rate $\dot{\gamma}_e$ as expressed in the case of simple shear flow, that is:

Then the power input is expressed by:

$$\tau_{r\theta}|_{r=d_e/2} = m\ |\dot{\gamma}_e|^n \tag{5}$$

$$P = \pi N \left[m\ |\dot{\gamma}_e|^n (\pi d_e H) d_e \right] \tag{6}$$

Substitution of Eq. 5 into Eq. 3 yields the following expression for the effective deformation rate:

$$\dot{\gamma}_e = \left[\frac{K_p' d^3}{\pi^2 d_e^2 H} \right]^{1/q} \left[\frac{d^2 \rho}{m} \right]^{(1-a)/q} N^{(2-a)/q} \tag{7}$$

where $q = n(1-a) + a$. This equation can be used to predict the effective shear rate using K_p' obtained for Newtonian fluids in the transition flow regime. The slope of the power curve changes with the Reynolds number and local values for K_p' and a are needed for the calculations.

5-4-1-2. Approach 2

The approach 2 is based on the assumptions of approach 1, but we make use of the power information for the laminar regime. At the turning point from the laminar to the transition flow regime, the effective deformation rate is taken to be continuous, that is:

$$\dot{\gamma}_e|_{trans} = \dot{\gamma}_e|_{lam} \tag{8}$$

and a = 1 (in Eq. 2) for the laminar regime. The effective deformation rate in the laminar regime was given by Carreau et al. (1993) to be:

$$\dot{\gamma}_e\ |_{lam} = k_s\ N = \left[\frac{K_p\ d^3}{\pi^2\ D^2 H} \right]^{1/(1-n)} \left[\frac{n\ [(D/d_e)^{2/n} - 1]}{4\pi} \right]^{n/(1-n)} \tag{9}$$

Attention should be drawn that the equivalent diameter, d_e in Eq. 9 may have a different meaning than that of Eq. 7, since they result from different approaches. The

effective deformation rate in Eq. 9 is evaluated from the generalized Reynolds number while in Eq. 7 it is related to the shear stress exerted on an imaginary inner cylinder of equivalent diameter d_e. For convenience, it is reasonable to assume the two equivalent diameter to be equal, for the transition regime not far away from the turning point. It follows from Eqs. 7, 8 and 9 that:

$$\left[\frac{K_p' d^3}{\pi^2 d_e^2 H}\right] = \left[\frac{K_p d^3}{\pi^2 D^2 H}\right]^{1/(1-n)} A \qquad (10)$$

where

$$A = \left[\frac{n\,[(D/d_e)^{2/n} - 1]}{4\pi}\right]^{n/(1-n)} \qquad (11)$$

Using Eq. 10 in Eq. 7, the effective deformation rate for the transition regime in terms of K_p is given by:

$$\dot{\gamma}_e = \left[\frac{K_p\, d^3}{\pi^2 D^2 H}\right]^{1/q} \left[\frac{d^2 \rho}{m}\right]^{(1-a)/q} A^{1/q}\, N^{(2-a)/q} \qquad (12)$$

In comparison with Eq. 7, the merit of Eq. 12 is that the Newtonian power proportionality constant K_p for the laminar flow regime, rather than the local K_p' for the transition regime, is needed to estimate the effective deformation rate. Newtonian power data and model predictions for the laminar regime are readily available in the literature. In both Eqs. 7 and 12, the value a for the local slope of the power curve has to be used for predicting the effective deformation rate. It should be stressed that Eq. 12 may not be applied into the transition regime far away from the turning point since Eq. 10 is strictly valid only at the turning point between the laminar and the transition

regime.

5-4-1-3. Approach 3

As mixing proceeds in the transition flow regime, inertial forces become more and more important. Secondary flows gradually increase and the axial velocity may no longer be neglected compared to the tangential velocity. For shear-thinning fluids, the viscosity is affected by both the tangential and axial velocity gradient components. To account for that we examine a two dimensional flow configuration, that is closer to the real flow field for the transition flow regime in a mixing reservoir. So hereby, in this third approach, we consider the two dimensional helical flow between two concentric cylinders, as illustrated in Figure 1. Notice that the axial velocity at the inner cylinder is not zero since the inner cylinder represents the action of an (inclined) helical blade. The effective deformation rate obtained from the following analysis will be compared with the results obtained from one dimensional approaches via Eqs. 7 and 12. For this steady-state helical flow, the two velocity components are assumed to be unique functions of the radial position, that is:

$$v_\theta = v_\theta(r), \quad v_z = v_z(r) \tag{13}$$

The θ-component of the equations of motion is:

$$-\frac{1}{r^2}\frac{d}{dr}\left(r^2\tau_{r\theta}\right) = 0 \tag{14}$$

Integration yields:

$$\tau_{r\theta} = \frac{c_1}{r^2} \tag{15}$$

For power-law fluids in a two dimensional flow, the viscosity has to be expressed in terms of the second invariant of the rate-of-strain tensor, that is:

where $II_{\dot{\gamma}}$ is the second invariant of the rate-of-strain tensor which is expressed as:

$$\eta = m\,|\dot{\gamma}|^{n-1} = m\left|\sqrt{1/2\ II_{\dot{\gamma}}}\right|^{n-1} \tag{16}$$

$$\underline{\underline{\dot{\gamma}}} = \nabla\underline{v} + \nabla\underline{v}^{+} = \begin{pmatrix} 0 & \dot{\gamma}_{r\theta} & \dot{\gamma}_{rz} \\ \dot{\gamma}_{\theta r} & 0 & 0 \\ \dot{\gamma}_{zr} & 0 & 0 \end{pmatrix} \tag{17}$$

where the shear rate components are defined as

$$\dot{\gamma}_{r\theta} = \dot{\gamma}_{\theta r} = r\,\frac{d}{dr}(v_\theta/r) = r\,\omega' \tag{18}$$

$$\dot{\gamma}_{rz} = \dot{\gamma}_{zr} = \frac{dv_z}{dr} = v_z' \tag{19}$$

where $'$ stands for the derivative with respect to r. Then, the second invariant is expressed by:

$$II_{\dot{\gamma}} = \underline{\underline{\dot{\gamma}}}:\underline{\underline{\dot{\gamma}}} = 2v_z'^{\,2} + 2r^2\omega'^{\,2} \tag{20}$$

and the viscosity is expressed by:

$$\eta = m\left(v_z'^{\,2} + r^2\omega'^{\,2}\right)^{(n-1)/2} \tag{21}$$

The $r\theta$-component of the stress tensor is given by:

$$\tau_{r\theta} = -\eta\ |\dot{\gamma}_{r\theta}| \tag{22}$$

Eq.14 can be rearranged by combining Eqs. 17, 20 and 21 to obtain:

$$-m\left(v_z'^{2} + r^2\omega'^{2}\right)^{(n-1)/2} r\omega' = \frac{c_1}{r^2} \tag{23}$$

Hereby, it is reasonable to assume that the z-component of the velocity is linear. From the previous work of Carreau et al. (1976), we expect that the axial velocity at the

inner cylinder (equivalent to the impeller), at r=d_e/2, is proportional to the tangential velocity. That is:

$$v_z|_{r=d_e/2} = C\, v_\theta|_{r=d_e/2} \tag{24}$$

where C is a proportional constant, assumed to be 0.25 for the transition regime not very far away from the turning point (for the laminar regime, the maximum axial velocity was found by Carreau et al. (1976) to be about 15% of the maximum tangential velocity in the vicinity of the impeller blade). An increase of the C value with increasing rotational speed is expected.

We obtain the shear stress exerted on the inner cylindrical (imaginary) wall by solving Eq.22 numerically with the boundary conditions $v_\theta = v_z = 0$ at r = D/2 and $v_\theta = \Omega d_e/2$ at r = d_e/2, as well as Eq. 23:

$$\tau_{r\theta,wall} = m\, r\omega'\left(v_z'^2 + r^2\omega'^2\right)^{1/2}\Big|_{r=d_e/2} \tag{25}$$

The effective deformation rate $\dot{\gamma}_e$ can be expressed in terms of the inner wall conditions, by combining Eqs. 3, 4 and 24. The results is:

$$\dot{\gamma}_e = \left[\frac{K_p' d^3}{\pi^2 d_e^2 H}\right]^{1/s}\left[\frac{d\rho}{m}\right]^{(1-a)/s} N^{(2-a)/s}\left[\left(\frac{d_e}{2\omega'}\right)\left(v_z'^2 + \left(\frac{d_e}{2}\right)^2\omega'^2\right)^{1/2}\right]^{-n/s} \tag{26}$$

where $s=a(1-n)$ and the values for v_z' and ω' are calculated at the inner cylinder wall (at $r = d_e/2$). Eq. 26 contains K_p' for the transition regime and the approximate velocity gradients for the two dimensional flow. Obviously, as mentioned before, Eq. 26 has to be solved numerically. More refined results could be obtained by solving a more complex flow situation using a more sophisticated numerical method, such as the finite element method as proposed by Tanguy et al. (1992) for solving the three dimensional "laminar" flow in a reservoir mixed with helical ribbon agitators.

5-5. EXPERIMENTAL

A detailed description of the rheological and power measurements, and of the equipment set-up is available elsewhere (Carreau et al., 1993). The mixing system consists of a cylindrical plexiglas vessel equipped with a helical ribbon impeller. The major geometric parameters of three different agitators used in this work are defined in Figure 2, and their values are listed in Table 1. The torque measurements were carried out using a torquemeter mounted on the impeller shaft and the response signals were recorded by a data acquisition system (Lab Master, PGL 40). The torquemeter was pre-calibrated using a dynamic method (see Ulbrecht, 1980, for the criteria for the dynamic and static methods). The accuracy of torque measurement is within $\pm$ 2.0 %.

Mixing and circulation times were measured using both conductivity and thermal methods. The thermal probes (T type, 1/16", Thermo Electric) and conductivity probes (stainless, 1/8") were placed in different positions in the vessel wall and at the top of the vessel, as shown in Figure 2. The different probe locations allowed us to assess the mixing behaviour in the whole reservoir. The signals were also recorded using the same Lab Master data acquisition system. The delay in the signal response for both types of probe is within 0.40 s. Approximately 40 mL of fluid sample at 60 ^{0}C or containing about 0.1 mass % sodium chloride salt (NaCl) were quickly injected to the mixing vessel. The vessel contained approximately 20 L and the initial temperature was 25 ^{0}C. The effects of salt concentration and temperature on the liquids' rheological properties were examined, and the mixing and circulation times were measured within concentration and temperature ranges for which the effects were negligible. A typical curve used for the determination of the mixing and circulation times is reported in Figure 3. The mixing time is taken as the time for which the response curve is within $\pm$ 5 % of the average value of the final signal, whereas the circulation time is taken as the period between two consecutive peaks of the signal.

Test fluids

Several Newtonian and non-Newtonian fluids have been used to investigate the influence of the rheological properties on mixing. The viscosity and primary normal stress difference of test fluids were measured using a R-18 Weissenberg rheogoniometer in simple shear flow. Glycerol and corn syrup were used as Newtonian liquids (glycerol of viscosity equal to 0.470 Pa·s was the only Newtonian fluid used for the measurement of the mixing and circulation times). Several 2.5 mass % and 1 mass % CMC aqueous solutions were employed as the shear-thinning inelastic fluids, whereas a 0.5 mass % xanthan in a mixture containing 85 mass % glycerol and 15 % water exhibited both shear-thinning and elastic behaviour. A 800 ppm polyacrylamide (PAA) in corn syrup showed elastic behaviour with a shear-independent viscosity. The rheological properties are discussed in more details in Carreau et al. (1993). The values for the key rheological parameters are reported in Table 2.

5-6. RESULTS AND DISCUSSION

5-6-1. Effective Shear Rate

The effective shear rate, $\dot{\gamma}_e$, is evaluated by comparing the non-Newtonian with the Newtonian power data for the same geometry and at the same impeller rotational speed, according to the Metzner-Otto (1957) scheme. Typical experimental power data for the Newtonian and non-Newtonian fluids agitated by impeller HR3 are reported in Figure 4. For the non-Newtonian fluids, the generalized Reynolds number, as defined in Eq. 3, with k_s value obtained from the laminar regime, is used. As mixing proceeds into the transition flow regime, the Newtonian power number is no longer inversely proportional to the Reynolds number. As seen in Figure 4, an extended laminar power curve for the highly shear-thinning inelastic 2.5 % xanthan aqueous solution ($n = 0.183$) is observed, while the power curve for the moderately shear-thinning 1 % CMC ($n = 0.409$) coincides with the corresponding Newtonian one. A

marked deviation of the power curve from the Newtonian curve is found for the shear-thinning elastic 0.5 % xanthan in the glycerol/water mixture, and considerably higher power numbers are observed after the departure.

Metzner et al. (1961) were the first authors to notice that the power number in the transition flow regime for non-Newtonian inelastic fluids was smaller than the corresponding Newtonian case at the same Reynolds number. That is, the effective deformation rate increases with impeller speed more sharply and is no longer proportional to the rotational speed. In the following sections, we compare experimental values of the effective deformation rate for various types of agitator in the transition regime with the predictions of the three models presented in the previous section. The agitators are classified as: helical ribbon, and other impellers (anchor and blade turbine, flat disk).

5-6-1-1. Helical Ribbon Agitators

In the recent work of Carreau et al.(1993), it was found that the effective deformation rate for highly shear-thinning liquids increases more drastically with the impeller speed than predicted by the linear Metzner-Otto expression. As shown in Figures 5 and 6, the departures from the linear expression are quite obvious for the transition regime. Our findings are in agreement with the results obtained by Brito et al. (1991) for a highly shear-thinning xanthan aqueous solution, also mixed with a helical ribbon impeller. For moderately shear-thinning fluids (0.5% and 0.8% xanthan and 1% and 3% CMC aqueous solutions, for which the n values are larger than 0.25), the linearity of the effective deformation rate with the rotational speed extends throughout the transition flow regime covered by this work (see Carreau et al., 1993). Typical results are shown in Figure 7 for a 1 % CMC solution. Nagata et al. (1971) reported similar trends for slightly shear-thinning CMC and PVA aqueous solutions in a helical ribbon mixing system up to the turbulent flow regime.

The predictions of the effective shear rate, $\dot{\gamma}_e$, using the three different models

(Eqs. 7, 12, and 26), are shown in Figures 5 and 6 for the highly shear-thinning 2.5 % xanthan aqueous solution mixed with impellers HR1 and HR3. As seen in the figures, Eqs. 7 and 26 give quite good predictions, while overestimation is obtained using Eq. 12. For highly shear-thinning fluids, the use of the K_p values (obtained from the laminar regime) is not adequate since the K_p' values (in the transition regime) are considerably lower, and K_p' decreases with as mixing proceeds far beyond the laminar regime. Comparing the values of the effective deformation rate estimated using Eq. 7 and Eq. 26, better predictions are obtained by using Eq. 26. However, the predictions of Eq. 7 are also adequate and it is much simpler to use, because of its analytical form which avoids the numerical solution of non-linear differential Eq.26.

For the moderately shear-thinning 1% CMC aqueous solution, the three models overpredict the effective deformation rate at high values of the rotational speed, as seen in Figure 7. For this solution, the linear Metzner-Otto relation remains valid throughout the transition regime. It seems to be the case for all inelastic fluids with low or moderate shear-thinning properties (see Carreau et al., 1993).

5-6-1-2. Anchor, Blade Turbine and Flat Disc Agitators

Sharp increases of the effective shear rate with impeller rotational speed have been reported for anchor and blade turbine agitators by Metzner et al. (1961), Pollard and Kantyka (1969), Nagata et al. (1971), Bourne et al. (1981), Höcker et al. (1981), and Forschner et al.(1991). This strong dependence on the rotational speed has been obtained even for slightly shear-thinning inelastic fluids, in contrast to results obtained for helical ribbon agitators.

The experimental data of Bourne et al. (1981) for a 63 mass % $CaCO_3$ suspension in ethylene glycol mixed with an anchor agitator are compared with the predictions of Eqs. 7 and 12 in Figure 8. The flow index $n \approx 0.60$, the average value of $a \approx 0.38$, and the ratio of the vessel diameter over the equivalent diameter of the impeller, D/d_e, is estimated using Eq. 9 to be 1.25. As seen in the figure, for the small scale mixer (d =

0.109m) Eq. 12 gives very good predictions and underestimation is obtained using Eq. 7 , whereas for the large scale (d = 1.52m) Eq. 12 overestimates the data and Eq. 7 gives good predictions.

The predictions of Eqs. 7 and 12 are compared in Figure 9 with the data of Pollard and Kantyka (1969) for a chalk-water slurries mixed by an anchor agitator (D/d =1.2). The value of D/d_e is calculated to be 1.38 via Eq. 9, using their power data in the laminar flow regime. As seen in the figure, Pollard and Kantyka (1969) obtained a highly pronounced enhancement of the effective deformation rate in the transition regime, with increases by almost two folds over a very small increase of the impeller rotational speed. Their regression for the transition regime is $\dot{\gamma}_e = 32\ N^{3.75}$ (not shown in the figure). The exponent of 3.75 is considerably larger than the exponent of 2 obtained by Bourne et al. (1981). The predictions of Eqs. 7 and 12 are in a good agreement with the data, but Eq. 7 gives slightly better predictions.

Metzner et al. (1961) were the first authors to note the negative deviations of the power curve for shear-thinning and shear-thickening fluids from the corresponding Newtonian curve in the transition flow regime for several different types of blade turbine impellers. They pointed out that the effective shear rate for the shear-thickening fluids was higher than that predicted by the Metzner-Otto linear expression (Eq.1). However, no correlation was proposed to account for the increases. Some typical values for the effective shear rate have been calculated based on the power data of Metzner et al. (1961) for shear-thinning carbopol solutions with n = 0.21 ~ 0.26 mixed with a 6-bladed fan turbine agitator. The results are shown in Figure 10. The calculated values are somewhat scattered, and apparently there are no obvious differences in the effective shear rate for the different values of the D/d ratio. The predictions of Eq. 7 are excellent whereas Eq. 12 slightly overpredicts the data. Both models show very little effects of the D/d ratio.

The data points in Figure 11 are recalculated from the extended laminar power curve for a 3.8 % CMC aqueous solution mixed with a 6-blade turbine agitator (D/d

= 2.0, D/d_e =3.14), from the subsequent work of Nagata et al. (1971). The three models apparently underestimate the experimental values which show a much pronounced increase of the effective shear rate as mixing proceeds in the transition regime. At the higher values of the rotational speed, surprisingly the effective shear rate is shown to decrease, but this is due to the minimum in the power number curve observed for turbine agitators in the transition regime. The same Newtonian power curves were obtained for mixing with and without baffles. This could shed some doubt on the accuracy of the transition regime data.

Höcker et al. (1981) also reported an extended laminar power curve, or lower power number values compared with the corresponding Newtonian curve. They studied CMC aqueous solutions with values for the flow index n ranging from 0.37 to 0.91 mixed with several different blade turbine and disc agitators. The more shear-thinning the fluid was, the lower was the power value, compared with the Newtonian case. The values for the effective shear rate calculated from their power curves for a typical CMC aqueous solution (n = 0.37) mixed with a flat disc impeller (D/d = 2.67) are compared with the predictions of Eqs. 7 and 12 in Figure 12. The agreement is quite good, especially for the predictions of Eq. 7. The value for D/d_e is calculated to be 6.68.

Recently, an attempt has been made by Forschner et al. (1991) to obtain a corrected effective shear rate, to use for the industrial scale-up of a turbine mixer in the transition flow regime. They found that the effective viscosity was overestimated when using the methods of Metzner-Otto (1957) and of Rieger-Novak (1974). Therefore, they proposed an empirical correlation to evaluate the generalized Reynolds number, which is expressed by:

$$Re_g = \left(\frac{D^2 N^{2-n} \rho}{k_{1,\,lam}\, k_{2,\,trans}} \right)^{1/(1+a)} \qquad (27)$$

where $k_1 = m\, k_s^{n-1}$. However, they did not report any values for $k_{2,\,trans}$, due to

commercial concerns. The effective deformation rate was calculated through reported effective viscosity data for a 2.2 % CMC aqueous solution ($n = 0.45$) and this is shown in Figure 13. The rate of increase for the effective shear rate with the impeller rotational speed is found to be between the lower rate reported by Bourne et al. (1981) and the higher rate obtained by Pollard and Kantyka (1967). The agreement between the experimental data and the predictions of Eqs. 7 and 12 are quite good, and even surprisingly excellent in the case of Eq. 7.

In contrast to experimental evidences obtained for helical ribbon agitators from this work and from the previous work of Nagata et al. (1971), the effective shear rate in the transition regime is considerably enhanced, even in low shear-thinning fluids, when using anchor, blade turbine and disc agitators. It can be argued that anchor, blade turbine and disc impellers may create much irregular flow and higher fluctuating velocities which, in turn, lead to more deformation in the fluids, compared to the more uniform and lower deformation rate created by helical ribbon agitators. Kamiwano et al. (1990) observed that the maximum axial velocity is more than 40 % of the maximum tangential velocity for a shear-thinning 1.2 mass % aqueous hydroxyethyl cellulose solution agitated by a 6-bladed turbine impeller at $Re_g = 100$, compared with about 15 % for the same ratio obtained by Carreau et al. (1976) for helical ribbon agitators.

All of the non-Newtonian fluids discussed above exhibit shear-thinning behaviour. The effective deformation rate in shear-thickening liquids has also been found to show similar enhancement as in shear-thinning fluids (Calderbank and Moo Young, 1957, Metzner et al., 1961). Metzner et al. (1961) found that $\dot{\gamma}_e$ varied with the impeller speed at an exponent of 2, for shear-thickening liquids agitated by blade turbine impellers.

For engineering applications, the interest is focused on the power requirement rather than on the effective deformation rate. The predictions of power requirement using the effective deformation rate values calculated via the three models are

compared in Figure 14 with the experimental power data for the 2.5 % xanthan solution mixed with the HR3 impeller. The open circle points were calculated using a constant k_s value of 18.7 obtained from the laminar regime. The points are shifted towards the Newtonian curve at the same power number using Eqs. 7 and 26, while Eq. 12 considerably overpredicts the power consumption for this highly shear-thinning inelastic fluid.

Finally, a summary of the predictions for the three models is presented in Table 3. The numerical model, e.g. Eq. 26, gives very good predictions, denoted by the sign "+++", at least for the fluids and mixing systems used in this work. The analytical model (Eq. 7) based on the Newtonian power information in the transition regime (namely, K_p' and a) produces good (++), and, in some cases, very good estimations. Finally, the other analytical model (Eq. 12), which is derived from the Newtonian power knowledge in both the laminar and transition flow regimes (K_p and a), gives poor (-) to very good predictions depending on the circumstances. More information in the transition flow regime, such as flow patterns, velocity profiles, etc., may lead to more satisfactory predictions using the numerical model (Eq. 26). However, the analytical model of Eq. 7 is highly attractive for design purposes, because of its simplicity (analytical form) and the adequate predictions.

5-6-2. Mixing and Circulation Times

The significance of mixing time is to demonstrate the mixing performance of a agitator. It is the time necessary to achieve a given level of homogenization and it should used only on a comparative basis with data obtained using the same scheme. For instances, Nagata et al. (1956), Gray (1963) and Johnson (1967) compared the mixing time with respect to power consumption for different types of impeller and concluded that the helical ribbon agitator is much more efficient for blending highly viscous and viscoelastic liquids.

The dimensionless mixing time, Nt_m, is plotted in Figure 15 as a function of the

generalized Reynolds number, Re_g, for a Newtonian and several non-Newtonian fluids, ranging from the inelastic shear-thinning to the viscoelastic Boger fluids, for three different agitator geometries. As seen in the figure, at lower Reynolds numbers, the dimensionless mixing time is apparently independent of the Reynolds number, then above certain Re_g values, Nt_m decreases sharply and becomes approximately independent of the fluids' rheology. The average values for Nt_m at the plateau are also listed in Table 4. In the laminar regime, the dimensionless mixing time is considerably longer in the non-Newtonian fluids, especially in the viscoelastic liquids, compared with the Newtonian glycerol. These results are in line with previous observations made by Hoogendoorn and den Hartog (1967), Chavan et al. (1975b), Ford and Ulbrecht (1975 and 1976), and Carreau et al.(1992). The non-Newtonian character has a strong influence on the dimensionless mixing time: the values of Nt_m for a Boger type fluid (800 ppm PAA in corn syrup) are more than *4* fold larger than that for the Newtonian glycerol of comparable viscosity. For the viscoelastic 0.5 % xanthan in glycerol/water mixture, and for the shear-thinning 1 % CMC aqueous solution, the Nt_m values are 2 ~ 3 times higher compared with the Newtonian case. Similar trends have been reported in the literature. Carreau et al. (1976) obtained 2.5 ~ 4.3 folds higher mixing times for shear-thinning CMC and viscoelastic Separan solutions compared with glycerol in helical ribbon mixing systems. Comparable increases of Nt_m in non-Newtonian liquids have been reported by Chavan et al.(1975a, 1975b), Ford and Ulbrecht (1975) and Carreau et al. (1992).

The effect of the impeller geometry on the mixing time is clearly seen in both Figures 15 and Table 4. The best performances for the three geometries reported here, in terms of Nt_m, are achieved using impeller HR3, characterized by a larger blade width and a smaller pitch, while the poorer performances are observed for impeller HR2, with a small blade width and large pitch. These results are also in agreement with the literature findings.

The circulation time reflects the pumping capacity of an agitator. The axially

pumping agitators, such as helical ribbons, have been found to be quite efficient for blending viscous and viscoelastic fluids (Coyle et al., 1970, Jonson, 1976). The circulation time appears in the literature in terms of a dimensionless circulation time, Nt_c, or in terms of a circulation number, Ci, which was first introduced by Chavan and Ulbrecht (1973) and is related to the pumping rate per fluid volume. It can be expressed as follows

$$Ci = \frac{Q}{Nd^3} \sim \frac{V}{t_c N d^3} \qquad (28)$$

The experimental circulation number is reported as a function of the Reynolds number in Figure 16. At lower Re_g values, the circulation number appears to be independent of the Reynolds number. For large Reynolds numbers, Ci starts to increase sharply, which indicates a better pumping performance, compared to the pumping achieved at lower Re_g values (laminar regime). This is in agreement with the previous works in the literature (Chavan and Ulbrecht, 1973, Chavan et al., 1975b, Guérin et al., 1984, and Carreau et al., 1992). As seen in Figure 16, the Ci values are about 20% ~ 70% lower for the shear-thinning elastic 0.5% xanthan in glycerol/water and for the Boger 800 ppm PAA fluid, compared with values obtained for glycerol. This suggests that the non-Newtonian properties dampen the pumping capacity of the impeller. This trend is in agreement with the typical findings of Chavan et al.(1975b) and Carreau et al.(1992). The geometry influence on the circulation time is similar to that discussed above for the mixing time.

Three circulation paths have been observed by Guérin et al. (1984) for helical ribbon agitators, with a bimodal distribution of circulation times, for glycerol and a moderately shear-thinning 1% CMC solution. These findings were confirmed by Takahashi et al. (1991), for hydroethyl cellulose solutions (n ranging from 0.67 to 0.83), agitated by helical ribbon impellers. In this work, a bimodal distribution was observed for the 0.5 % xanthan in glycerol/water as shown in Figure 17 for impeller HR1. Here,

the bimodal distribution is probably due to the high-shear constant viscosity that the fluid exhibits, which may result in a similar behaviour as a Newtonian fluid at high enough deformation rates (see the viscosity curve reported by Carreau et al., 1993).

The ratio of mixing time over circulation time, t_m/t_c, is plotted against the Reynolds number in Figure 18. At lower Re_g values, t_m/t_c appears to be independent of the Reynolds number. Over critical Re_g values, it starts to decrease sharply and becomes almost independent of the fluids' rheology. The average values of t_m/t_c at plateau regime are also listed in Table 4. In the case of glycerol, the average value is about 4.4, compared to 3 reported by Coyle et al.(1970), 3.5 by Carreau et al.(1976), 2.6 by Brito et al.(1991), all for helical ribbon agitators. In the laminar regime, the shear-thinning and elasticity increase the t_m/t_c value from 4.4 obtained for the Newtonian glycerol up to 10.6 for the Boger fluid. These results are in agreement with the findings of Carreau et al.(1976), who found that the ratio ranged from 4.3 to 8.5 for mixing 2 % CMC aqueous solution with different helical ribbon impellers. In contrast, Brito et al. (1991) observed no effect of rheology on this ratio and a value of 2.6 was found for Boger fluids as well as for Newtonian fluids.

Finally, it is worthwhile to report an observation on the flow pattern in the transition regime. Depending on the direction of the impeller rotation, the fluid is pumped upwards at the vessel wall and pumped down in the center, or the reverse. With increasing impeller rotational speed, the fluid motion appears to be more and more at random. At the very high speeds investigated in this work (e.g. ~300 rev/min), the main axial flow pattern could be inverse, for shear-thinning elastic fluids under some circumstances, with respect to the usual patterns observed at lower speeds. This stresses the complexity of the flow field when mixing non-Newtonian fluids in the transition regime.

5-7. CONCLUSIONS

Using the experimental data of this work and of previous works in the literature, we have shown that the effective deformation rate in the transition flow regime is no longer proportional to the rotational speed, as suggested by Metzner and Otto (1957) for the laminar regime. For helical ribbon agitators, the effective deformation rate increases sharply in the transition regime when mixing highly shear-thinning fluids; however, an extended linearity of the Metzner-Otto expression was found for the moderately shear-thinning fluids in the flow regime investigated in this work. This is in agreement with the power data reported in the literature for similar fluids, for which the power number versus the Reynolds number coincides with the Newtonian curve. When examining results for other types of impeller (anchor, blade turbine and flat disc), reported in the literature, a strong dependence of the effective deformation rate with the impeller rotational speed was found even for moderately shear-thinning fluids.

Two analytical and one numerical models, based on one or two dimensional equivalent Couette flow using Newtonian power information in either laminar or transition flow regimes, are proposed to estimate the effective deformation rate in the transition flow regime. The predictions of three models are compared with the experimental data of this work and data extracted from the literature. The agreement is very good for most systems examined.

The dimensionless mixing time, Nt_m, and the circulation number, Ci, were investigated for the laminar and the transition flow regimes with Newtonian and non-Newtonian fluids mixed with three different helical ribbon agitators. In the laminar flow regime, the dimensionless mixing time and the circulation number were found to be independent of the Reynolds number. At high Reynolds numbers, Nt_m was found to decrease whereas Ci increased. In the laminar regime, the elasticity and shear-thinning properties increased considerably the dimensionless time and decreased similarly the circulation number. At very Reynolds numbers, the fluids' rheology was shown to have little effect on both the dimensionless mixing time and circulation

number. The impeller with a larger blade width and a smaller pitch gave the best mixing performance.

5-8. Acknowledgement

We acknowledge the financial support received from the FCAR program of the Province of Québec.

5-9. REFERENCES

Bird, R.B., R.C. Armstrong and O. Hassager, *Dynamics of Polymeric Liquids,* Vol.1, Fluid Mechanics, Wiley, New York (1977).

Boger, D.V. and R. Binnington, " Separation of Elastic and Shear Thinning Effects in the Capillary Rheometer", *Trans. Soc. Rheol.*, **21**, 515-534(1977).

Bourne, J.R., and H. Bulter, "Power Consumption of Helical Ribbon Impellers in Inelastic Non-Newtonian Liquids", *Chem. Eng. J.* **47**, 263-270(1969).

Bourne, J.R., M. Buerli and W. Regenass, "Power and Heat Transfer to Agitated Suspensions: Use of Heat Flow Calorimetry", *Chem. Eng. Sci.,* **36**, 782-784 (1981)

Brito E., J.C. Leuliet, L. Choplin and P.A. Tanguy, "On the Role of Elasticity on Mixing with a Helical Ribbon Impeller", *Trans. IChemE.* **69,** 324-331(1991).

Calderbank, P.H. and M.B. Moo Young, "The Prediction of Power Consumption in the Agitation of non-Newtonian Fluids," *Trans. IChemE.* **37**, 26-(1959).

Carreau, P.J., W.I. Patterson and C.Y. Yap, "Mixing of Viscoelastic Fluids with Helical Ribbon Agitators, I - Mixing Time and Flow Patterns", *Can. J. Chem. Eng.,* **54**, 135-142(1976)

Carreau, P.J., J. Paris and P. Guérin, "Mixing of Newtonian and Non-Newtonian Liquids: Screw Agitator and Draft Coil System", *Can. J. Chem. Eng.,* **70**, 1071-1082 (1992)

Carreau, P.J., R.P. Chhabra and J. Cheng, "Effect of Rheological Properties on Power Consumption with Helical Ribbon Agitators", *AIChE J.,* **39,** 1421-1430(1993).

Chavan V.V., and J.J. Ulbrecht, "Internal Circulation in Vessels Agitated by Screw Impellers", *Chem. Eng. J.*, **6**, 213-223(1973).

Chavan V.V., M. Arumugam and J. Ulbrecht, "On the influence of Liquid Elasticity on Mixing in a Vessel Agitated by a Combined Ribbon-Screw Impeller", *AIChE J.* **21**, 613-615(1975a).

Chavan V.V., D.E. Ford and M. Arumugam, "Influence of Fluid Rheology on Circulation, Mixing and Blending", *Can. J. Chem. Eng.* **53,** 628-635(1975b).

Coleman, B.D., and W. Noll, "Helical Flow of General Fluids", *J. Appl. Phy.,* **30,** 1508-(1959).

Coyle, C.K., H.E. Hirschland, B.J. Michel and J.Y. Oldshue, "Mixing in Viscous Liquids", *AIChE J.*, **16,** 903-905 (1970).

Dierckes, A.C. and W.R. Schowalter, "Helical Flow of a Non-Newtonian Polyisobutylene Solution" , *Ind. Eng. Chem. Fund.,* **5**, 263-271 (1966).

Dostál, M., R. Žitný, J. Sesták and M. Houska, "Helical Flow of Power-Law Fluids", *AIChE J.,* **39,** 189-192 (1993).

Ford, D.E., R.A. Mashelkon and J. Ulbrecht, "Mixing Times in Newtonian and Non-Newtonian Fluids", *Proc. Tech. Int.,* **17**, 803-806 (1972).

Ford, D.E., and J. Ulbrecht, "Blending of Polymer Solutions with Different Rheological Properties", *AIChE J.,* **21,** 1230-1233(1975).

Ford, D.E., and J. Ulbrecht, "Influence of Rheological Properties of Polymer Solutions upon Mixing and Circulation Times", *Ind. Eng. Chem. Proc. Des. Dev.* **15**, 321-326 (1976).

Forschner, P., R. Krebs and T. Schneider, "Scale-up Procedures for Power Consumption of Mixing in Non-Newtonian Fluids, *7th European Cong. on Mixing,* Brugge, Belgium, 161-165(1991),

Gray, J.B., "Batch Mixing of Viscous Liquids", *Chem. Eng. Prog.,* **59,** 55-59 (1963).

Guérin, P., P.J. Carreau, W.I. Patterson and J. Paris, "Characterization of Helical Impellers by Circulation Times", *Can. J. Chem. Eng.,* **62**, 301-309(1984)

Guy, C., P.J. Carreau and J. Paris, "Mixing Characteristics and Gas Hold-up in a Bubble Column", *Can. J. Chem. Eng.*, **64**, 23-35 (1986).

Höcker, H., G. Langer and U. Werner, "Power Consumption of Stirrers in Non-Newtonian Liquids", *Ger. Chem. Eng.,* **4**, 113-123(1981).

Hoogendoorn, C.J. and A.P. Den Hartog, "Model Studies on Mixers in Viscous Flow Region", *Chem. Eng. Sci.*, **22**, 1689-1699 (1976).

Johnson, R.T., "Batch Mixing of Viscous Liquids", *Ind. Eng. Chem. Proc. Des. Dev.* **6**, 340-345(1967).

Kamiwano, M., F. Saito and M. Kaminoyama, "Velocity Distribution and Apparent Viscosity of a Pseudoplastic Liquid in a Stirred Vessel", *Internal. Chem. Eng.*, **30**, 274 -280(1990).

Metzner, A.B. and R.E. Otto, "Agitation of Non-Newtonian Fluids", *AIChE J.,* **3**. 3-10 (1957).

Metzner, A.B., R.H. Feehs, H. Lopez Ramos and J.D. Tuthill, "Agitation of Viscous Newtonian and Non-Newtonian Fluids", *AIChE J.*, **7**, 3-9 (1961).

Nagata, S., T. Yanagimoto and T. Yokoyama, "A Study of the Mixing of High Viscosity", *Mem, Fac., Eng. Kyoto Univ.* **18.** 444-454(1956)

Nagata, S., M. Nishikawa, H. Tada and S. Gotoh, "Power Consumption of Mixing Impellers in Pseudoplastic Liquids", *J. Chem. Eng. Japan,* **4,** 72-76 (1971).

Nagata, S., Mixing: Principles and Applications, Kodansha, Wiley, Tokyo (1975).

Pollard, J. and T.A. Kantyka, "Heat Transfer to Agitated non-Newtonian Fluids", *Trans. IChemE J.,* **47,** T21-T27 (1969).

Rieger, F. and V. Novak, "Power Consumption of Agitators in Highly Viscous Non-Newtonian Liquids", *Trans. IChemE.*, **51**, 105-111 (1973).

Smith, J.M., "Industrial Needs for Mixing Research", *Trans. IChemE.*, **68**, 3-6 (1990).

Takahashi, K., M. Iwoki, T. Yokota and H. Konno, "Circulation Time for Pseudoplastic Liquids in a Vessel Equipped with a Variety of Helical Ribbon Impellers", *J. Chem. Eng. Japan,* **22,** 413-418(1989).

Tanguy, P.A., R. Lacroix, F. Bertrand, L. Choplin and E. Brito, "Finite Elament Analysis of Viscous Mixing with a Helical Ribbon-Srew Impeller", *AIChE J.*, **38**, 939-944(1992).

Tatterson, G.B., Fluid Mixing and Gas Dispersion in Agitated Tanks, McGraw-Hill, New York (1991).

Vorcken, R.M., "Homogenization of miscible liquids", *British Chem. Eng.*, **10**, 12-18 (1965).

Ulbrecht, J.J., "Comments on Sawinsky et al.", *Chem. Eng. Sci.*, **35**, 2372-2373(1980)

Ulbrecht, J.J. and P.J. Carreau, Mixing of Viscous Non-Newtonian Liquids, *in Mixing of Liquids by Mechanical Agitation,* (Eds: Ulbrecht J.J. and Patterson G.K.), Gordon and Breach, New York (1985).

Table 1. Agitator Geometry

Impeller	Characteristics	*D/d*	*w/d*	*p/d*	*H/d*
HR1	small blade width, large pitch	1.11	0.097	0.695	1.05
HR2	small blade width, large pitch	1.11	0.133	0.850	1.05
HR3	large blade width, small pitch	1.11	0.133	0.695	1.05

Table 2. Rheological Properties of Test Fluids

Test Fluids	n	m	t_1	η_0	η_s	n′	m′
	-	$Pa.s^n$	s	Pa.s	Pa.s	-	$Pa.s^{n'}$
Glycerol	1	0.470					
2.5% xanthan (H_2O)	0.183	22.4					
1% CMC (H_2O)	0.409		0.110	1.57			
0.5% xanthan (glycerol/H_2O)	0.199	4.13			0.19	0.782	7.85
800 ppm PAA (corn syrup)	0.94	1.03				1.67	0.15

n, m: parameters in the power-law model: $\eta = m|\dot{\gamma}|^{n-1}$

t_1, η_0: parameters in Cross model: $\eta = \eta_0 / [1+(t_1|\dot{\gamma}|)^{1-n}]$

η_s: parameter in the expression: $\eta = m|\dot{\gamma}|^{n-1} + \eta_s$

n′, m′: parameters in the expression: $N_1 = m'|\dot{\gamma}|^{n'}$

Table 3. Summary of the predictions of three models

Impeller	helical ribbon	anchor		blade turbine			flat disc
	I	II	III	IV	V	VI	VII
n	0.183	0.60	0.35	0.50	0.21~0.26	0.45	0.37
D/d	1.11	1.04	1.2	2.0	1.3~3.0	1.43	2.67
D/d_e *	1.37	1.25	1.38	3.15	3.15~8.90	2.97	6.68
Eq. 7	++	+ [a] ++ [b]	++	—	+++	+++	+++
Eq. 12	—	+++ —	+	—	+	+	++
Eq.26	+++			—			

I: this work (geometries: HR1 and HR3);
II: Bourne et al.(1981), a: small scale (d=0.109m), b: large scale (d=1.52m);
III: Pollard and Kantyka (1967);
IV: Nagata et al.(1971) (6 blade turbine);
V: Metzner et al.(1961) (6 blade fan turbine);
VI: Forschner et al.(1991);
VII: Höcker et al.(1981);
*: values of D/d_e are calculated via Eq.8 using the power information in the laminar flow regime;
mark order: +++: very good, ++: good, +: adequate, —: poor.

Table 4. Effect of Fluid Properties and Geometry on Nt_m and t_m/t_c

Fluids	Rheological characteristics	Nt_m			t_m/t_c		
		HR1	HR2	HR3	HR1	HR2	HR3
glycerol	Newtonian	--	--	49.1	--	--	4.4
1% CMC (H_2O)	Shear-thinning	116	--	--	8.2	--	--
0.5% xanthan (gly./H_2O)	Viscoelastic	143	162	133	7.5	10.6	9.6
800 ppm PAA (corn syrup)	Boger	242	--	207	7.2	--	6.4

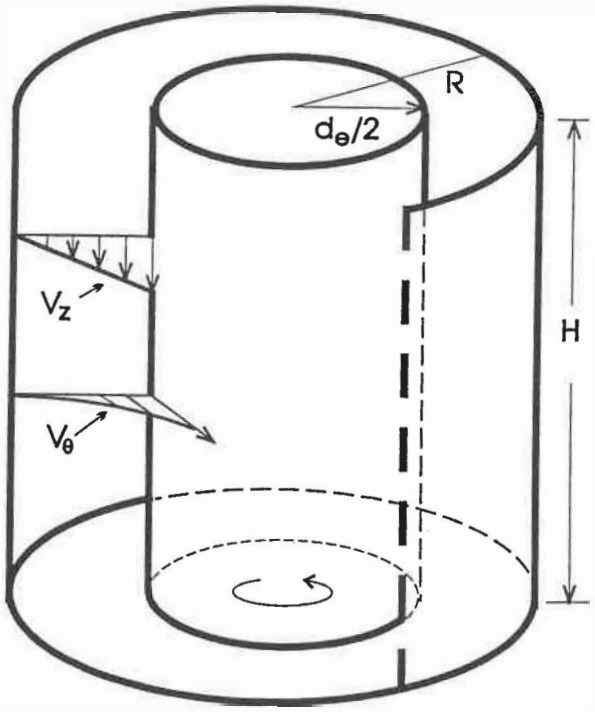

Figure 1 Sketch of the two dimensional equivalent Couette flow

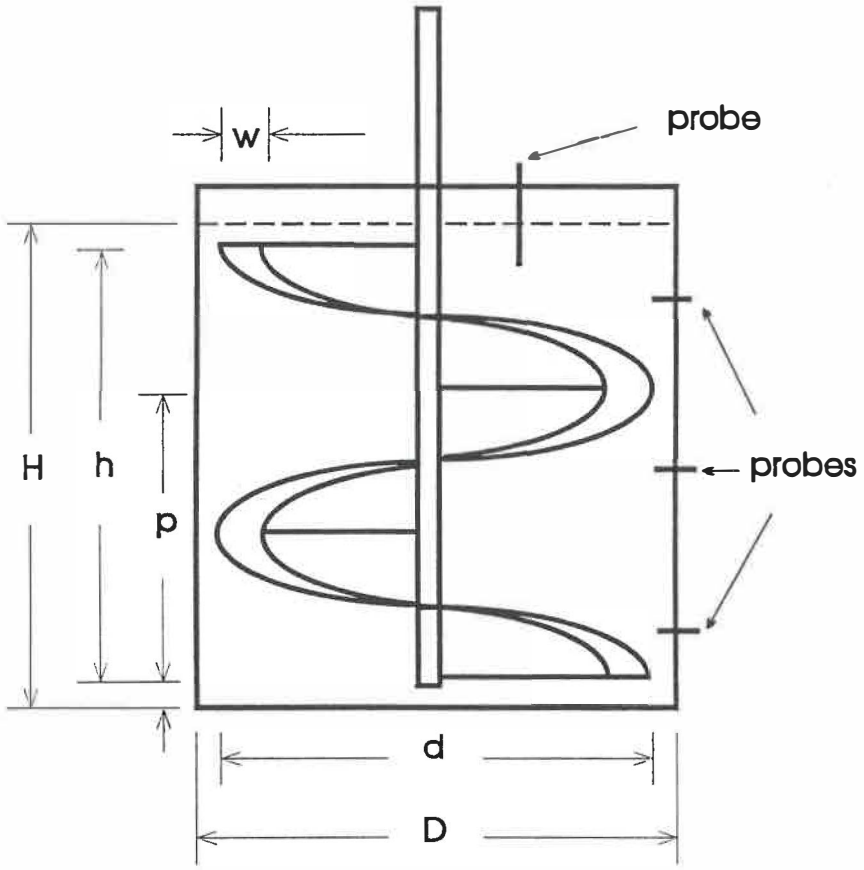

Figure 2 Helical ribbon system

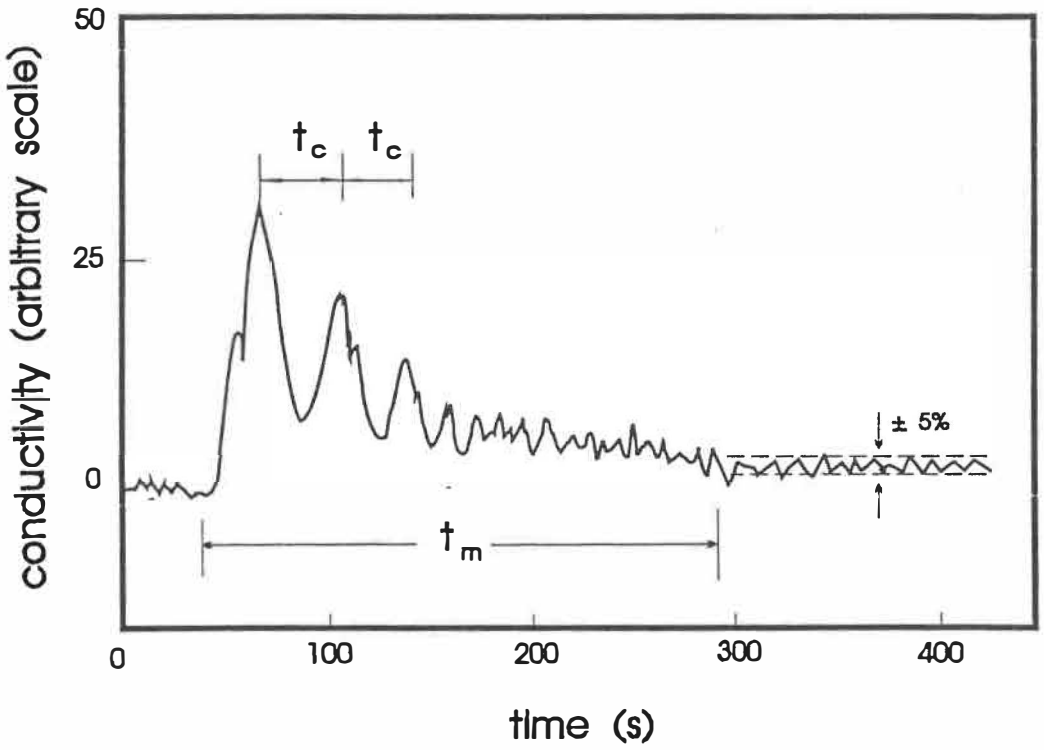

Figure 3 Measurement of mixing and circulation times for 800 ppm PAA in impeller HR1 system, at 59 rev/min

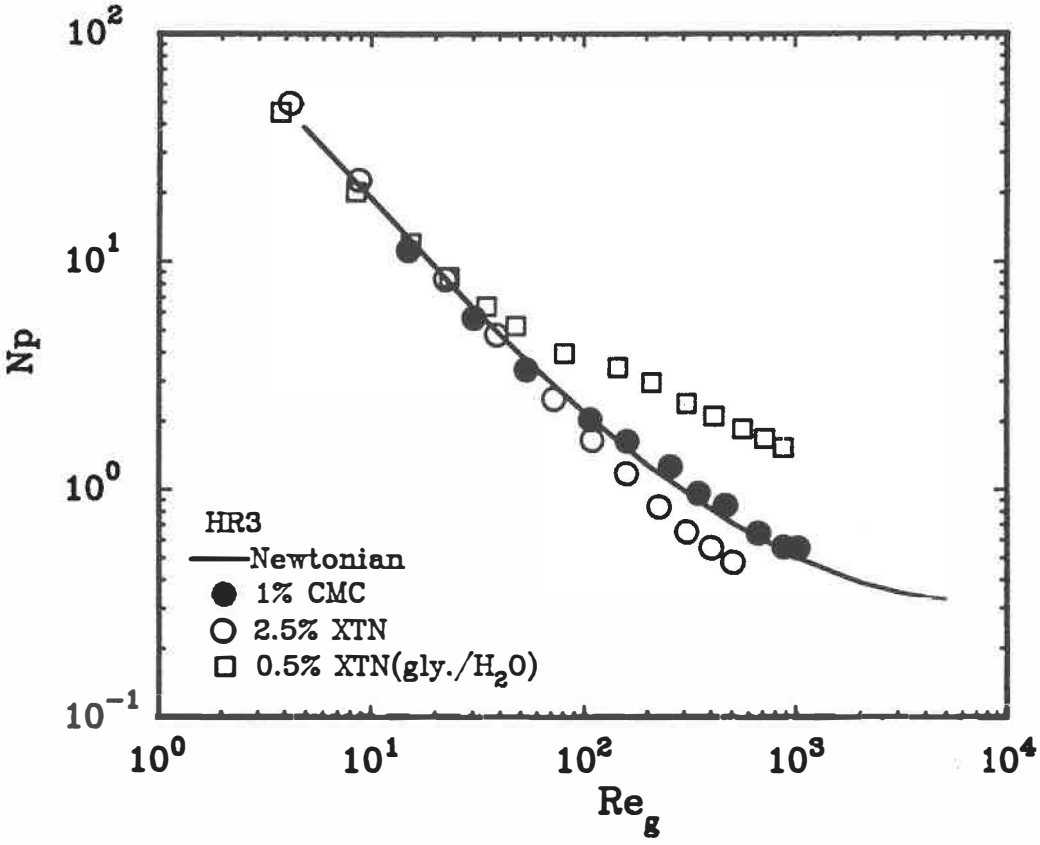

Figure 4 Power curves for Newtonian and non-Newtonian test fluids

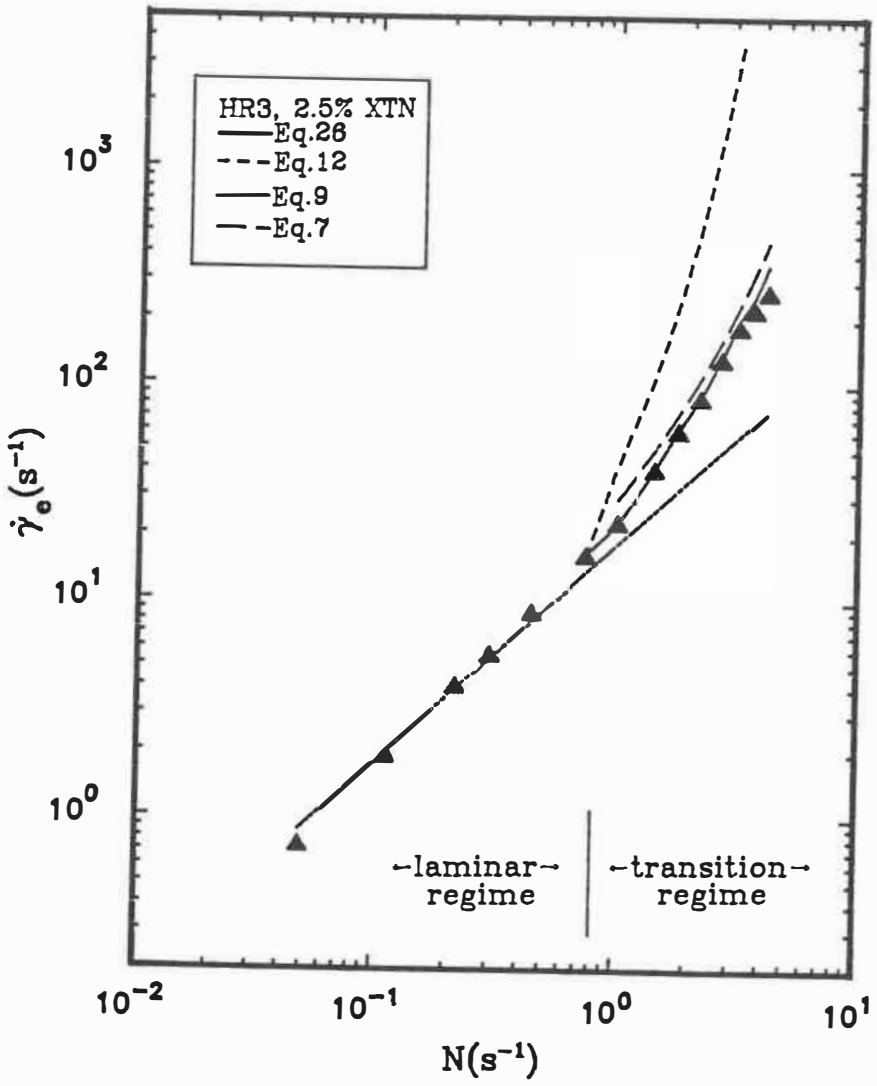

Figure 5. Predictions of $\dot{\gamma}_e$ compared with the experimental data for the highly shear-thinning 2.5% xanthan solution with impeller HR3

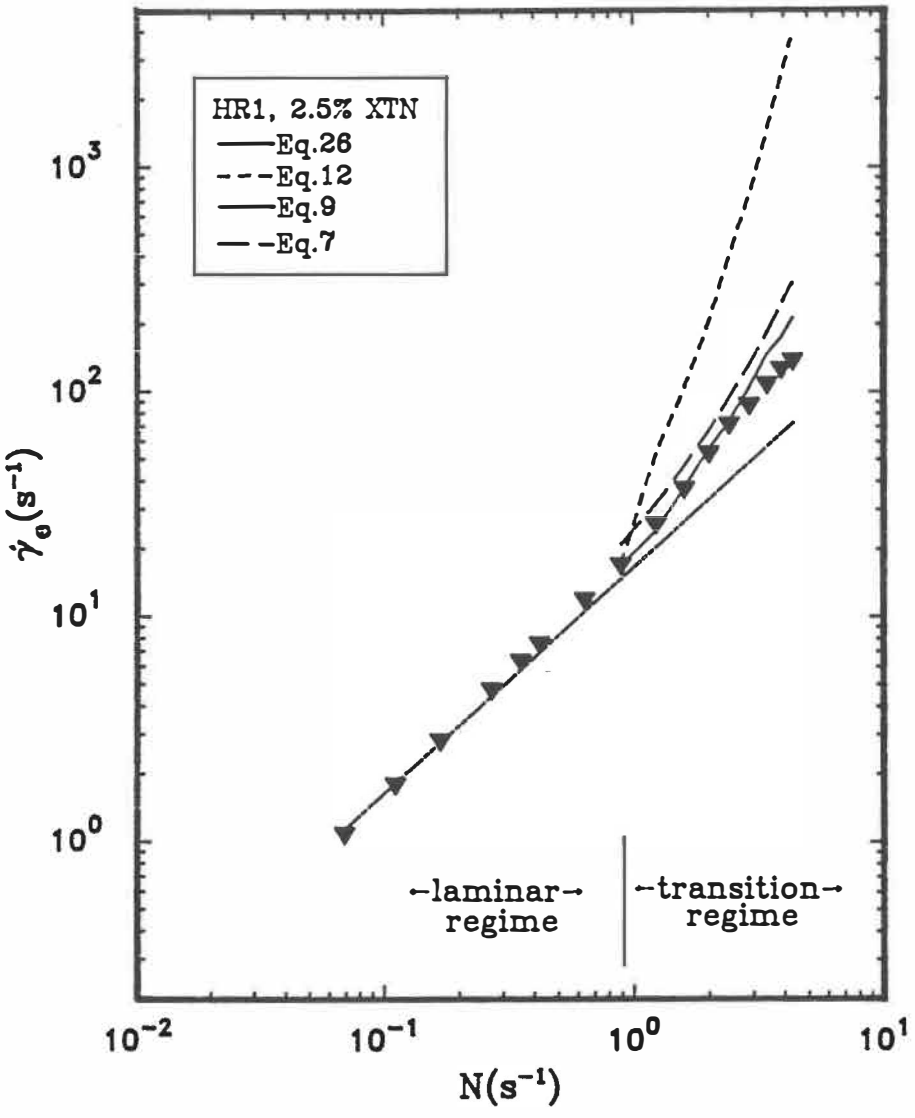

Figure 6. Predictions of $\dot{\gamma}_e$ compared with the experimental data for the highly shear-thinning 2.5% xanthan solution with impeller HR1

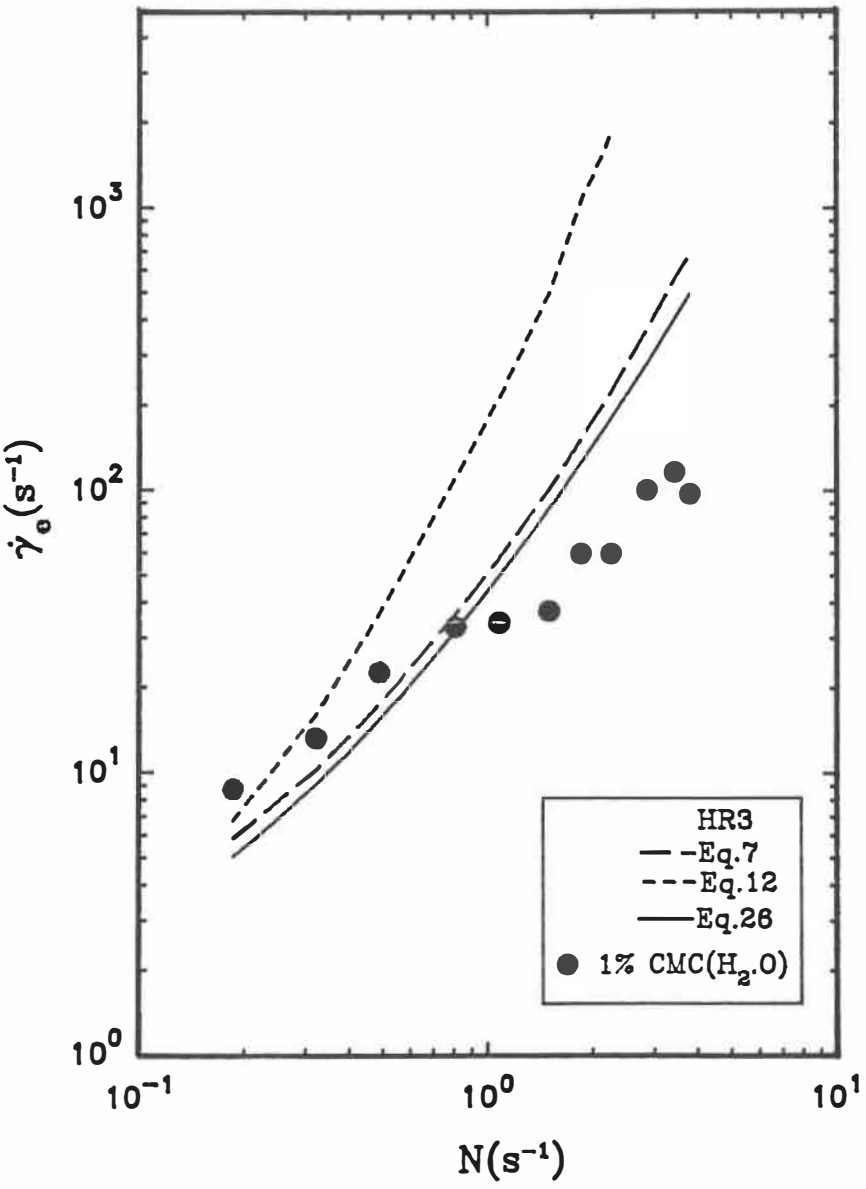

Figure 7 Predictions of $\dot{\gamma}_e$ compared with the experimental data for the moderately shear-thinning 1% CMC solution with impeller HR3

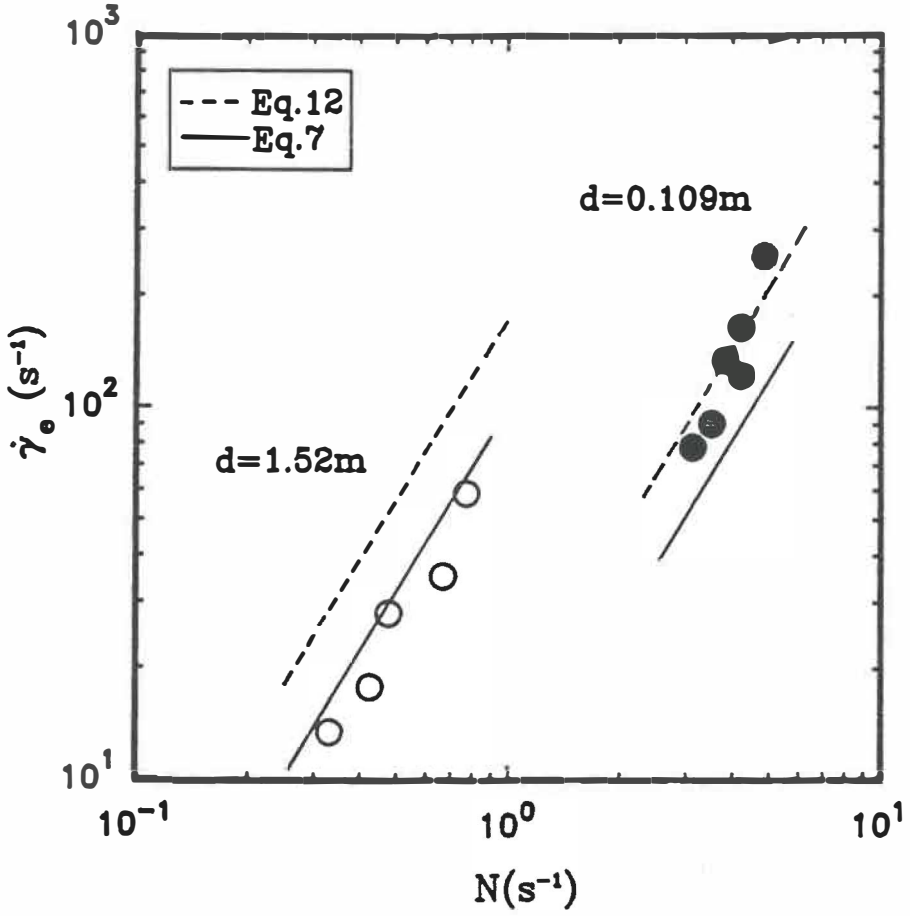

Figure 8. Predictions of $\dot{\gamma}_e$ compared with the data of Bourne et al.(1981) with anchor

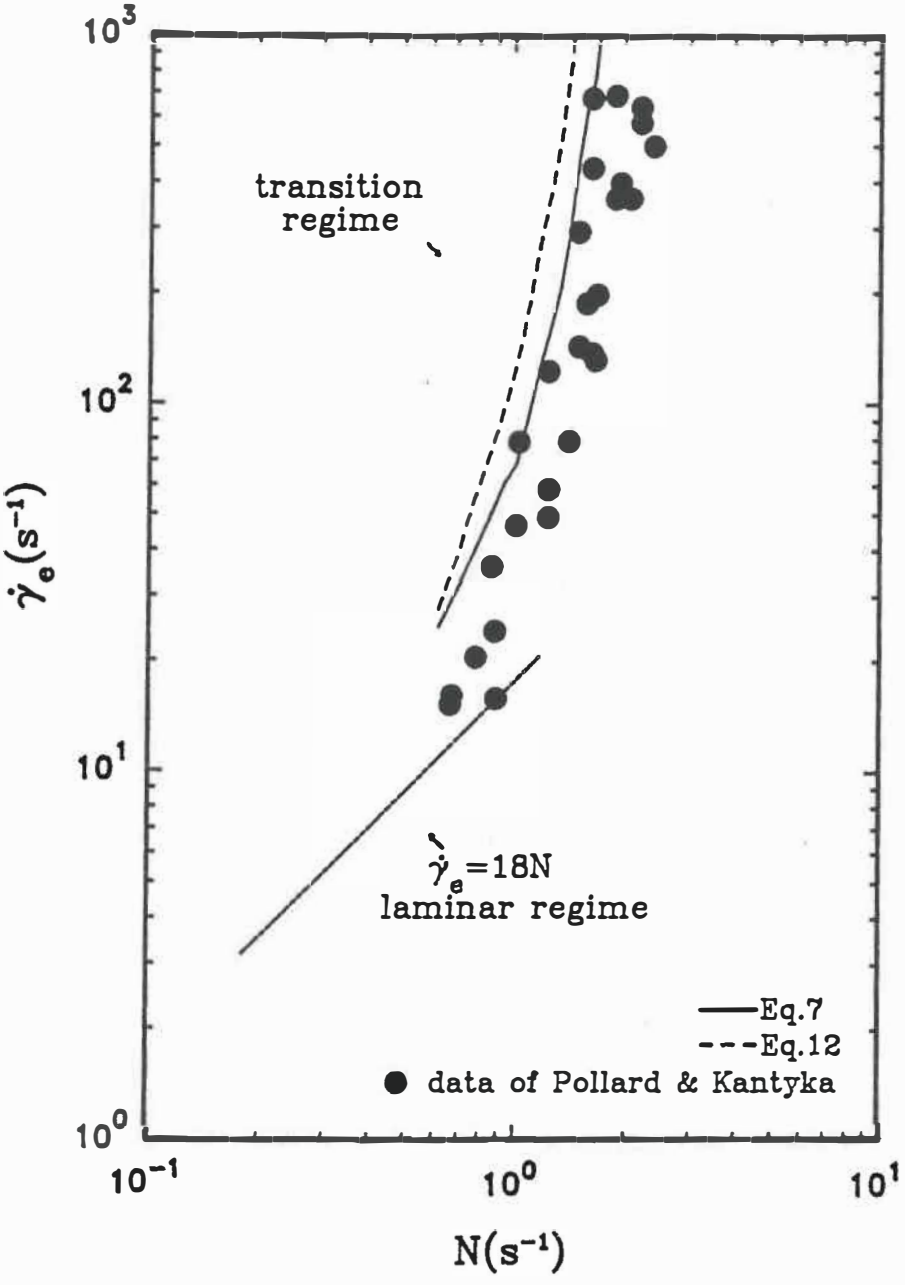

Figure 9 Prediction of $\dot{\gamma}_e$ compared with the data of Pollard and Kantyka (1969) with anchor impeller

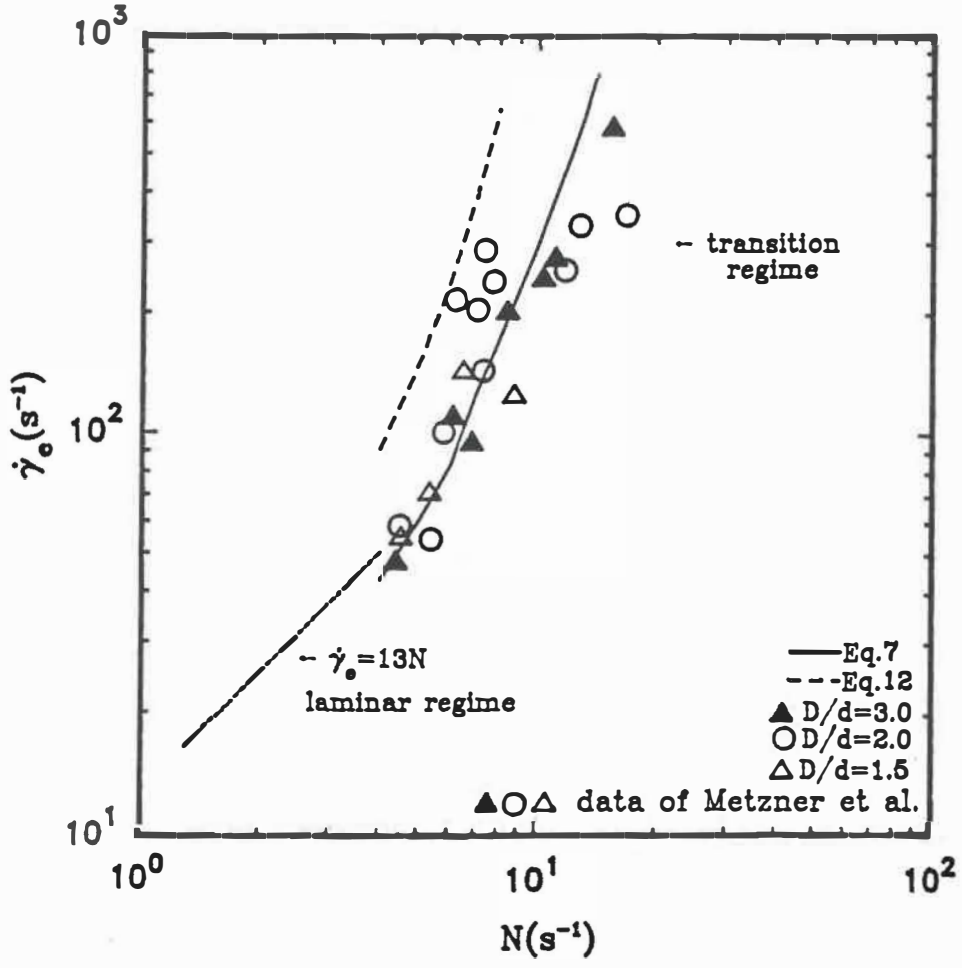

Figure 10 Prediction of $\dot{\gamma}_e$ compared with the data of Metzner et al. (1961) with 6-bladed fan turbine impeller

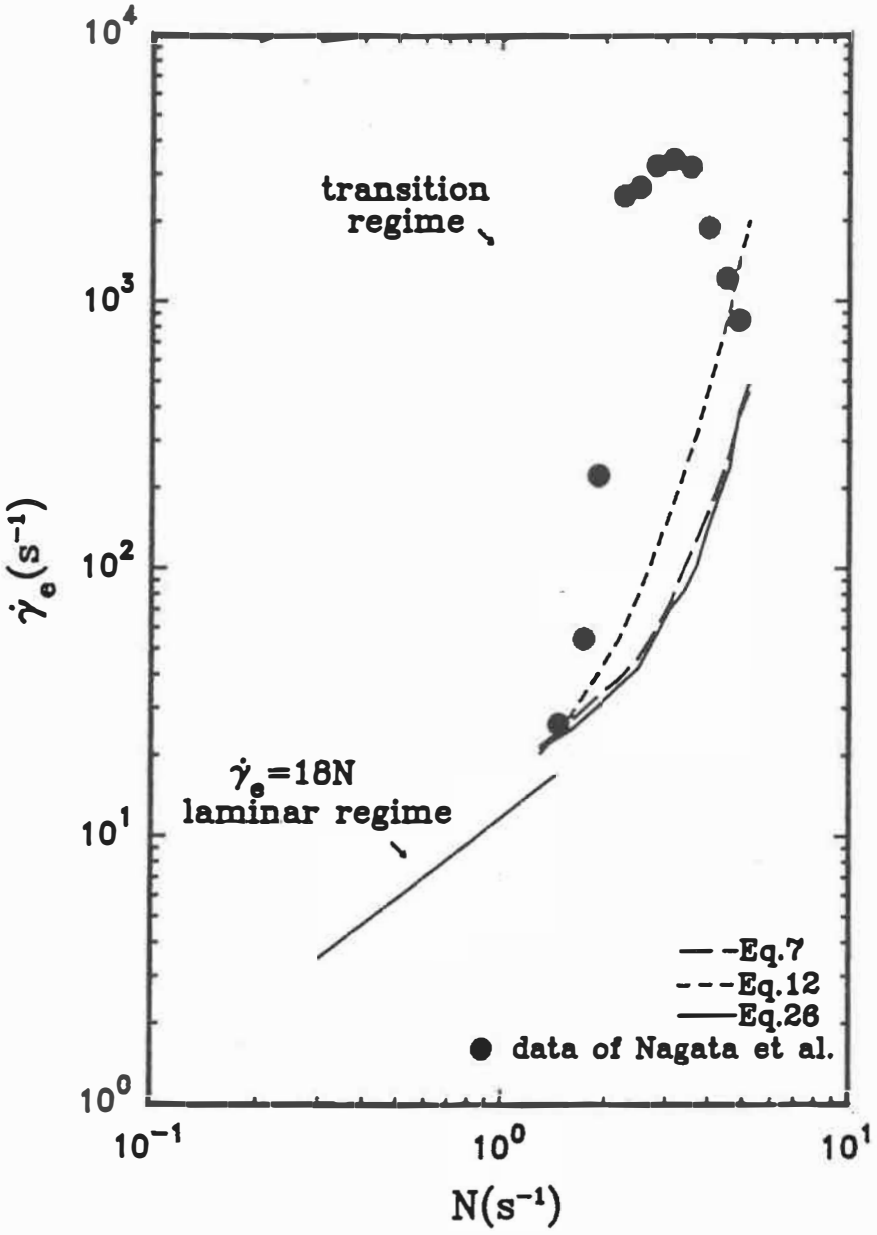

Figure 11 Prediction of $\dot{\gamma}_e$ compared with the data of Nagata et al.(1971) with 6-blade turbine impeller.

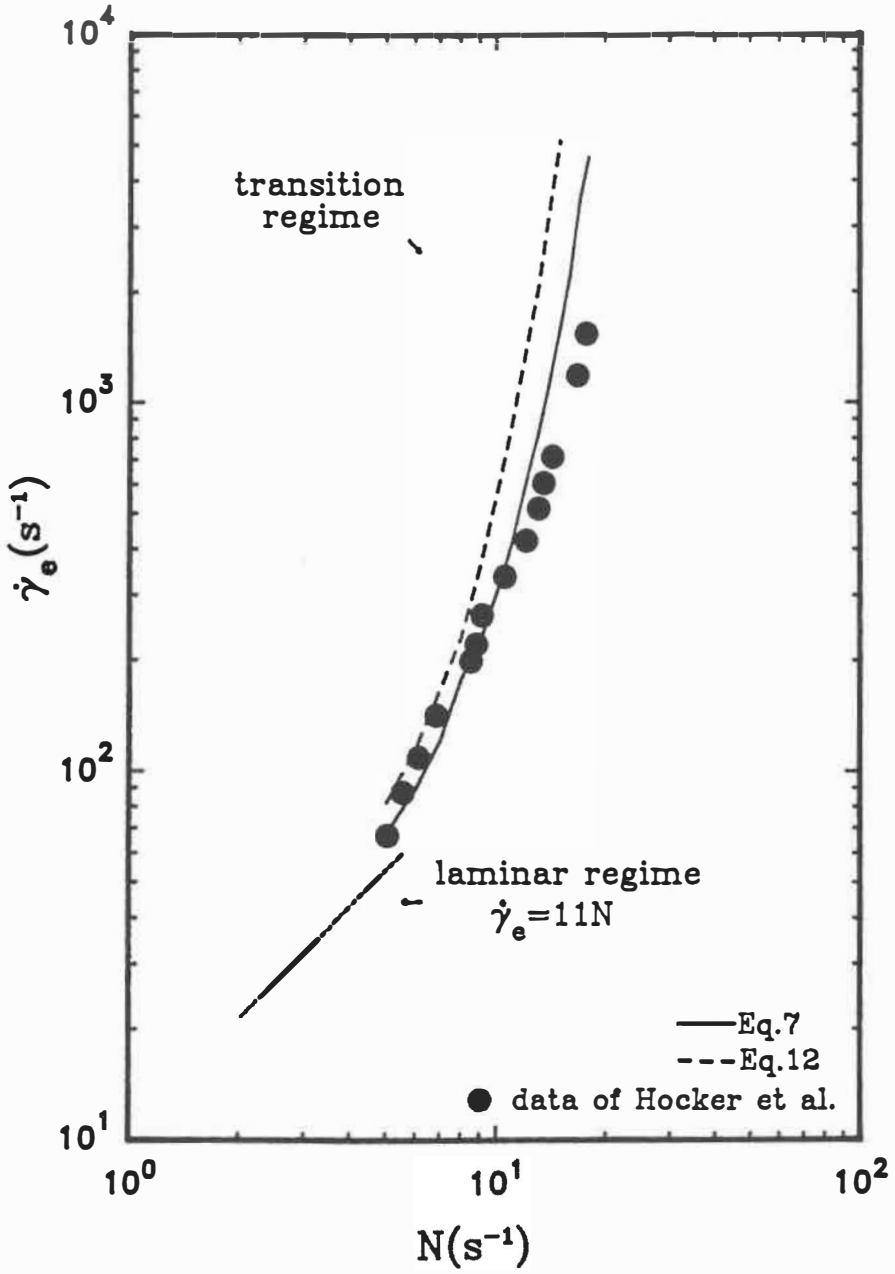

Figure 12 Prediction of $\dot{\gamma}_e$ compared with the data of Höcker et al. (1981) with flat disc impeller

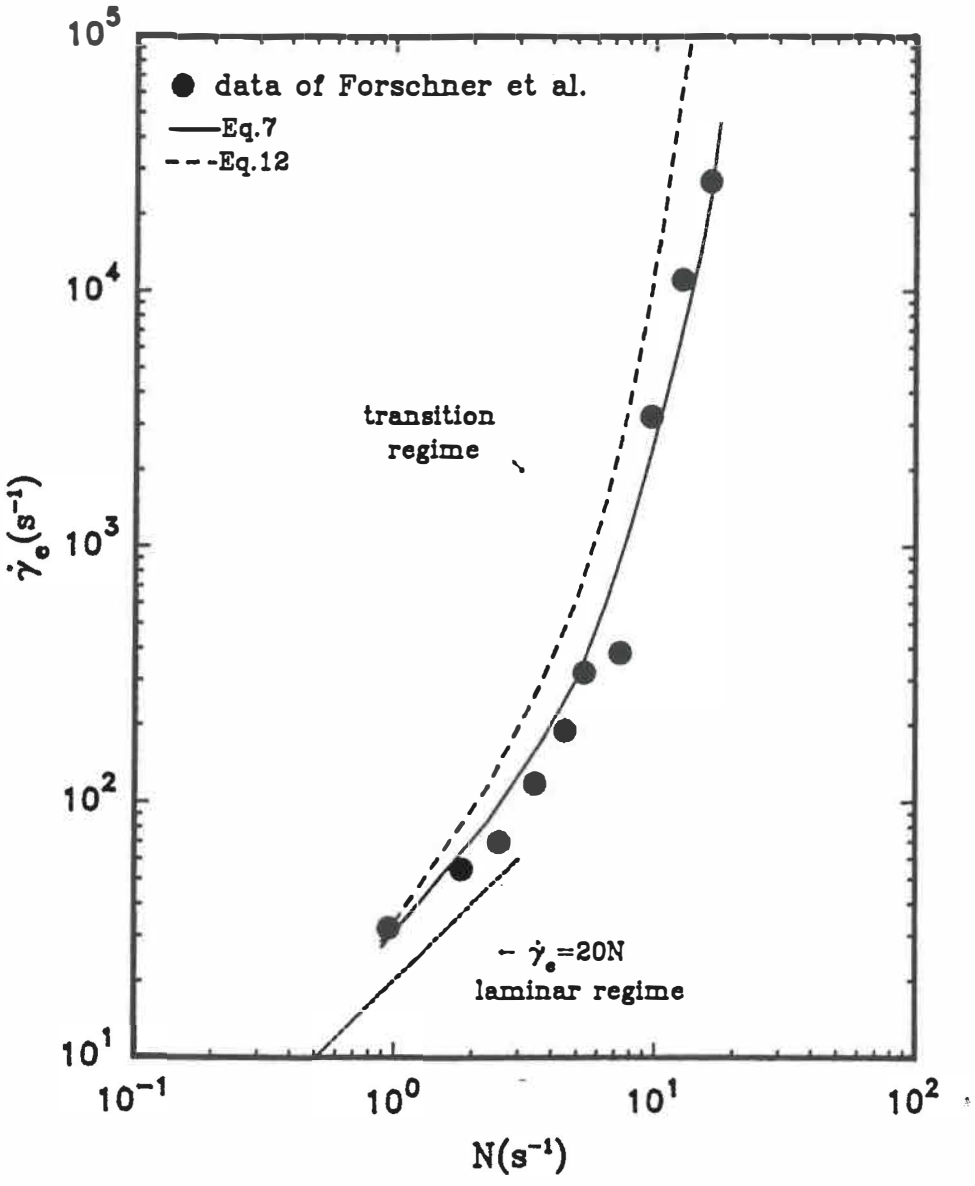

Figure 13 Predictions of $\dot{\gamma}_e$ compared with the data of Forschner et al.(1991) with Inter-Mig turbine impeller

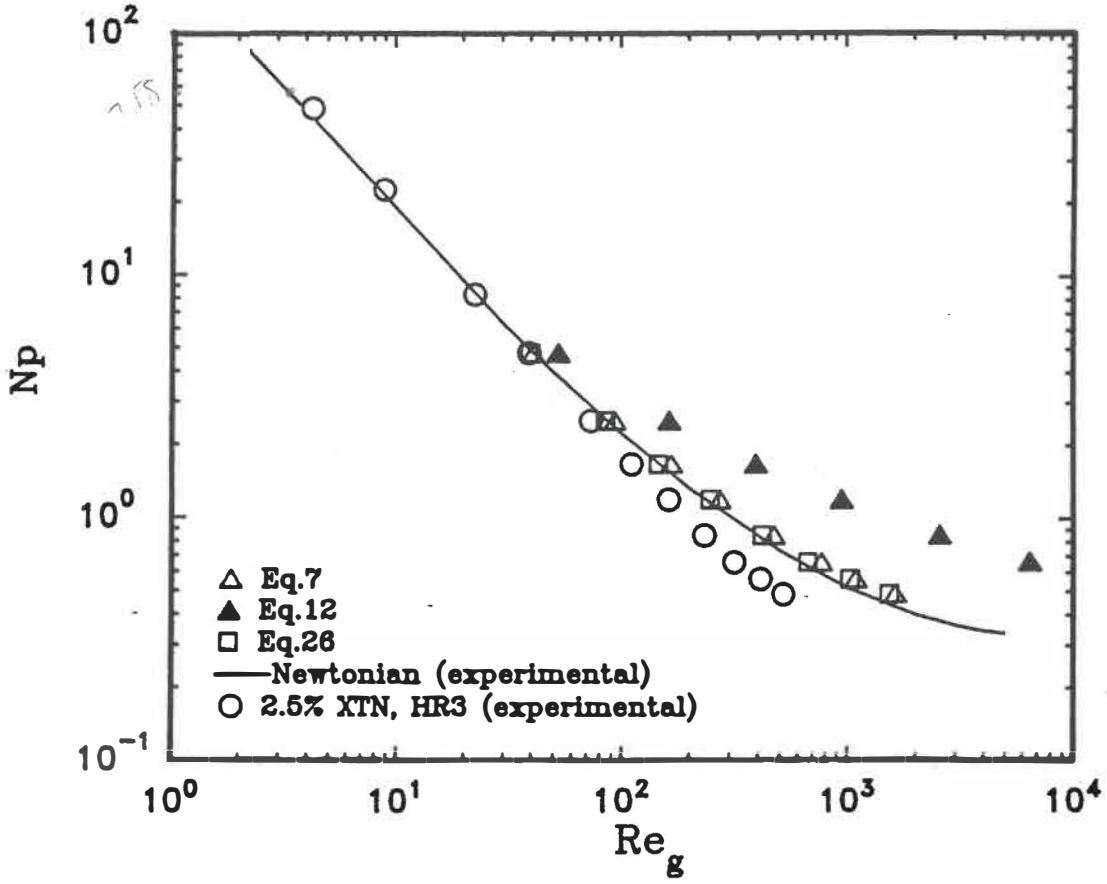

Figure 14 Comparison of power data evaluated via the effective shear rate obtained from Metzner-Otto's expression (Eq.1) and via Eqs. 7, 12 and 26

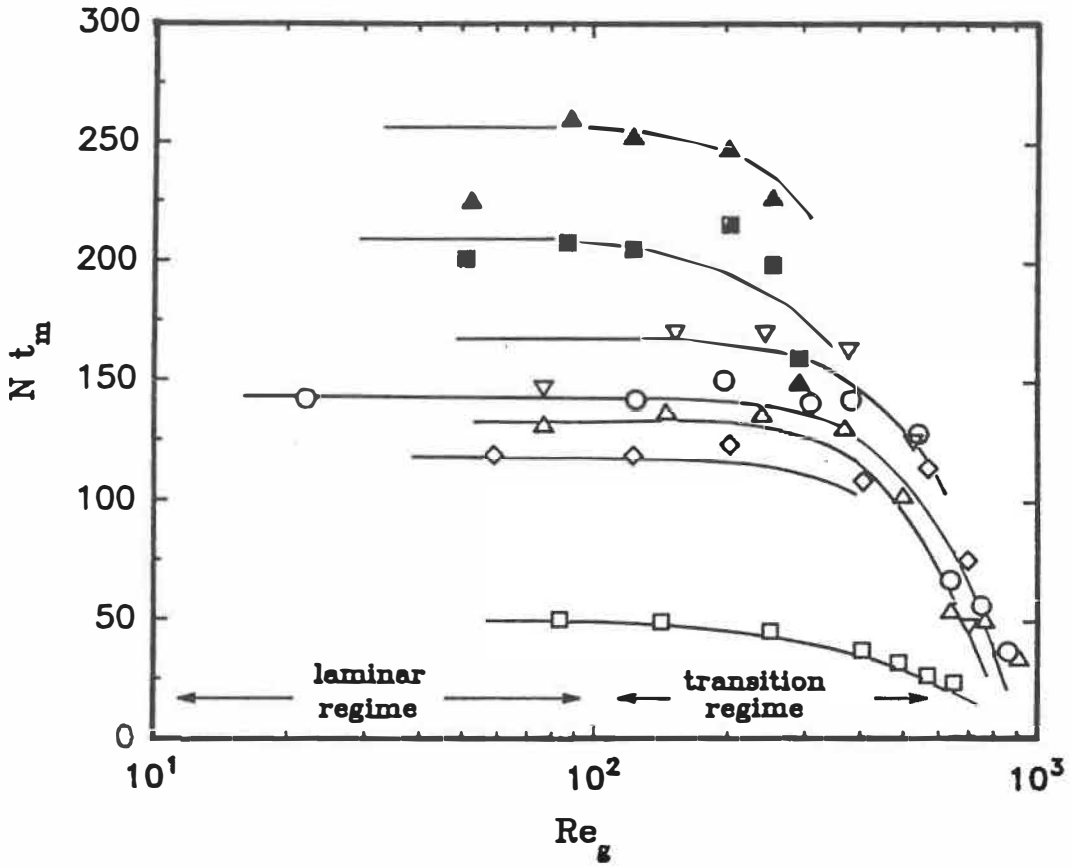

Figure 15 Dimensionless mixing time, Nt_m, versus generalized Reynolds number Re_g. □: glycerol (μ = 0.47 Pa.s), ◇: 1% CMC (H_2O), ◯ ▵ ▽: 0.5 % xanthan in glycerol/H_2O, ▲ ■: 800 ppm PAA in corn syrup; ◇ ◯ ▲: HR1 impeller, ▵: HR2 impeller, □ ▽ ■: HR3 impeller

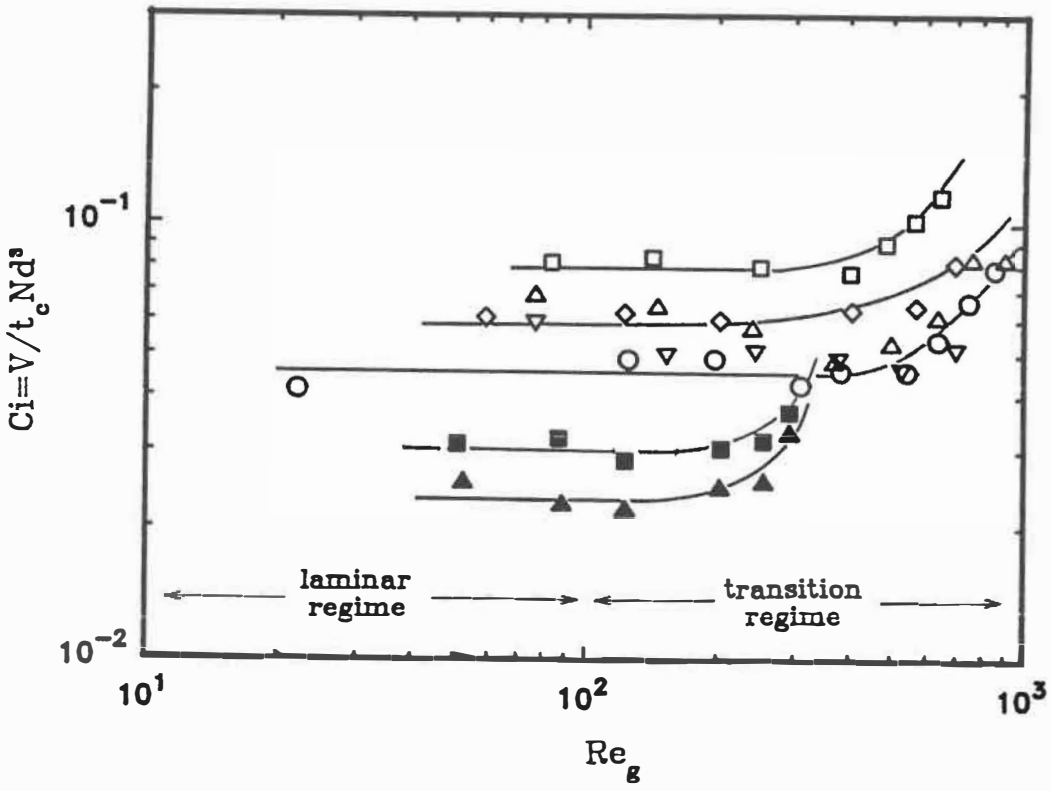

Figure 16 Circulation number, *Ci*, versus generalized Reynolds number. □: glycerol (μ = 0.47 Pa.s), ◇: 1% CMC (H_2O), ◯ ▵ ▽: 0.5 % xanthan in glycerol/H_2O, ▲ ■: 800 ppm PAA in corn syrup; ◇ ◯ ▲: HR1 impeller, ▵: HR2 impeller, □ ▽ ■: HR3 impeller

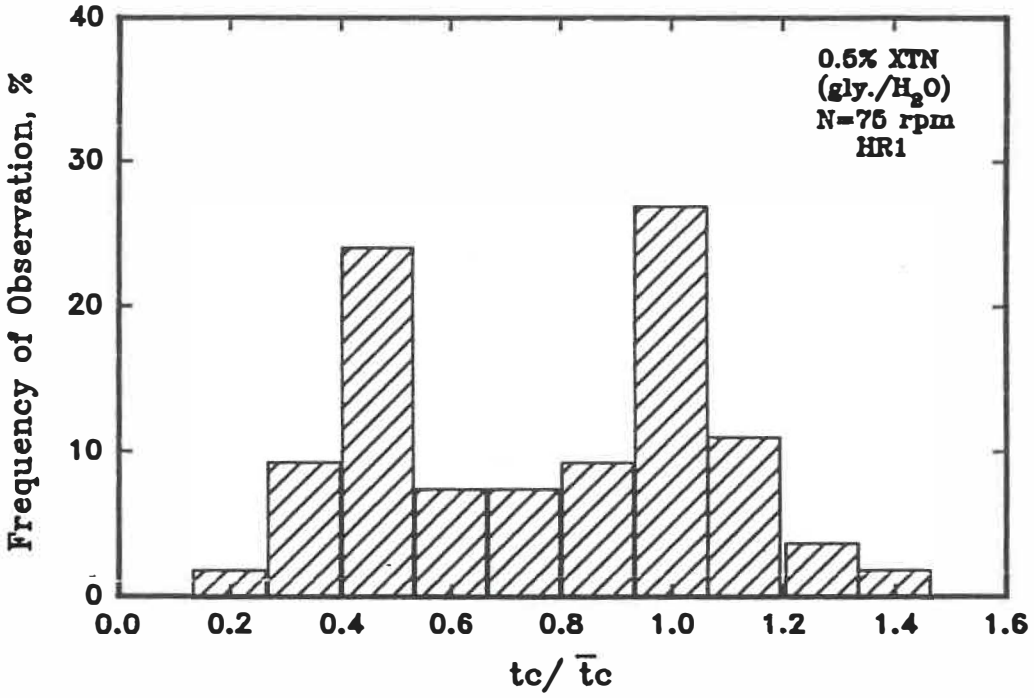

Figure 17 Distribution of circulation time for 0.5% Xanthan in glycerol/H_2O

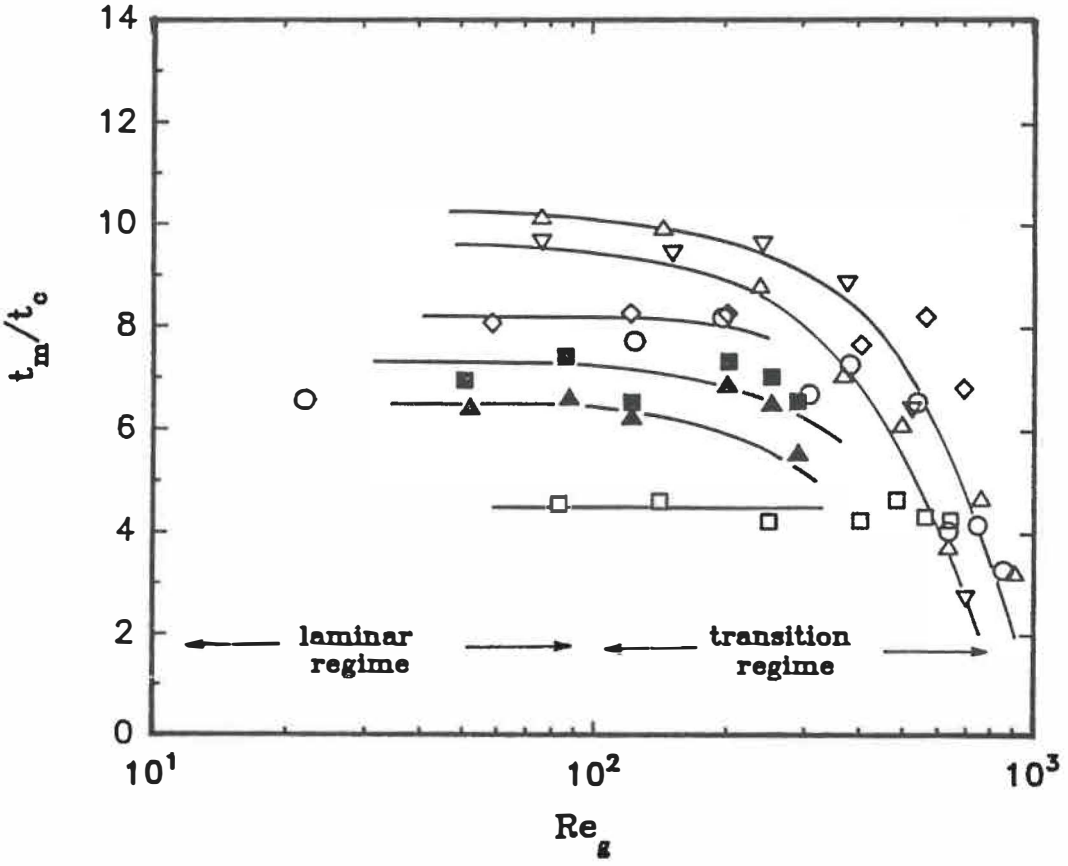

Figure 18. Dependence of t_m/t_c with generalized Reynolds number □: glycerol (μ = 0.47 Pa.s), ◇: 1% CMC (H_2O), ◯ ▵ ▽: 0.5 % xanthan in glycerol/H_2O, ▲ ■: 800 ppm PAA in corn syrup; ◇ ◯ ▲: HR1 impeller, ▵: HR2 impeller, □ ▽ ■: HR3 impeller

Chapter 6

CONCLUSIONS

6-1 Conclusions

The influence of the complex rheological properties of non-Newtonian fluids on the mixing performance has been examined. Two scale mixers agitated by close clearance helical ribbon agitators of different geometric combinations has been investigated in the laminar and in the transition flow regimes with and without aeration. Several models based on the analysis of the equivalent Couette flow have been developed to predict the effective deformation rate in both the laminar and transition flow regimes. The main achievements of this work are presented in the following paragraphs.

- The experimental results for the helical ribbon agitators have shown that for highly shear-thinning inelastic fluids, the power number has an extended laminar flow regime, that is, the onset of the transition flow regime is somewhat delayed to higher Reynolds number. However, for moderately shear-thinning inelastic fluids, the power consumption does not deviate from the corresponding Newtonian one through the laminar to the transition regime. A early departure of power number from the corresponding Newtonian curve was observed for elastic fluids, even within the laminar regime. Elasticity tends to increase the power requirement dramatically, by a factor up to 3.5 in case of the 0.35% PIB solution. The more elastic the fluids is, the sooner is the departure.
- For shear-thinning inelastic fluids, the effective deformation rate constant k_s from Metzner-Otto's method was found to be a function of the flow index, n, in the laminar flow regime. The k_s value increases considerably with increasing the flow index. Two models based on the analysis of the equivalent Couette flow are proposed to predict the effective deformation rate and the power requirement of inelastic shear-thinning fluids in the laminar regime with close clearance helical ribbon impellers.
- The power consumption for the Boger fluids (elastic with shear independent

viscosity) under aerated conditions was found, for the first time, to be much higher than for ungassed conditions at low Reynolds numbers and increases with increasing gas flow rate. This phenomena coincides with the enhancement of the apparent viscosity of gassed fluids measured using a rheometer. With increasing Reynolds number, the power decreases and approaches to value obtained for ungassed conditions. For shear-thinning inelastic fluids, the power under aerated conditions is lower than for ungassed conditions, and with increasing Reynolds number, it levels off. A concept of aerated shear deformation rate is outlined to correct the effective deformation rate under gassed circumstances. Two empirical correlations based on dimensional analysis are presented, in terms of the aeration number, the Weissenberg number and aerated Reynolds number, which is evaluated from the aerated deformation rate. The correlations predict well the power under aerated conditions for both the laminar and transition flow regimes.

- For the transition flow regime, the experimental data of this work have confirmed the previous findings that the effective deformation rate is no longer proportional to the impeller rotational speed. From a closer examination, it was found that the effective shear rate increases sharply for highly shear-thinning inelastic fluids agitated by close clearance helical ribbon impellers, whereas the extended linear relation of Metzner-Otto (1957) is still valid for fairly shear-thinning fluids. As reviewing the literature, in contrast to the results obtained for helical ribbon agitators, a drastic enhancement of the effective deformation rate was observed even for moderately shear-thinning fluids agitated by other types of impeller such as anchor, blade turbine, flat disc. Three models based on one or two dimensional analysis of the equivalent Couette flow are proposed to predict the effective deformation rate in the transition flow regime. The predictions are compared with experimental data obtained for various non-

Newtonian fluids mixed by helical ribbon agitators, and with literature data for anchor, blade turbine and flat disc agitators. The agreement between the predictions and experimental values is quite good.

- The elasticity and shear-thinning properties apparently have no significant effect on the dimensionless mixing and circulation times in the transition flow regime, compared with Newtonian data. However, in the laminar regime, the effects of non-Newtonian behaviour on the mixing and circulation times are quite pronounced, for instance, more than five fold higher dimensionless mixing time was obtained for the viscoelastic fluids compared with that for glycerol of comparable viscosity. The best performances are given by the impeller with a larger blade width and a smaller pitch. Flow of irregularities in the transition regime are much drastic. Bottom clearance between the impeller and vessel has negligible effect on the power consumption in the laminar and transition flow regime.

6-2 Recommendation for Future Work

As pointed in the first chapter, mixing is still in the developing, rather than developed stage of investigation, that is, many unmapped areas obviously need to be explored. Hereby, the author would like to emphasize two of them: mixing under aerated conditions, and mixing in the transition flow regime, which are of considerable practical industrial interest.

- First, bridges should be built to bring in more appropriate rheological data, rather than obtained under the ideal steady simple shear flow, to describe the flow field in a mixing reservoir. A specific case is mixing under aeration. What is anxiously needed as one deals with gassed mixing, is the corrective gassed rheological parameters which are almost missing in the literature. No effort has been ever devoted to this domain although the question of using ungassed

rheological data for gassed conditions has raised (Nienow et al., 1983). Even a glance into this area can be very helpful for a better understanding of the mixing performance under gassed conditions

- The effective deformation rate has been gradually accepted as a subject of high interest, since it is related to the power consumption. It can be argued that the effective deformation rate is one of the macro-expression of flow field in a mixing reservoir (related to the local fluid's deformation). The expression of the effective deformation rate under gassed conditions or in the transition flow regime is expected to be much more complicated than for under ungassed conditions and in the laminar flow regime. However, the values used in the literature for the effective deformation rate under gassed conditions are essentially the values obtained from ungassed conditions. Obviously, these data can not properly describe the real deformation fluids experience under gassed circumstances. Intensive exploration in this area is definitely necessary. One of the approaches is likely to combine the deformations caused by bubbles' presence and caused by the impeller mechanical blending. This combination may not be as simple as proposed in this work. Available information from the bubble columns or on the deformation of bubbles may be quite useful to describe a more refined model for the effective deformation rate under aerated conditions.
- The effective deformation rate for the transition flow regime is highly difficulty to predict. Needs of detailed flow field in the mixing systems for the transition regime emerge, to develop valid models to correctively predict the effective deformation rate. An investigation of the detailed flow behaviour and velocity profiles can result in more sophisticated models which are essential for the industrial scale-up and designs (Ulbrecht and Carreau, 1985).
- The influence of elasticity on the mixing performance in the transition flow

regime is far from being clarified. The elastic effect was is expected to be much pronounced. Investigations should be carried out to confirm the observations of this work on the effects of elasticity on the power consumption, mixing and circulation times, flow patterns, etc. The effect of elastic deformation on the gassed mixing is also needed to be studied intensively.

APPENDICES

Appendix I

Effective deformation rate in the laminar flow regime including bottom clearance effect

Following Bourne and Bulter (1969), we make use of an one-dimensional analogy of the equivalent Couette flow to simulate the fluid's flow in an agitated mixer. The fluid movement caused by a rotating helical ribbon impeller can be replaced by a coaxial cylindrical configuration with the inner cylinder rotating in an angle speed Ω. The inner cylinder has an equivalent diameter of d_e. A typical sketch of a helical ribbon mixer is shown in Figure 1 of Chapter 3. It is assumed that the energy dispersion (in terms of viscous dispersion) in this system is caused by the simple shear deformation of the fluid in the clearance from the out cylindric wall to the impeller tip, and in the clearance from the bottom wall to impeller blade. We examine the effects of wall and bottom clearances, respectively, on the energy dispersion in terms of the torque, then the sum of these two effects, to obtain the expression of the effective shear rate in the laminar flow regime.

Wall effect

First, we study the influence of wall clearance. The hypotheses in this simple shear flow field of steady state can be reasonably given as:

$$v_r = v_z = 0 \ , \quad v_\theta = v_\theta(r) \tag{1}$$

$$\tau_{rz} = \tau_{\theta z} = 0 \ , \quad \tau_{r\theta} = f(r) \tag{2}$$

The θ-component of motion equation can be reduced to:

$$\frac{\partial}{\partial r}\left(r^2 \tau_{r\theta}\right) = 0 \tag{3}$$

For the *power-law* fluids, the shear stress can be given by:

$$\tau_{r\theta} = -m\,\dot{\gamma}_{r\theta}^{n} = -m\left[r\frac{\partial}{\partial r}\left(\frac{v_\theta}{r}\right)\right]^n \tag{4}$$

Substitution of Eq.4 into Eq.3 yields:

$$\frac{d}{dr}\left(r^2\left[r\frac{d}{dr}\left(\frac{v_\theta}{r}\right)\right]^n\right) = 0 \tag{5}$$

Eq. 5 can be integrated with respect to r with the boundary conditions: $v_\theta = \Omega d_e/2$ when $r = d_e/2$, $v_\theta = 0$ when $r = D/2$, to give the velocity profile:

$$\frac{v_\theta}{r} = \frac{\Omega}{(D/d_e)^{2/n} - 1}\left[\left(\frac{R}{r}\right)^{2/n} - 1\right] \tag{6}$$

and the shear stress can be expressed in terms of the equivalent diameter, d_e, that is:

$$\tau_{r\theta} = m\left[\frac{2\Omega}{n\left[(D/d_e)^{2/n} - 1\right]}\right]^n \left(\frac{R}{r}\right)^2 \tag{7}$$

The torque exerted on the inside cylinder is taken as:

$$\Gamma_{wall} = (2\pi RH)(-\tau_{r\theta})\big|_{r=R}\, R \tag{8}$$

Substituting Eq. 7 into Eq. 8 gives

$$\Gamma_{wall} = \frac{\pi}{2} mD^2H\left[\frac{2\Omega}{n\left[(D/d_e)^{2/n} - 1\right]}\right]^n \tag{9}$$

Bottom effect

Hereby, we focus on to the effect of the bottom clearance on the torque. The reader

may be refereed to Bird et al, 1987 for elaboration for a similar flow configuration. The hypotheses can be speculated as:

$$v_r = v_z = 0 \ , \quad v_\theta = rf(z) \tag{10}$$

The θ-component of the motion equation can be simplified to:

$$-\left(\frac{1}{r^2}\frac{\partial}{\partial r}\left(r^2\tau_{r\theta}\right) + \frac{\partial \tau_{z\theta}}{\partial z}\right) = 0 \tag{11}$$

The magnitude of $\tau_{r\theta}$ is very small comparing to $\tau_{z\theta}$ and it can be neglected:

$$\frac{\partial \tau_{z\theta}}{\partial z} = 0 \tag{12}$$

For power law fluids, the shear stress can be defined as:

$$\tau_{z\theta} = -m\ \dot{\gamma}_{z\theta}{}^{n} = -m\left(\frac{\partial v_\theta}{\partial z}\right)^{n} \tag{13}$$

Substituting Eq. 13 into Eq. 12 yields:

$$\frac{\partial}{\partial z}\left[-m\left(\frac{\partial v_\theta}{\partial z}\right)^{n}\right] = 0 \tag{14}$$

Eq. 14 can be integrated with respect to z with the boundary condition: $v_\theta|_{z=he} = \Omega r$, and $v_\theta|_{z=0} = 0$,

$$v_\theta = \frac{\Omega r z}{h_e} \tag{15}$$

Then the shear stress can be obtained:

$$\tau_{z\theta} = -m\left(\frac{\Omega}{h_e}\right)^{n} r^{n} \tag{16}$$

The torque due to the bottom contribution is given by:

$$\Gamma_{bottom} = \int_0^{d_e/2} r \left[\tau_{z\theta}|_{r=d_e/2}\right] 2\pi r dr \tag{17}$$

$$\Gamma_{bottom} = \frac{2\pi m}{n+3}\left(\frac{d_e}{2}\right)^{n+3}\left(\frac{\Omega}{h_e}\right)^n \tag{18}$$

The total torque exerted on the impeller's shaft can be the sum of the wall and bottom ones:

$$\Gamma_{total} = \Gamma_{wall} + \Gamma_{bottom} \tag{19}$$

$$\Gamma_{total} = \frac{\pi}{2} m D^2 H \left[\frac{2\Omega}{n\left[(D/d_e)^{2/n}-1\right]}\right]^n + \frac{2\pi m}{n+3}\left(\frac{\Omega}{h_e}\right)^n\left(\frac{d_e}{2}\right)^{n+3} \tag{20}$$

The torque is related to the power consumption, P, that is:

$$P = 2\ \pi\ \Gamma_{total}\ N \tag{21}$$

Substituting Eq.19 into Eq.20 gives:

$$P = m\pi^{n+2}\ N^{n+1}\left\{ D^2 H \left[\frac{4}{n\left[(D/d_e)^{2/n}-1\right]}\right]^n + \frac{D^3}{2(n+3)}\left(\frac{H}{h_e}\right)^n\left(\frac{D}{H}\right)^n\left(\frac{d_e}{D}\right)^{n+3}\right\} \tag{22}$$

The experimental correlation of power number as function of Reynolds number at laminar flow region can be expressed as:

$$N_P\ Re_g = K_p \tag{23}$$

Follow the Metzner-Otto concept, the generalized Reynolds number, Re_g, in Eq.23 is evaluated from the effective viscosity, η_e, which is related to the effective deformation

rate, $\dot{\gamma}_e$. The effective viscosity is given in terms of power, P, from Eq.23, that is:

$$\eta_e = \frac{P}{K_p\, d^3\, N^2} \tag{24}$$

For *power-law* fluids, the effective viscosity is related to the effective shear rate:

$$\eta_e = m\ |\dot{\gamma}_e|^{n-1} \tag{25}$$

Combining Eq.24 and 25, the effective shear rate is given by:

$$\dot{\gamma}_e^{n-1} = \frac{P}{m\ K_p\, d^3\, N^2} \tag{26}$$

Eq. 26 can re-arranged by substituting Eq. 22 into Eq. 26, that is:

$$\frac{\dot{\gamma}_e}{N} = k_s = \left[\frac{\pi^{n+2}}{K_p d^3}\right]^{1/(n-1)} \left\{ D^2 H \left[\frac{4}{n\left[(D/d_e)^{2/n}-1\right]}\right]^n + \frac{D^3}{2(n+3)}\left(\frac{H}{h_e}\right)^n\left(\frac{D}{H}\right)^n\left(\frac{d_e}{D}\right)^{n+3} \right\}^{1/(n-1)} \tag{27}$$

In Eq.27, the effective deformation rate is function of the equivalent diameter, d_e, flow index, n, power number constant, K_p, and mixer geometry. If the bottom effect is neglected, the second term inside the braces in the right hand of Eq.27 can be erased. Then, Eq.27 is reduced to the Eq.13 in Chapter 3.

The predictions of the k_s values with different values of the bottom clearance (h_e values range from 5 mm to 200 mm) for impellers HR3 and HR4 are shown in Figures A1 and A2. The predictions were calculated using the values of D/d_e obtained for Newtonian fluids. As seen in the figures, the predictions with different values of h_e are much close to each other at lower values of the flow index and show fair differences with increasing flow index. The k_s values calculated using h_e values of 5, 10, 50 and 200 equal to 18.0, 18.6, 19.4 and 19.7 at the flow index of 0.2 for impeller HR4. Similar tendency is seen for impeller HR3. It should be noted that the curve of k_s

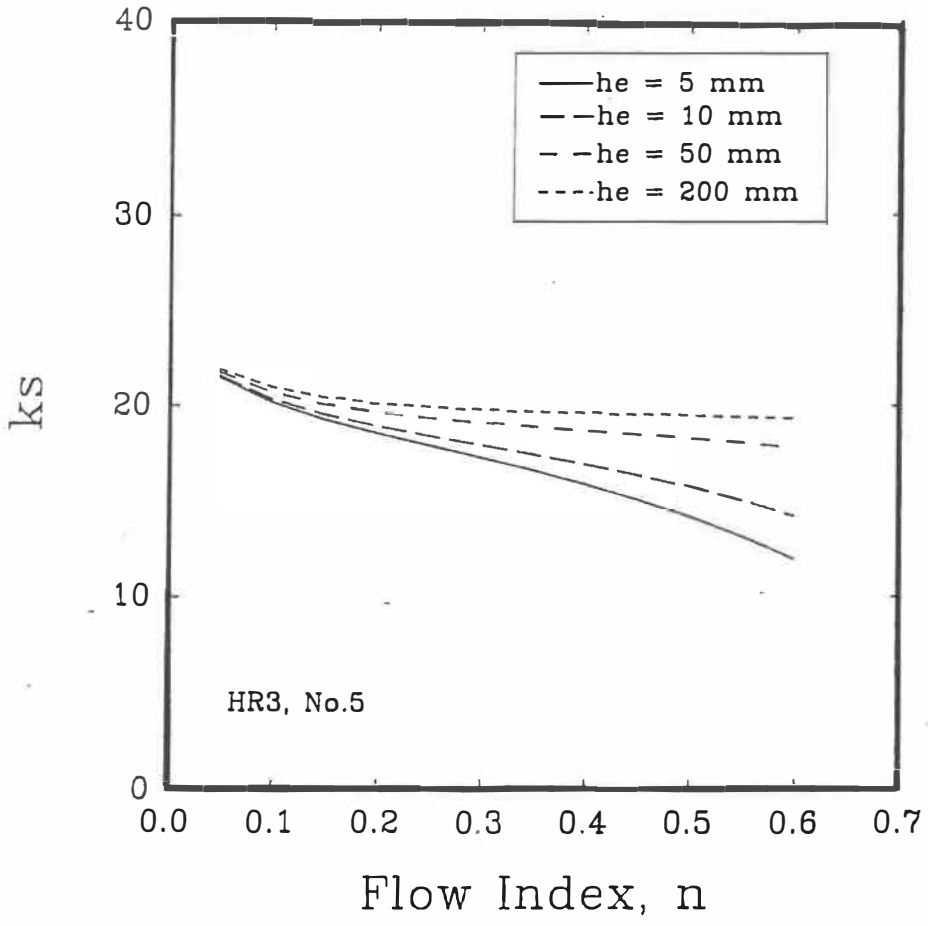

Figure A1 Effect of the equivalent bottom clearance on k_s for impeller HR3

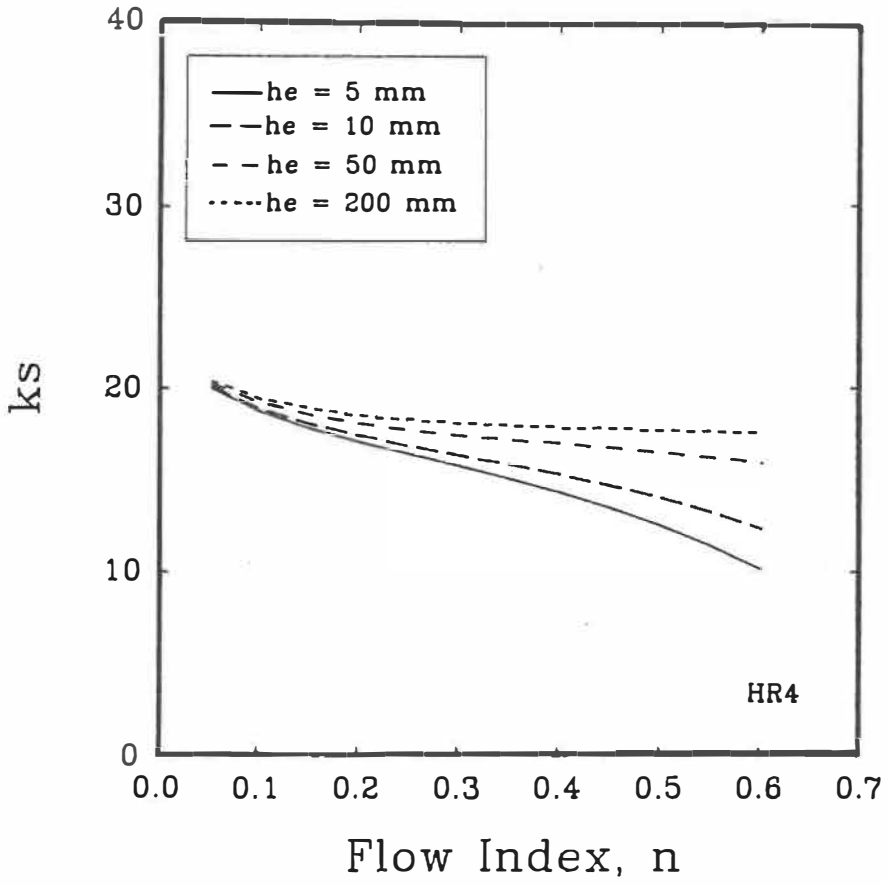

Figure A2 Effect of the equivalent bottom clearance on k_s for impeller HR3

predicted with the bottom effect is much close to the curve with h_e of 200 mm and most power data of this work were measured at h_e equal to 10 mm.

The power values predicted using h_e values equal to 5, 10, 25 and 100 mm are reported in Figure A3. The predicted curves are almost coincided as seen in this figure. These predictions confirm the experimental data of this work, that the bottom clearance has negligible effect on the power requirement.

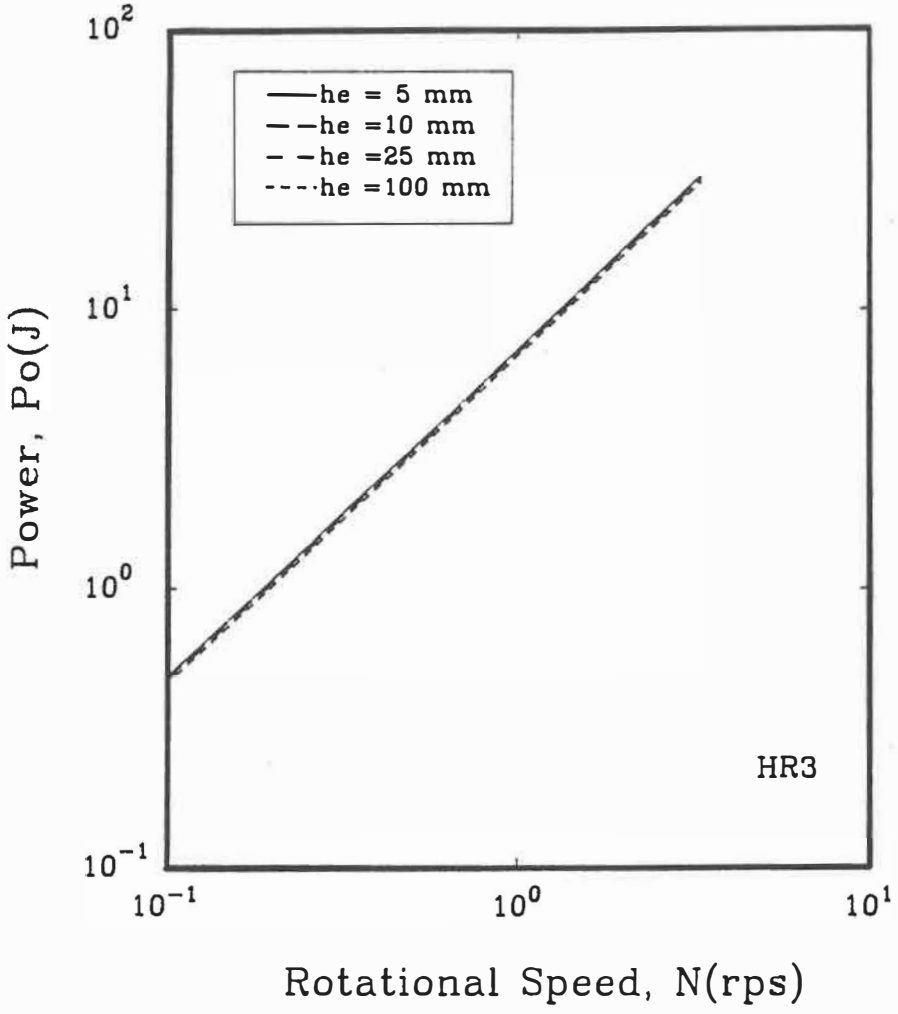

Figure A3 Effect of the equivalent botton clearance on the power consumption for impeller HR3

Appendix: II

Computer program for solving Model 3 in Chapter 5

In Chapter 5, three models based on one or two dimensional analysis of the equivalent Couette flow were developed to predict the effective shear rate in the transition flow regime. Model 3 (Eq. 26 in Chapter 5) is evaluated from a two dimensional analysis of the equivalent Couette flow, in other words, that is a two dimensional helical flow geometry. Eq.26 in Chapter 3 is given by

$$\dot{\gamma}_e = \left[\frac{K_p' d^3}{\pi^2 d_e^2 H}\right]^{1/s} \left[\frac{d\rho}{m}\right]^{(1-a)/s} N^{(2-a)/s} \left[\left(\frac{d_e}{2\omega'}\right)\left(v_z'^2 + (d_e/2)^2\omega'^2\right)^{1/2}\right]^{-n/s} \quad (1)$$

In the model, the θ-component of the velocity gradient, ω' must be solved via a numerical method. One mehtod to obtain ω' is to solve Eq.23 in Chapter 3, which is expressed as:

$$-m\left(v_z'^2 + r^2\omega'^2\right)^{(n-1)/2} r\omega' = \frac{c_1}{r^2} \quad (2)$$

In this equation, there are two parameters being determined, one is C_1 in Eq.23 and another is an integration constant. Two known boundary conditions of first type (e.g.: $v_\theta = v_z = 0$ at $r = D/2$ and $v_\theta = \Omega d_e/2$ at $r = d_e/2$), now allow us to solve Eq.23. By re-arranging Eq.23, a target function is a function of ω':

$$F(\omega') = \frac{c_1}{r^2} + m\left(v_z'^2 + r^2\omega'^2\right)^{(n-1)/2} r\omega' \quad (3)$$

A program algorithm is shown in Figure A2. First, an initial value of c_1 is given, so ω' values at given a position r, can be obtained by obtaining the roots of the target function $F(\omega')$, using Newton's method. Then, the θ-component velocity profile can be obtained by integrating ω' using Ronge-Kouta's method, and using one boundary

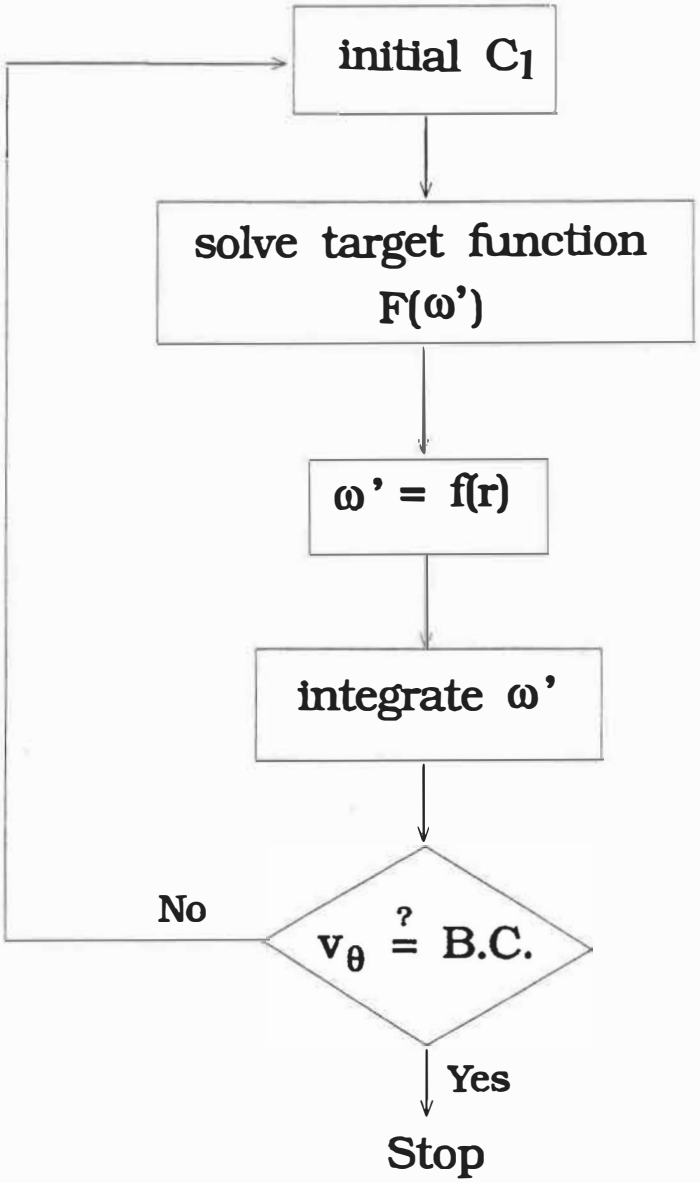

Figure A4 Frame of computer program for solving Model 3 in Chapter 5.

condition (for instance, at $r=D/2$). The resulted v_θ at $r=d_e/2$ is compared with the boundary condition. If the difference is smaller than a given error precision (10^{-5}), then the calculation is terminated; otherwise other c_1 value is given once again, the procedure of the calculation is repeated until the difference is within the given error precision.

The computational program is listed as following.

```
C     PROGRAM (Two Dimensional Helical Flow)
      INTEGER N5, NN, M, J
      DIMENSION  C(50)
      REAL C, H2, RO, XL, S, AA, BB, H, FM, FN
      REAL YR, R, DY, Y, DF, L2
      DIMENSION  DF(100), L2(100)
      DIMENSION DY(50,50), Y(50,50), R(100)


      V=5.655
      FN=0.18
      FM=22.4
      Y(1,1)=10.46
      AA=0.0
      BB=50.0
      H=0.5
      M=1
      YR=0.0

      J=0
2     J=J+1
      IF(J.LE.2) THEN
      C(1)=0.05
      C(2)=0.1
      GOTO 8
      ENDIF
      IF(J.EQ.3) THEN
      C(3)=(C(1)+C(2))/2.0
      GO TO 8
      ENDIF

      IF(DF(J-1)*DF(J-2).LE.0.0) THEN
      C(J)=(C(J-1)+C(J-2))/2.
      go to 8
      ENDIF
```

```
      IF(DF(J-1)*DF(J-3).LE.0.0) THEN
      C(J)=(C(J-1)+C(J-3))/2
      ENDIF
8     H2=0.002
      RO=0.106
      XL=0.146-RO
      S=XL/H2
      N5=INT(S)+1
      DO 100 I=1, N5
      L2(I)=H2*I
      IF (L2(I).GT.XL) THEN
      R(I)=0.146
      ELSE
      R(I)=L2(I)+RO
      ENDIF

      CALL ROOT(AA, BB,H,M,NN, 1E-5,1E-5,R(I),V,FN,FM,C(J),DY,J,I)
      WRITE(*, *) 'DY=',DY(J,I), 'I=',I,'J=',J
      Y(J,I)=Y(J,I)+H2*DY(J,I)
      WRITE(*,*) 'Y=',Y(J,I)
C     FORMAT(3 E 20.10)
100   CONTINUE
      DF(J)=Y(J,20)-YR
      IF(ABS(DF(J)).GE.1E-3) THEN
      GO TO 2
      ENDIF
101   CONTINUE
      WRITE(*,*) 'C=',C
      STOP
      END

      SUBROUTINE ROOT(AA, BB, H, M, N, E1, E2,R,V,FN,FM,C,DY,J,I)
      DIMENSION  DY(50,50)
      N=0
      A=AA
      FA=F(FM,V,R,A,FN,C)
10    B=A+H
      B1=B
      FB1=F(FM,V,R,B1,FN,C)
      WRITE (*,*) 'FB1=',FB1
      K=0
      IF(ABS(FA).LE.E1) GO TO 16
      IF(ABS(FB1).LE.E1)  GO TO 11
      IF(FA*FB1.GT.0.0)   GO TO 11
12    A0=(A+B)/2.0
      K=K+1
```

```
      F0=F(FM,V,R,A0,FN,C)
      IF(ABS(F0).LE.E1) GO TO 13
      IF(ABS(B-A0).LE.E2) GO TO 13
      IF(FA*F0.GT.0.0) GO TO 14
      B=A0
      GO TO 12
14    FA=F0
      A=A0
      GO TO 12
16    A0=A
13    N=N+1
      DY(J,I)=A0
      WRITE(*,*) 'DY=',DY(J,I)
      IF(N.GE.M) GO TO 15
11    IF(B1.GT.BB) GO TO 15
      A=B1
      FA=FB1
      GO TO 10
15    RETURN
      END

      FUNCTION F(FM,V,R,DY,FN,C)
C     F=M1*((V**2+((R(I)*DY(J,I))**2))**((N1-1)/2))*R(I)*DY(J,I)+C(J)/R(I)**2
      F=-FM*((V**2+((R*DY)**2))**((FN-1)/2))*R*DY+C/R**2
      RETURN
      END
```

Appendix: III

Effects of wall clearance on K_p and k_s

Influence of wall clearance on K_p

The power constant, K_p (=*NpRe*), has been found to be dependent of the mixer geometry. One of the important geometrical effects is the clearance between the vessel wall and the impeller blade. The wall clearance is given by, $c=(D-d)/2$.

In this work, three vessels with different diameters along with three impellers with the same diameter but different impeller pitch and width were used to assess the influence of the wall clearance on K_p. Typical power data for corn syrup in three vessels with different clearance ratios for the laminar flow regime are shown in Figure A1. As seen in this figure, the power number at the same Reynolds number increases with decreasing wall clearance. The experimental data of K_p are reported in Table A3. Also listed in this table are the predicted values calculated by using the correlations of Chavan and Ulbrecht (1973), Yap et al.(1979), and Shamlou and Eduards (1985). The reader is referred to Section 2.4 in Chapter 2 for the detailed forms of these correlations. As seen in the table, at the same impeller geomtry, the K_p value is considerably dependent of the wall clearance, c/D. The predictions of the correlations of Chavan and Ulbrecht (1973) and Yap et al. (1979) are fairly in agreement with the experimental data, whereas the correlation of Shamlou and Eduards (1985) overestimate the experimental values.

Influence of wall clearance on k_s

Beyond the flow index influence, the effective shear rate constant, k_s, is function of the agitator geometry. A typical dependence of k_s on the wall clearance for the 3% CMC solution mixed with impellers HR2 and HR3 is shown in Figure A5. Also illustrated in this figure is the values predicted using Shamlou and Eduards' model

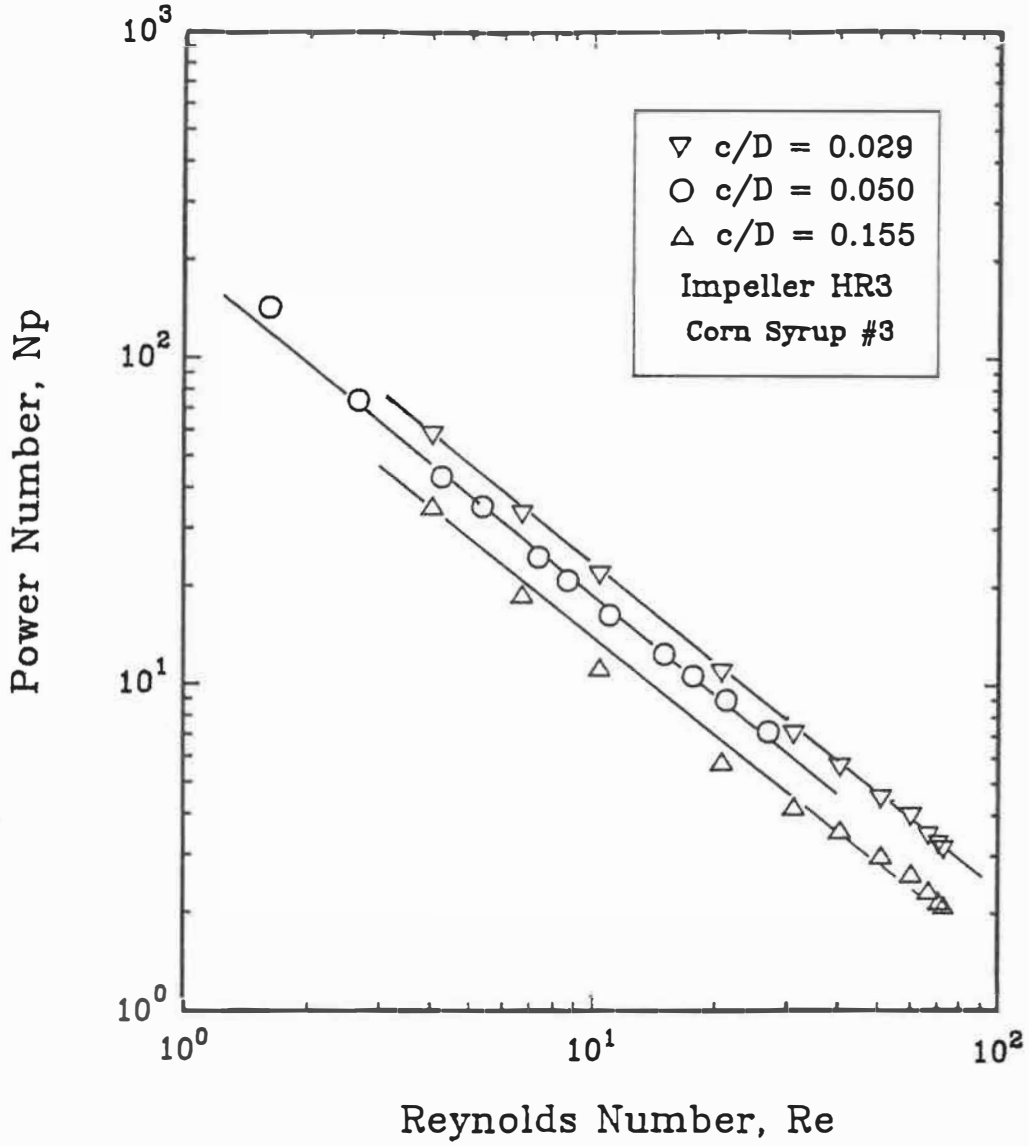

Figure A5 Influence of the wall clearance on power number for corn syrup agitated by impeller HR3

Table A1. Influence of wall clearance on K_p

No.	c/D	Impeller	K_p exp.	K_p Chavan and Ulbrecht	K_p Yap et al.	K_p Shamlou and Eduards
1	0.029	HR1	--	239.1		283.1
2		HR2	217.2	227.4		234.2
3		HR3	227.6	266.3		413.8
4	0.050	HR1	164.1	180.9	136.2	226.7
5		HR2	132.2	176.7	103.0	229.5
6		HR3	192.2	206.8	129.8	253.9
7	0.155	HR1	--	92.7		161.0
8		HR2	108.0	96.4		169.7
9		HR3	132.1	112.1		179.2

Correlation of Chavan and Ubrecht (1973) is Eq.37 in Chapter 2;
Correlation of Yap et al. (1979) is Eq.41 in Chapter 2;
Correlation of Shamlou and Eduards (1985) is Eq.42 in Chapter 2.

(1985). As seen in Figure A6, the k_s value increases with decreasing wall clearance, and increases much sharply at the lower values of wall clearance. This indicates that the effective deformation rate in the mixing vessels with smaller clearance is much larger that in larger clearance reservoirs. The prediction of shamlou and Eduards (1985) (Eq. 17 in Chapter) is fairly in agreement of the experimental results. However, their correlation did not account other geometrical effects such as impeller width and pitch. The flow index influence is also not taken into account.

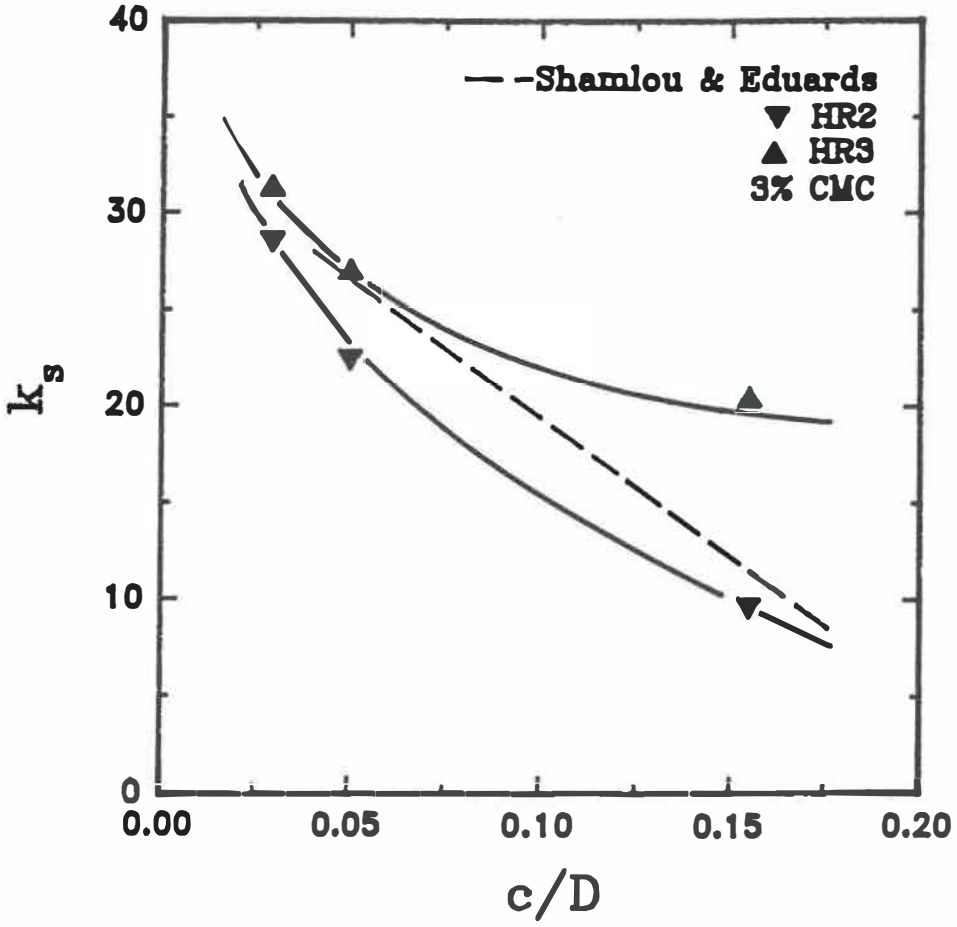

Figure A6 Influence of wall clearance on k_s for 3% CMC with impeller HR2 and HR3.

Appendix: IV

Comparison of gassed power data with Michel and Miller's correlation

The correlation of Michel and Miller (1962) has been found to be much successful to correlate power data under aerated conditions. However, as indicated in Chapter 2, this correlation does not account for geometrical effects. Furthermore, non-Newtonian characteristics are not taken into account in this expression. It is still worthwhile to compare the gassed power data of this work with their correlation, although two correlations based on dimensional analysis were proposed in this work. The correlation of Michel and Miller is expressed as:

$$P_g = C\left(\frac{P_0^2 N D^3}{Q^{0.56}}\right)^{0.45} \qquad (1)$$

The gassed data plotted as P_g against $P_o^2ND^3/Q^{0.45}$ are reported in Figure A7. The straight line in this figure is the prediction of the Michel and Miller's correlation. The predictions are in fair agreement only for the Newtonian glycerol and for the moderately shear-thinning 0.5% xanthan aqueous solution. For highly shear-thinning, viscoelastic and Boger fluids, the gassed power is considerably higher than predicted.

With a closer examination, the constant C in their expression is found to be a function of the shear-thinning property, e.g. flow index, n, and the elastic characteristic, elastic constant, λ, defined in Eq. 21 of Chapter 3. The results are shown in Figure A8. The flow index is shown to have no effect on the gassed power.

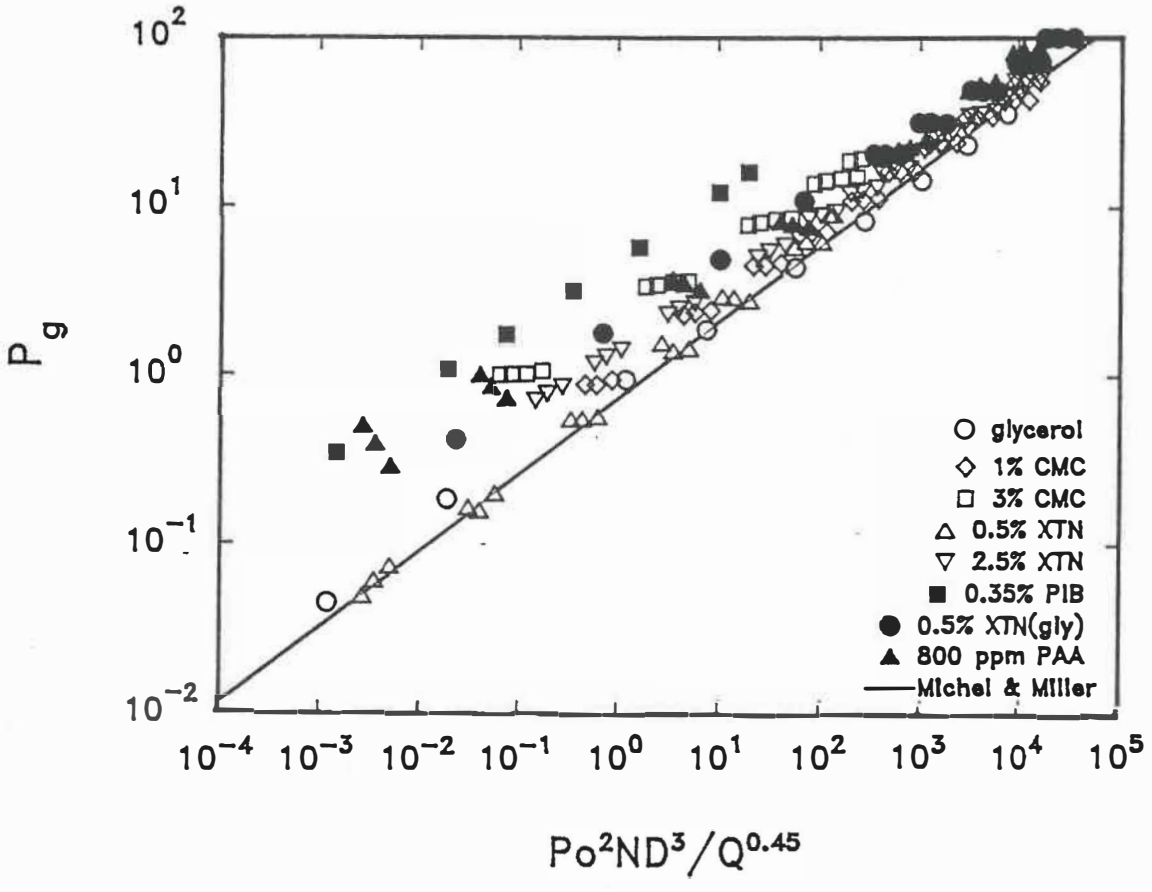

Figure A7 Comparison of gassed power data with Michel and Miller's correlation.

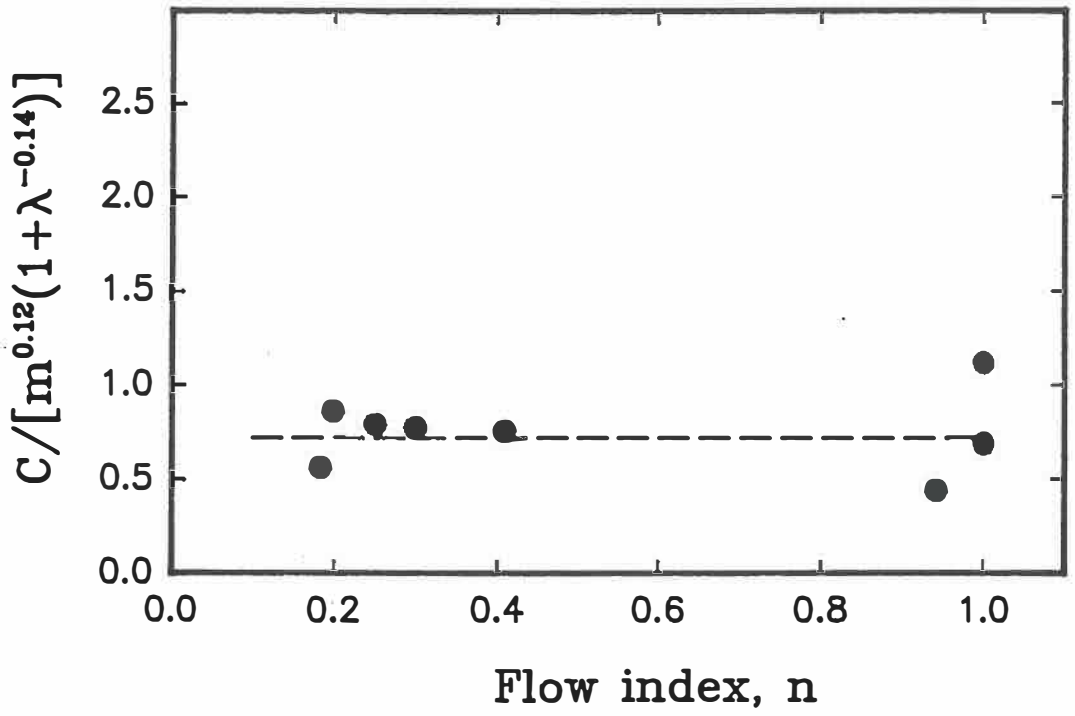

Figure A8 Dependence of C in Michel and Miller's correlation on flow index, n, and elastic constant, λ.

Appendix V

Reproduction of the effective deformation rate from the power data reported in the literature

In Chapter 5, the predictions of the three models for the effective deformation rate were compared with the data reported in the literature, which were reproduced through the power data reported in the literature. The procedure of this reproduction of the effective deformation rate is illustrated as following.

The extended linear power curve for the shear-thinning fluids in the transition occurs in the transition flow regime, comparing to the corresponding Newtonian power curve, as illustrated in Figure A9.At same power number, *Np*, a value of generalized Reynolds number, Re_g, is obtained from the extended linear power curve for shear-thinning fluids while a value of Reynolds number, *Re*, is obtained from the

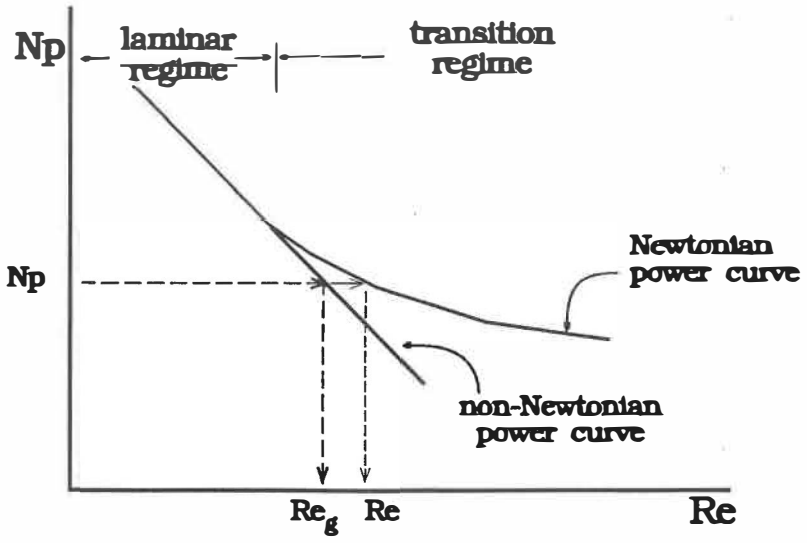

Figure A9 Illustration of reproducing the effective deformation rate from the power data reported in the literature

corresponding Newtonian power curve, in a given mixer. The generalized Reynolds number, Re_g, is calculated using a known effective deformation rate constant, k_s, obtained for the laminar flow regime, that is:

$$Re_g = \frac{d^2 N_1 \rho}{\eta_e} = \frac{d^2 N_1 \rho}{m \dot{\gamma}_e^{n-1}} = \frac{d^2 N_1 \rho}{m (k_s N_1)^{n-1}} \quad (1)$$

where the N_1 is the rotational speed at which the non-Newtonian fluid is mixed. N_1 can be obtained by re-ranging Eq. 1:

$$N = \left(\frac{m k_s Re_g}{d^2 \rho} \right)^{1/(2-n)} \quad (2)$$

Following the Metzner-Otto concept of the effective deformation rate, the generalized Reynolds number, Re_g, should be equal to the Reynolds number, Re, at the same power number, that is:

$$Re = Re_g = \frac{d^2 N_1 \rho}{\eta_e} = \frac{d^2 N_1 \rho}{m \mid \dot{\gamma}_e \mid_{trans.}^{n-1}} \quad (3)$$

Then the effective deformation rate in the transition regime can be obtained from Eq.3 in terms of Re and N_1:

$$\dot{\gamma}_e \mid_{trans.} = \left[\frac{d^2 N_1 \rho}{m Re} \right]^{1/(n-1)} \quad (4)$$

The power data reported in the literature which were cited in this work for reproducing the effective deformation rate are list in Figures A10, A11 and A12.

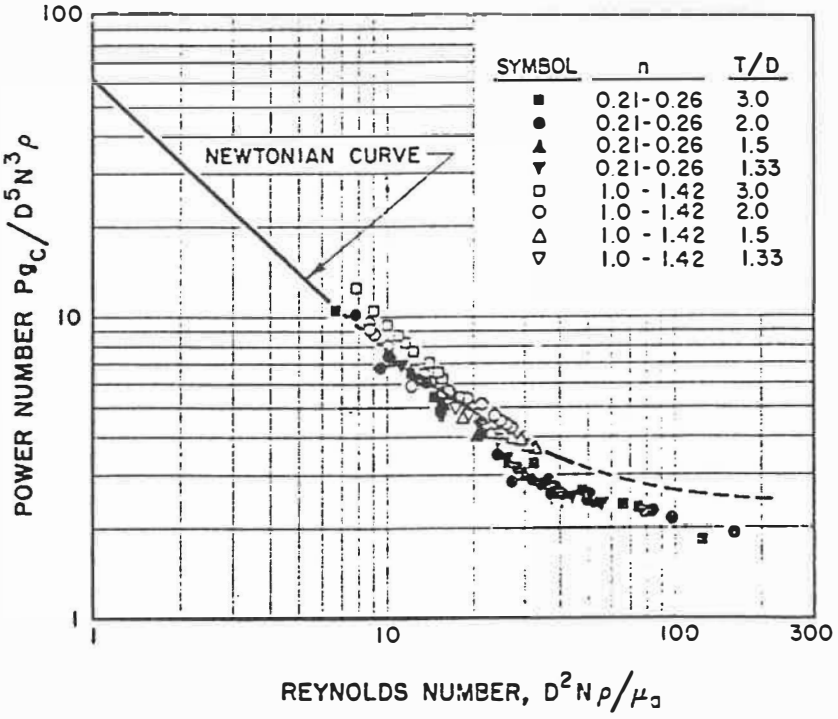

Figure A10 Power data of Metzner et al. (1961)

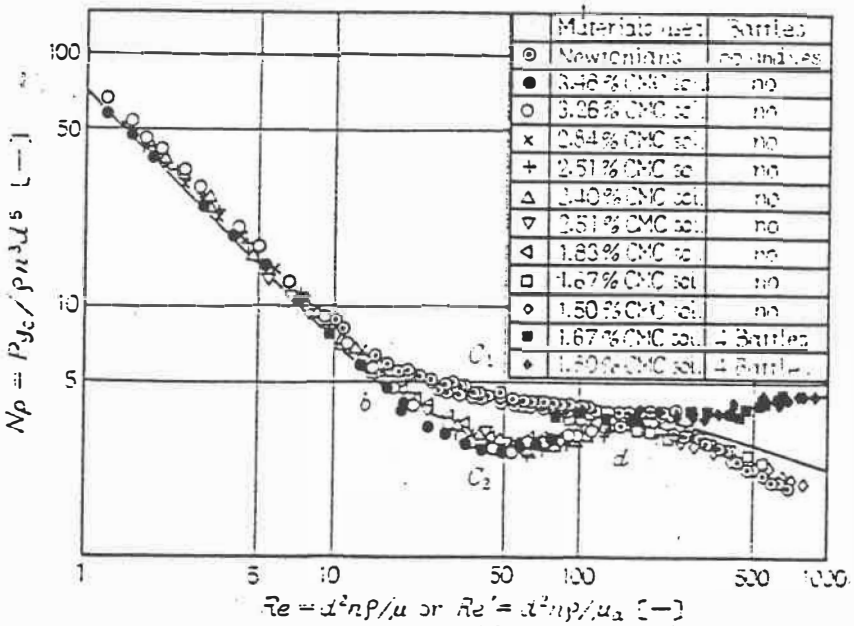

Figure A11 Power data of Nagata et al. (1971)

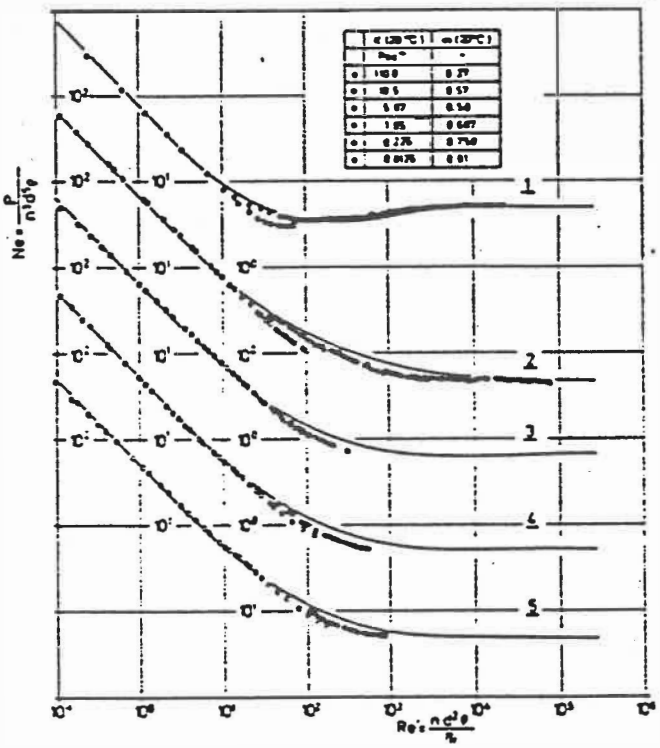

Figure A12 Power data of Höcker et al. (1981)

ÉCOLE POLYTECHNIQUE DE MONTRÉAL
3 9334 00276916 2